(12)

SCIENTIFIC REPORT

BEHAVIOR OF ALUMINUM IN SOLID PROPELLANT COMBUSTION

By

E. W. Price, R. K. Sigman, J. K. Sambamurthi and C. J. Park

Prepared for

AIR FORCE OFFICE OF SCIENTIFIC RESEARCH
BOLLING AIR FORCE BASE, DC 20332

Under

Contracts AFOSR F 49620–76–C–0003
and AFOSR F 49620–82–C–0013

June 1982

GEORGIA INSTITUTE OF TECHNOLOGY
A UNIT OF THE UNIVERSITY SYSTEM OF GEORGIA
SCHOOL OF AEROSPACE ENGINEERING
ATLANTA, GEORGIA 30332

1982

UNCLASSIFIED

SECURITY CLASSIFICATION OF THIS PAGE *(When Data Entered)*

REPORT DOCUMENTATION PAGE		READ INSTRUCTIONS BEFORE COMPLETING FORM
1. REPORT NUMBER	2. GOVT ACCESSION NO. AD-A113 128	3. RECIPIENT'S CATALOG NUMBER
4. TITLE *(and Subtitle)* BEHAVIOR OF ALUMINUM IN SOLID PROPELLANT COMBUSTION		5. TYPE OF REPORT & PERIOD COVERED SCIENTIFIC REPORT 1 Oct. 1977 - 28 Feb. 1982
		6. PERFORMING ORG. REPORT NUMBER
7. AUTHOR(s) E. W. Price, R. K. Sigman, J. K. Sambamurthi and C. J. Park		8. CONTRACT OR GRANT NUMBER(s) AFOSR F49620-78-C-0003 AFOSR F49620-82-C-0013
9. PERFORMING ORGANIZATION NAME AND ADDRESS GEORGIA INSTITUTE OF TECHNOLOGY SCHOOL OF AEROSPACE ENGINEERING ATLANTA, GA 30332		10. PROGRAM ELEMENT, PROJECT, TASK AREA & WORK UNIT NUMBERS N/A
11. CONTROLLING OFFICE NAME AND ADDRESS AIR FORCE OFFICE OF SCIENTIFIC RESEARCH/NA BLDG. 410 BOLLING AIR FORCE BASE, DC 20332		12. REPORT DATE June 1982
		13. NUMBER OF PAGES 91
14. MONITORING AGENCY NAME & ADDRESS *(if different from Controlling Office)*		15. SECURITY CLASS. *(of this report)* UNCLASSIFIED
		15a. DECLASSIFICATION/DOWNGRADING SCHEDULE N/A

16. DISTRIBUTION STATEMENT *(of this Report)*

Approved for public release; distribution unlimited

17. DISTRIBUTION STATEMENT *(of the abstract entered in Block 20, if different from Report)*

18. SUPPLEMENTARY NOTES

19. KEY WORDS *(Continue on reverse side if necessary and identify by block number)*

SOLID PROPELLANT COMBUSTION,
ALUMINUM AGGLOMERATION,
ALUMINUM COMBUSTION.

20. ABSTRACT *(Continue on reverse side if necessary and identify by block number)*

This report is concerned with achieving improved combustion of the aluminum ingredient in solid propellant. The approach is to clarify understanding of the complex detailed processes exhibited by aluminum and relate them to control of propellant burning rate, combustion stability, combustion efficiency and two phase flow behavior in the motor. A series of experiments were contrived to elucidate the microscopic details of aluminum behavior and their relation to microscopic details of the propellant, and to behavior of the other propellant ingredients.

DD FORM 1 JAN 73 1473 EDITION OF 1 NOV 65 IS OBSOLETE

UNCLASSIFIED

SECURITY CLASSIFICATION OF THIS PAGE *(When Data Entered)*

ACKNOWLEDGEMENT

The research summarized in this report was sponsored by the Air Force Office of Scientific Research. Technical monitor of the project is Dr. L. H. Caveny. The authors are grateful for the opportunity to pursue this research in the depth necessary to unravel the controlling details of a very complex combustion process.

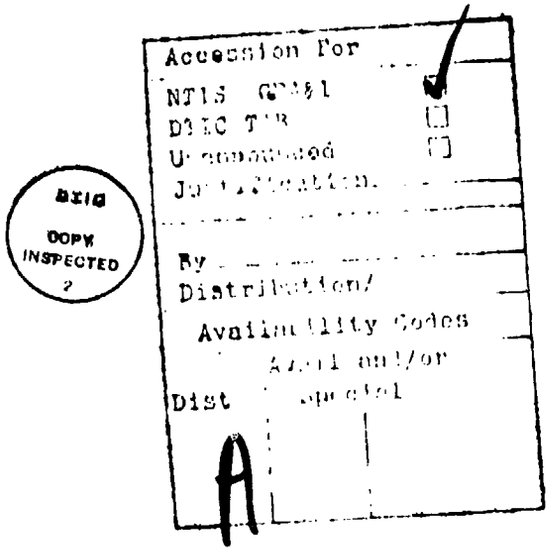

TABLE OF CONTENTS

INTRODUCTION

Metal powders are used as fuel components in solid propellants because of their high density, and high heat release when burned. The metals have other benefits as well, such as suppression of combustion instability, modification of burning rate, reduction of sensitivity to detonation, favorable supply, etc. These advantages are not all applicable to all metals in all rocket motors in all applications. Indeed, for rocket motor applications, only aluminum powder has seen widespread use. Even aluminum has been considered disadvantageous in some applications, particularly those in which the smoky exhaust trail of aluminized propellants compromises system effectiveness too severely. However, aluminum (and possibly other metals) is a highly desirable ingredient in many applications, and is the second most plentiful ingredient in roughly 50% of all propellant manufactured.

The advantages and disadvantages of aluminum, both real and potential, depend to a significant degree on the details of combustion of the aluminum. Combustion behavior is in turn relatively complex compared to other propellant ingredients, a circumstance resulting from the low volatility of the metal and its oxide. The fine metal particles go through a complex accumulation-concentration-agglomeration on the propellant burning surface, yielding relatively large and slow-burning droplets. The combustion behavior, and nature of the oxide products, are sensitive to details of the propellant and motor, and are difficult to predict in advance of testing the all-up system. Because of this, a number of efforts have been mounted in the past to achieve better understanding and/or engineering characterization of aluminum behavior in propellant combustion, and its effect on system performance. The present study has been aimed at understanding the detailed processes that determine the behavior of aluminum in the rocket motor, using methods that provide information at the microscopic level of the aluminum particles, agglomerates and oxide product droplets. Such understanding provides the basis for more rational "design" of propellant formulation, prediction of performance, and manipulation of design to achieve best performance.

In the interests of perspective, the combustion "metabolism" of aluminum is outlined in Fig. 1, which shows the routes by which ingredient aluminum particles in propellants can progress to their final reaction products (the figure is based on the usual case where the products are molten Al_2O_3). For any given propellant, there is

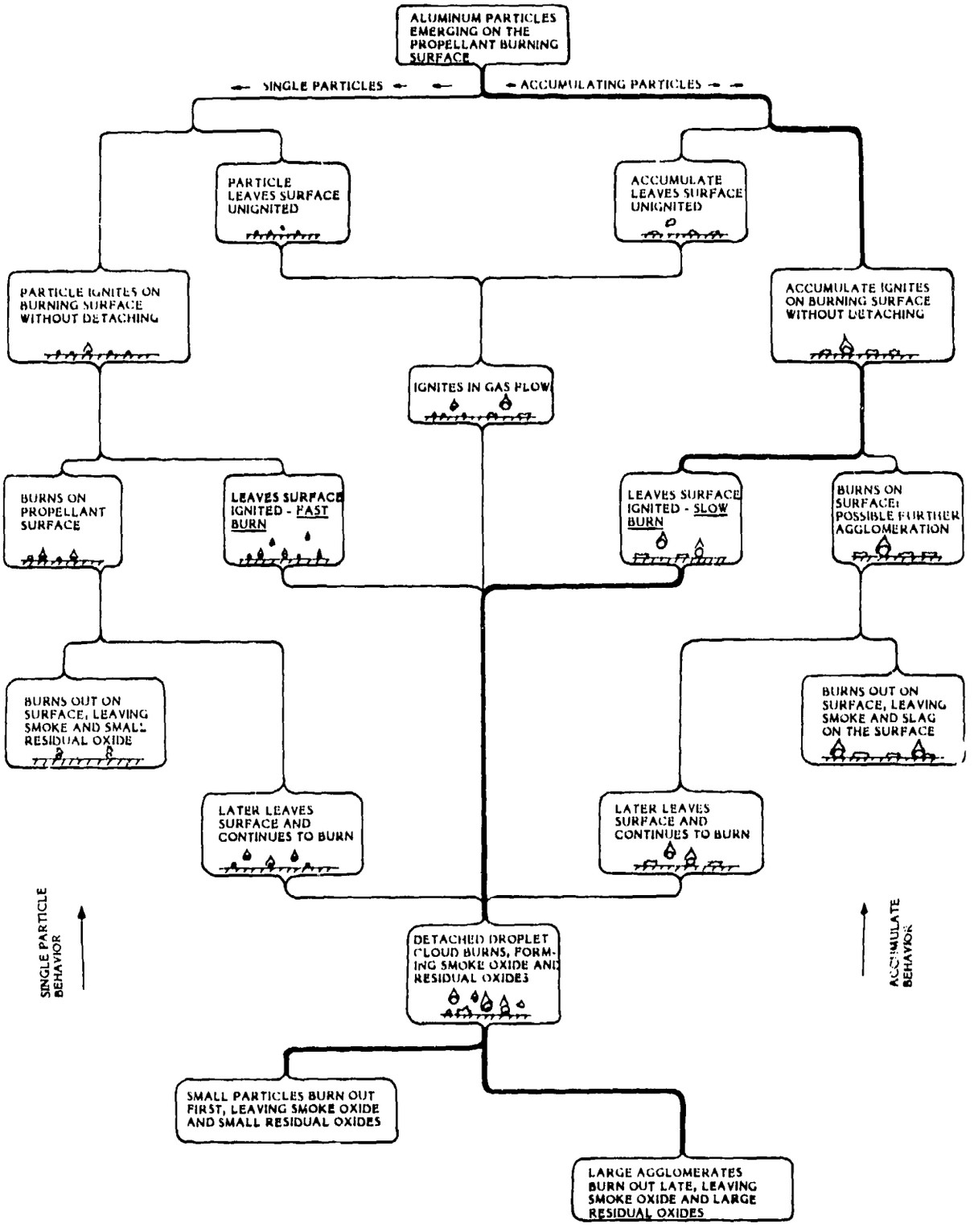

Fig. 1 Alternative paths of aluminum behavior in the combustion zone. The path emphasized by the heavy line is most typical with ammonium perchlorate-hydrocarbon binder propellants.

a "most typical" route, but some of the particles follow other routes, giving a statistical array of behavior. However under most conditions, aluminum concentrates on the burning surface (Fig. 2); agglomerates, ignites and detaches from the surface as a single complex event (Fig. 3); burns as 50 - 300 μm diameter agglomerates while moving away from the burning surface (Fig. 4); forms a fine Al_2O_3 smoke (< 2 μm) in a flame envelope about the agglomerate (Fig. 5); concurrently accumulates oxide on the surface of agglomerates that ends up as "residual" oxide droplets in the 5 - 100 μm range when the agglomerates burn out (Fig. 6). This sequence is noted by the heavy lines in Fig. 1.

It is this detailed behavior that determines the effect of aluminum on such combustion variables as

propellant burning rate
combustion stability
combustion efficiency
combustion quenching
aluminum slag residue

and such oxide product effects as

two-phase flow in the combustor and nozzle
thrust efficiency
component erosion
damping of combustor oscillations
oxide slag residue.

The combustion studies seek to understand the accumulation-concentration-agglomeration-ignition-detachment-agglomerate combustion sequence by studies that clarify these individual steps. This involves consideration of the original distribution of aluminum particles in the propellant microstructure; the relative dimensions of the combustion zone and the particulate ingredients; the forces conducive to retention and concentration of aluminum; the conditions that delay ignition during concentration; the processes that connect accumulated particles and set the stage for coalescence; the conditions that eventually break down sintered surface accumulations and cause agglomeration, ignition and detachment from the

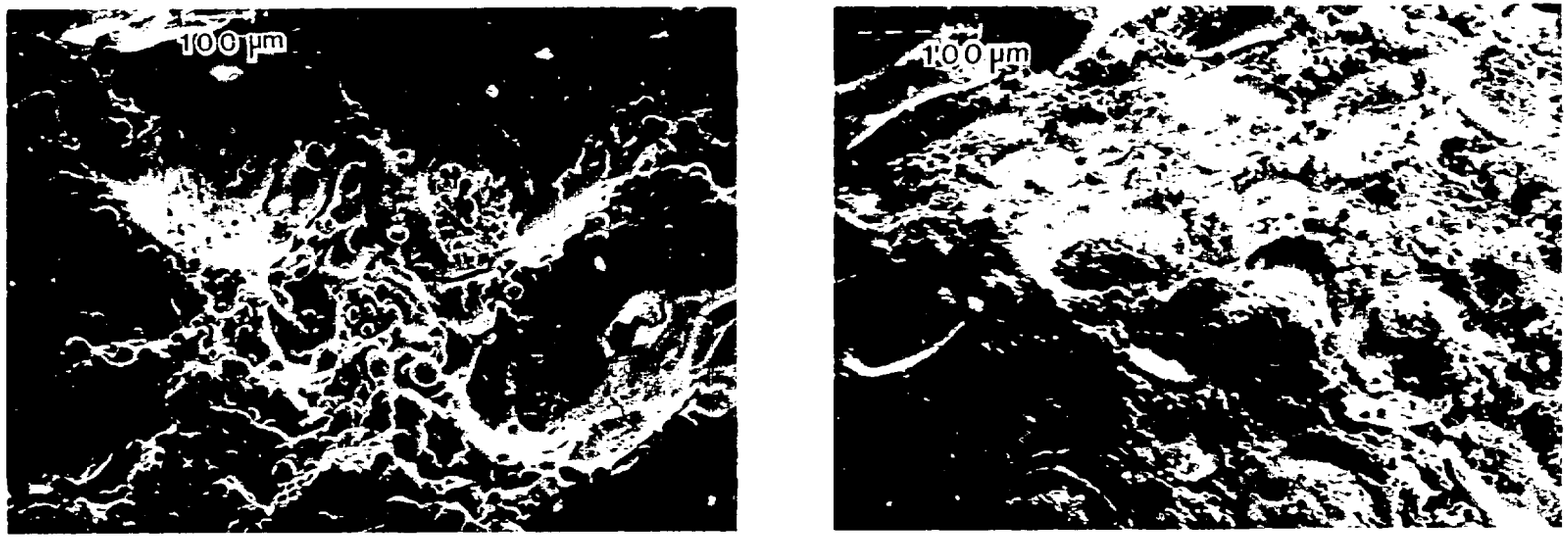

Fig. 2 Aluminum concentration on the burning surface. Scanning electron microscope pictures of surfaces quenched by rapid depressurization.
a) Aluminum concentration in a "pocket", with relatively visible evidence of binder melt (from 6.9 MPA test).
b) General pattern of aluminum concentration, selected to show also an example of relatively dry sintering of accumulated aluminum (from 0.7 MPa test).

Fig. 3 Formation of an agglomerate from a surface accumulation of alumin particles (from high speed motion pictu s by D. Zurn, Naval Weapons Center).

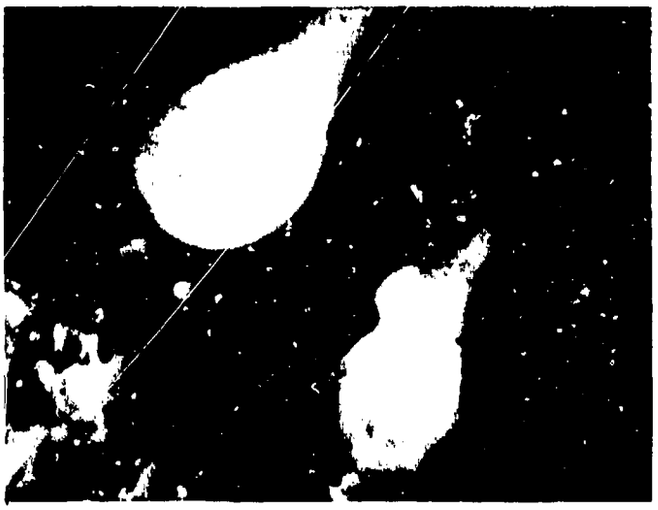

Fig. 4 Burning agglomerates, shortly after leaving the propellant burning surface.

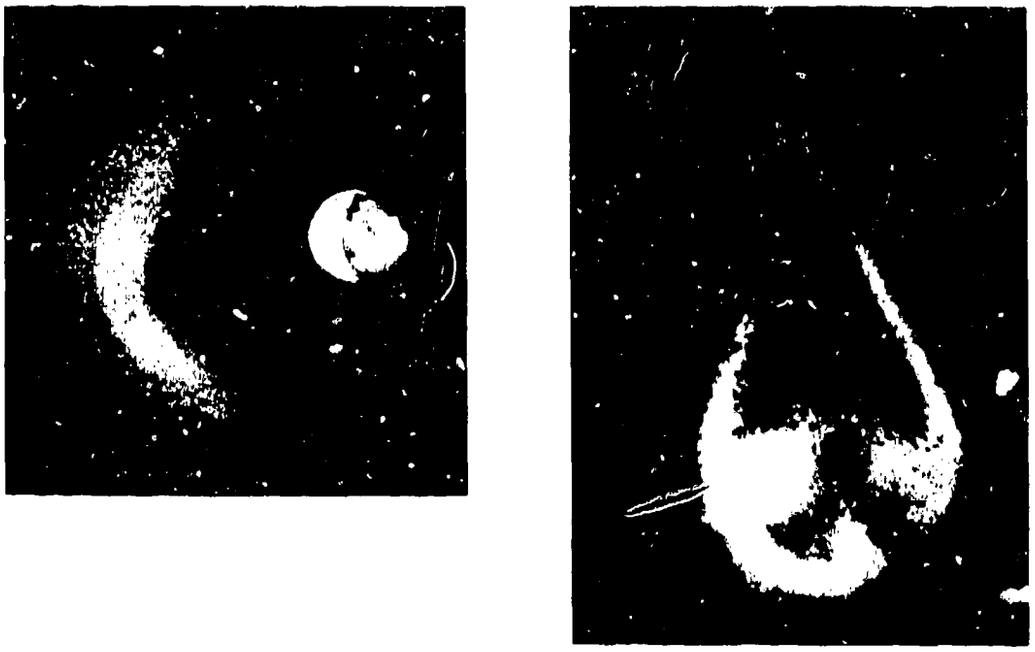

Fig. 5 Illustration of smoke oxide formation in the detached flame around the agglomerate.
a) Aluminum droplet with oxide lobe and smoke cloud deposited on a quench plate in an experiment burning single aluminum particles in air at 1 atm (photo by Prentice, NWC).
b) Burning aluminum agglomerate observed in high speed photography of propellant combustion.

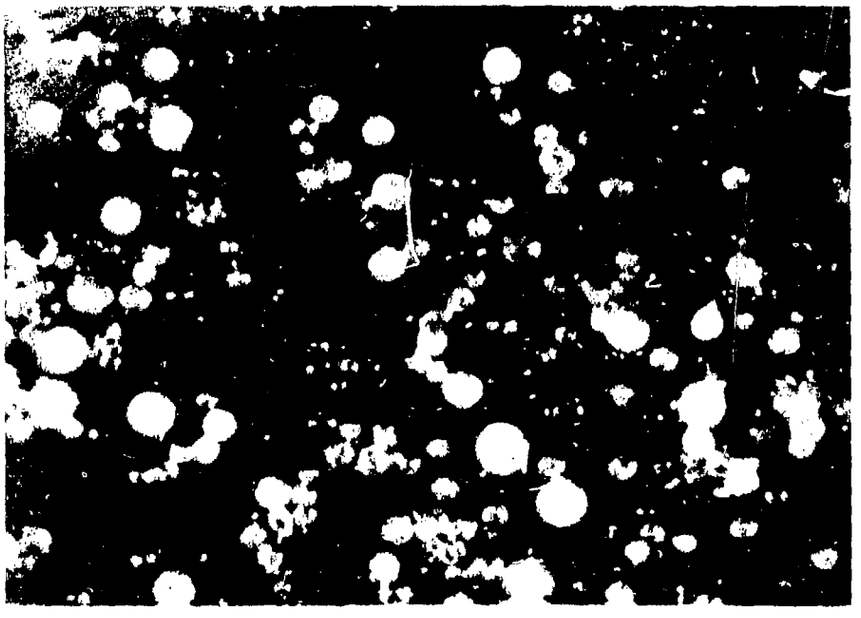

Fig. 6 Residual oxide, evolved from agglomerate oxide.

burning surface; and the combustion of agglomerates in the gas flow field. While it is not practical to seek complete understanding of all these complex processes, it is also not practical to ignore any of them because they are "branch points" for the alternative paths in Fig. 1, and each branch point can exercise decisive effects on combustion. The present investigations have sought to clarify these branch points, establish their roles at the microscopic level in real propellant combustion, and thus provide the basis for understanding the relation between conventional propellant variables (composition, particle size) and macroscopic combustion behavior (burning rate, stability, combustion efficiency, etc.). The discussion in the following seeks (in the first sections) to develop the arguments and summarize past results into a connected account of how aluminum behaves as it "moves through" the combustion wave. These sections are followed by accounts of several supporting studies that have not been reported previously. These studies were carried out as part of the basic study, and in part to explore potentially useful ideas emerging from the study (e.g., modifications of aluminum powder to control agglomeration, and use of high aluminum-content propellants).

PROPELLANT MICROSTRUCTURE

Typical composite propellants are made with oxidizer as a primary particulate ingredient (70 - 75% by weight for aluminized propellants), with particles ranging from 6 - 600 μ m (mass average 100 μm). Aluminum particles are typically 16% by weight, in the size range 5 - 40 μm. The balance of the mass (10 - 15%) is typically a polymeric material. In order to achieve a near-stoichiometric mixture, the binder content is made as low as possible consistent with acceptable processing characteristics and physical properties of the propellant. To achieve this, the size distribution of the particulate ingredients is normally chosen rather carefully so as achieve dense particle packing and minimize packing voids that that yield locally high concentrations of binder. On the other hand, it is required that the surface of all particles be "wetted" by binder in order to get acceptable mechanical properties, so all particles are surrounded by binder. In meeting all these requirements, propellant processors have to limit the "smallness" of particles (total surface area) to avoid processing problems (e.g., viscosity of the uncured mix). The net result is reflected in the typical figures noted above, but with oxidizer particle blends involving two to four different sizes, a substantial portion being in the coarse component (e.g., 200 - 400).

Given the foregoing practical realities and trade practices, a typical propellant looks like that shown in Fig. 7. An aggregate of coarse oxidizer particles is set in a "sponge" of binder and finer oxidizer and aluminum particles. In a low burning rate propellant, the coarse particles will be more densely packed (and possibly larger), with the "sponge" being correspondingly more tenuous and containing less fine oxidizer. Because the aluminum particles are normally relatively small in both size and total volume, they can be pictured as being part of the sponge. Thus the aluminum is not homogeneously distributed on the dimensional scale of the oxidizer particles, being located in that 30 - 50% of the volume occupied by the sponge. That volume is very fuel rich, containing only about 30% of the oxidizer in a propellant that is already fuel rich in overall formulation.

When a propellant burns, a burning front propagates through the matrix, with

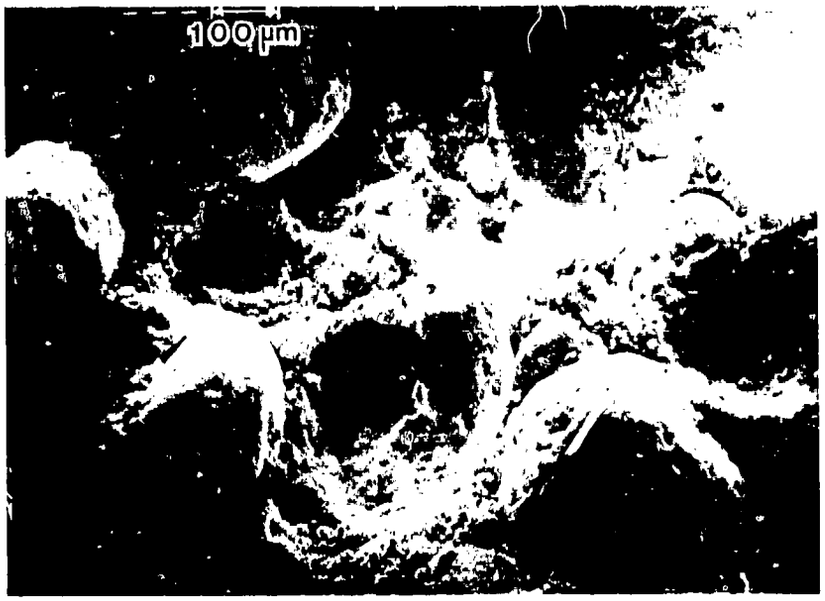

Fig. 7 Illustration of propellant microstructure. Scanning electron microscope picture of a surface produced by breaking the propellant (to show structure).

the burning surface representing a sort of "cross section" of the propellant microstructure (Fig. 8). Oxidizer particles are readily visible, as is the "cross section" of the sponge (in Fig. 8 a nonaluminized propellant was used to enhance the visibility of sponge structure). The binder area of the surface is revealed as a tenuous, interconnected structure with occasional patches of larger dimensions corresponding to voids or "pockets" in the packing pattern of the larger oxidizer particles. These pockets may contain smaller oxidizer particles, which are often difficult to distinguish. A similar structure is revealed with aluminized propellants, but the sponge pattern is usually dominated on the burning surface by aluminum particles (Fig. 9). The aluminum presents an appearance of an interconnected array, which to some extent is a reflection of its actual distribution in the propellant (i.e., as part of the sponge). However, the distribution of the aluminum is critically dependent on its particle size relative to the coarser AP particles. Very fine aluminum can be uniformly dispersed in the sponge, but coarser aluminum particles will be isolated from each other because they will not fit in the thinner elements of the sponge structure. Thus aluminum may be localized in the thicker sponge components corresponding to oxidizer packing voids (referred to in this report as "binder pockets"). The degree of interconnectedness between these aluminum concentrations will depend on the size of aluminum particles and their corresponding ability to "fit" in the connective structure of the sponge between pockets. These circumstances are important because they affect the continuity of the aluminum's array on the burning surface, which in turn affects the opportunity for coalescence between pocket concentrations of aluminum.

As noted earlier, oxidizer is usually present as a blend of particle sizes. The smaller fraction typically has a particle size of the same order as the aluminum (this was the case for the propellant in Fig. 9). Thus arguments regarding the distribution of aluminum particles in the sponge apply also to the finer part of the oxidizer particle population. As noted earlier, this means that the aluminum containing part of the sponge contains also oxidizer, yielding a very fuel-rich propellant (which will ordinarily not burn unaided). Obviously the distributions of fine oxidizer and aluminum in the sponge are amenable to some delicate tailoring by careful particle size tailoring, but the size distributions ordinarily available are too broad for such "fine tuning" of microstructure, and the effects on combustion are consequently unevaluated.

In the present work, particle size has been one of the principal variables in experiments. The foregoing description of microstructure was evolved as a

Fig. 8 Illustration of distribution of binder in a heterogeneous propellant. Scanning electron microscope picture of a quenched surface (non aluminized sample used to enhance visibility of binder; test pressure 6.9 MPa; propellant contains fine AP, visible in the binder).

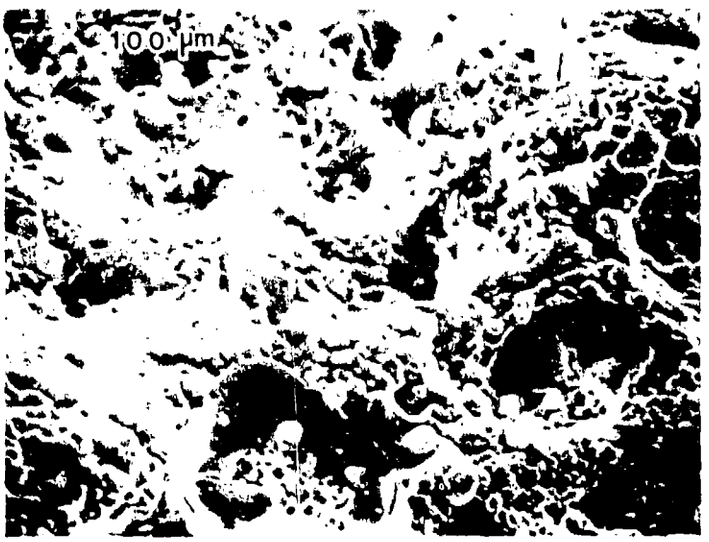

Fig. 9 Illustration of distribution of aluminum on the burning surface. SEM picture of a sample quenched from 6.9 MPa.

consequence of efforts to understand results of tests, and as a basis for design of test experiments. In hindsight, the description is fairly obvious, and a key element of the description (the concept of pockets) was presented by one of the authors earlier (Ref. 1). The more elaborate description presented here is designed to accomodate a more detailed understanding of aluminum behavior described in the following.

PRE-AGGLOMERATION BEHAVIOR OF ALUMINUM*

There is very little controversy over the thesis that aluminum forms agglomerates near the propellant burning surface, but there have been a variety of proposals as to what processes lead to agglomeration. These different proposals do not represent a controversy so much as divergent efforts to produce tractable idealized modeling schemes from which agglomeration behavior can be calculated (Ref. 2-4). The experimental evidence is largely in the form of combustion photography (which doesn't get published), and more controlled studies of response of aluminum powders to heating (available in diverse sources (Ref. 5)). In addition, some idea of intermediate steps leading to agglomeration can be gained from examination of quenched burning surfaces. These methods have all been used in one or more of past studies and the present study. The general interpretation is relatively unambiguous, and is summarized in the following.

Aluminum is seen to accumulate on the propellant burning surface, often residing there for much longer times than required for the burning surface to recede past the particles. In other words, particles typically adhere to the surface. Mobility is typically low, consistent with an "adhesive" surface retention. Knowing the propellant microstructure, it is evident that most adhering particles on a receding surface will be joined by underlying particles. This in turn implies that accumulation and concentration of aluminum particles will normally occur, an implication supported by countless observations by combustion photography and quenched sample studies. Low volatility of the metal, protective nature of the oxide skin, and initially low local concentration of oxidizing species prevent ignition of the metal during this surface accumulation (as seen later in this report, such accumulation occurs without ignition even on the burning surface of AP oxidizer). Finally, it is an observed fact that the accumulating particles eventually coalesce into agglomerates, implying that concentration proceeds to the point of contact between particles. Presence of relatively rigid structures of aluminum particles is manifested in combustion photography and quench tests; thus it is evident that particle contact progresses to a state of sintering, similar to that resulting from controlled heating of aluminum powder in oxidizing atmospheres. Indeed, acid etching of recovered accumulates shows them to consist of an

---

* This section is condensed from Ref. 7. See that reference for more extensive illustrations of relevant experimental results.

interconnected oxide shell structure filled with aluminum (Ref. 5 - 7).

In view of chaotic microstructure of the heterogeneous propellants, it is to be expected that some diversity and intermittency of behavior would occur. Some aluminum particles leave the surface without evident interaction with others. All aluminum eventually leaves the surface, and the extent of prior concentration and sintering can only be fully described with the aid of statistical language. Recalling the earlier discussion of the implications of propellant microstructure, the statistical language of accumulation, sintering and detachment must be linked to the statistical language of propellant microstructure, and concepts such as "pockets", "bridging" between pockets, and formation of "sintered filigrees" are terms used to connect propellant microstructure to the state of connectedness of accumulated aluminum on the burning surface. The ultimate size of an accumulate is thus dictated to some extent by the original concentration of aluminum in the propellant microstructure (pockets) and to some extent by the spatially nonuniform conditions that cause sintered structures to adhere to the propellant surface without ignition. Finally, ignition may precipitate detachment, and the ultimate size of the accumulate will in that case be determined by conditions necessary for ignition. Recalling the earlier reference to the reluctance of aluminum to ignite in the AP flame, it must be anticipated that ignition termination of surface accumulation may be as dependent on propellant microstructure as is the pattern of accumulation. This will be so when the ignition is induced by the local oxidizer-binder flamelets associated with oxidizer-binder interfacial regions of the burning surface microstructure. It is in or beyond these flamelets that high enough temperatures are reached to achieve ignition of sintered aluminum accumulates. The process of ignition and concurrent agglomeration is described in the following.

THE AGGLOMERATION EVENT

Agglomeration takes place when the progressive state of an accumulate reaches a point where the oxide containment of the molten aluminum breaks down. At this point, two processes come precipitously into dominance. The surface tension of the molten aluminum causes the metal to draw into a spherical configuration. Since the breakdown of the oxide containment does not occur simultaneously throughout the accumulate, this spheroidization is progressive. The second process that comes concurrently into dominance is the oxidation rate of the aluminum as it escapes the containment of the existing oxide shell. Thus it is typical in combustion photography, under conditions favorable for good resolution, to see areas of spheroidization in a surface accumulate, accompanied by onset of evidence of associated aluminum vapor flame and telltale oxide smoke trail.

The agglomeration event can be so rapid that it is not resolved in photography at a few thousand frames per second, or it can be fairly protracted and easy to observe (large accumulates at low pressure). The progressive nature of the event is obvious under favorable viewing conditions. Initiation appears to start at locations where the accumulate is best exposed to the high temperature of the diffusion flame elements (AP-binder flame). That region of the accumulate glows brightly, spheroidizes and develops darker reflective areas that are apparently molten metal. The smoke veil and trail develops over these areas when they appear. At this point, the oxide residue from the spheroidized portion is visible (at least in part) as a white glowing film over parts of the sphere, presumably molten. This is accompanied by increasing brightness of the neighboring portions of the accumulate. The molten portion starts to coalesce progressively into the rest of the accumulate, at the same time exhibiting a loss of any other attachment to the propellant surface. Under the conditions that give good resolution of these progressive features, the surface accumulation of aluminum is usually widely interconnected, so that the propagative aspect of a coalescence is relatively visible. Indeed, some investigators who observed the behavior without aid of the external illumination used to show the nonluminous part of the accumulate have interpreted the behavior as indicating a freely rolling droplet on the propellant surface (without accompanying rationale for the long delay before "lift-off" from the surface). In any case, the flaming agglomerate eventually burns itself free of surface attachment and moves away in a near spherical condition (Fig. 4), typically

showing burning metallic areas; bright molten oxide areas; and often darker or orange irregular areas of not yet melted material at the last point of contact of the droplet with the propellant surface. This is in effect the birth of an agglomerate, whose individual identity remains until burnout somewhere in the flow field. Such an agglomerate is typically 10 times the diameter of the original ingredient aluminum particles, implying an agglomeration of 1000 particles.

The foregoing description is based on interpretation of combustion photography, aided by a good deal of prior knowledge of the nature of surface accumulates, the propellant combustion zone, and aluminum combustion. It is basically a visualization of the agglomeration, seen from the outside. What's happening inside the coalescing mass, how does it affect the process, and what is the end effect on the fully developed agglomerate? This can be inferred from the nature of the situation, properties of materials involved, and the externally observable behavior.

When the accumulate first starts to break down and coalesce, it is a nonuniformly preheated structure consisting of an intricate solid oxide encasement of liquid aluminum. The metal of the original aluminum particles is probably mostly still unconnected, any contact points having oxidized to form the connected accumulate structure. Any localized breakdown of the oxide leading to onset of coalescence is initially insulated from the overall accumulate by the rigidity and low thermal conductivity of the oxide containment structure. However, the rise in local heat release due to the flame around the coalescing aluminum at the initial breakdown point melts the oxide locally, assuring continued and spreading reaction of aluminum.

As the oxide shell structure breaks down, it is swept up by the coalescing aluminum in the form of thin (sub micron) solid and melting sheets with varying degree of connectedness. Insoluble in the liquid aluminum, the oxide will be partly trapped in the interior of the agglomerate, and partly left as melting surface aggregations remaining after withdrawal of coalescing aluminum (Fig. 10 a). The quenched agglomerate in Fig. 10 b shows the tendency of the aluminum to spheroidize when the accumulate is not yet fully molten in the interior. Fig. 3 shows the tendency for much of the initial oxide to be left as a melting aggregate on the agglomerate surface. This external residue is the source of part of the oxide typically present as an oxide lobe on a fully burning agglomerate (Fig. 4). Acid etching of such agglomerates after quench-collection reveals the presence of a complex interior oxide structure (Fig. 11), probably evolved from the accumulate

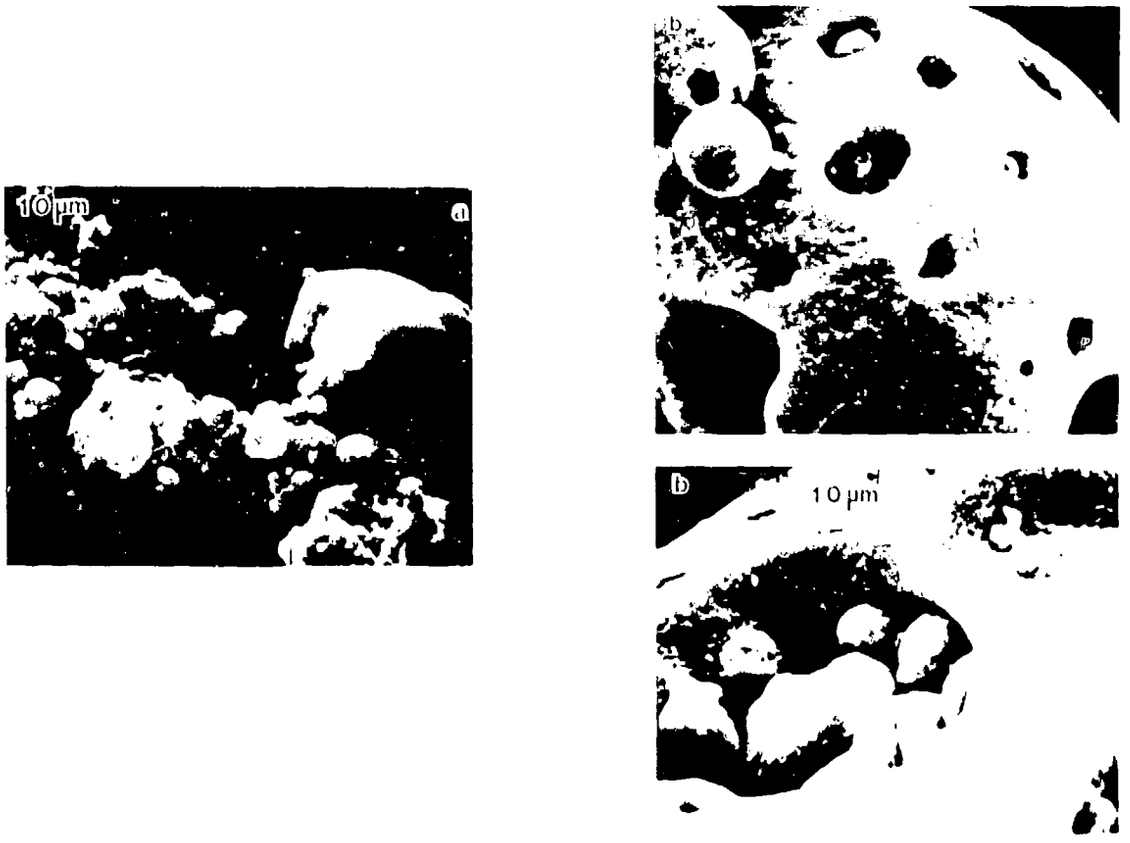

Fig. 10 Transition from accumulate to agglomerate.
a) Accumulate with sites where coalescence, burning and oxide lobe formation have occurred.
b) Spheroidization is largely complete, but not all original oxide has yet melted.

Fig. 11 Flake oxide in the interior of the aluminum portion of an agglomerate (revealed by acid etching). (From ethanol plume quench test at 1 atm.)

oxide that was trapped in the agglomerate during coalescence of the accumulate. Since the temperature of the burning agglomerates is above the melting point of the oxide, that oxide in the interior presumably survived as liquid sheets that solidified to the form in Fig. 11 during quenching. There is some evidence that the amount and structure of interior oxide is dependent on the abruptness of the agglomeration event, suggesting that the aluminum coalescence would exclude the oxide if it were completely free to flow. Thus agglomerates formed in the argon atmosphere in a hot stage microscope have little or no oxide trapped in the interior (Ref. 7,8). Combustion-produced agglomerates are observed in the present studies to have more interior oxide if formed in high pressure burning. The differences are conspicuous when one tries to cut the quenched agglomerate: "high pressure" agglomerates are brittle and give ragged cut surfaces, while "low pressure" agglomerates are soft, and cut smoothly. Thus it seems clear that the agglomeration is a dynamic event that yields a product that is dependent on a large complex of conditions. Indeed, the agglomerate may contain also carbon, nitrogen and/or chlorine and their compounds, probably only in small quantities.

A point of particular interest regarding the agglomeration event is its relation to ignition of the aluminum. Under most conditions, agglomerates are already burning at the moment of detachment from the propellant surface. When ingredient aluminum particles of agglomerate size are used in a propellant, they usually ignite some distance from the burning surface (and in some laboratory experiments, fail to ignite at all). This point may seem unimportant, since ingredient aluminum particles of a size comparable to that of typical agglomerates are usually not used in practical situations. The importance lies in the demonstration that the agglomeration process is an exothermic process, occurring in a loosely connected filigree on the propellant burning surface. Further, it is the initiation point of the sustained burning of the aluminum. Its responsiveness to combustor flow conditions (Ref. 9) and gas flow oscillations (Ref. 10) is likely to be a factor in erosive burning, g-force effects (Ref. 11), slag retention, combustor stability, propellant quench limits, combustion efficiency, and product oxide droplet size role in two-phase losses.

NATURE AND COMBUSTION OF AGGLOMERATES

The foregoing sections have described how aluminum agglomerates are formed in the propellant combustion. Much of that information was drawn from earlier research on this and other projects. A substantial part of recent effort on this project has been on the nature of the agglomerates and their combustion and (next section) on the nature of the oxide droplets formed during combustion. This work was reported in Ref. 7, and is presented here in summary form.

Test Methods

Experimental studies were based on analysis of samples collected in the outflow from the burning surface of real and model propellants. Collection was accomplished by directing the flow from the burning surface into a pool of ethanol. The method quenches burning agglomerates, and collects most of the condensed material in the flow except the fine oxide smoke formed in the flame envelope of the burning agglomerates (mass of that smoke is calculated from mass and composition of the original sample and collected sample). The collected samples were subjected to a variety of analyses, including: particle size analysis; determination of unreacted aluminum content; microscopic examination; and determination of interior structure by cleaving, breaking, acid etching and heat treatment. Such studies were made as a function of distance from the propellant surface, pressure, and propellant formulation variables. The objective was to reconstruct from quench sample data the combustion history of agglomerates.

Trends of Agglomerate Populations

When samples are quench-collected close to the propellant burning surface (1.5 cm), and washed to remove smoke oxide (i.e., $< 2\ \mu m$), they are mostly aluminum agglomerates (low pressure tests), consisting of a wide size range of agglomerates with small transparent oxide lobes. At greater distances from the propellant surface, the oxide lobe portion of each agglomerate becomes relatively large (Fig. 12), and a variety of small residual oxide particles appear in the collected samples (remnants of burnout of the initially small agglomerates). Figure 13 shows a typical sequence of agglomerate mass size distributions corresponding to quenches at increasing distances from the burning surface. The area under the curves is indicative of the total weight of the agglomerates in the quench sample

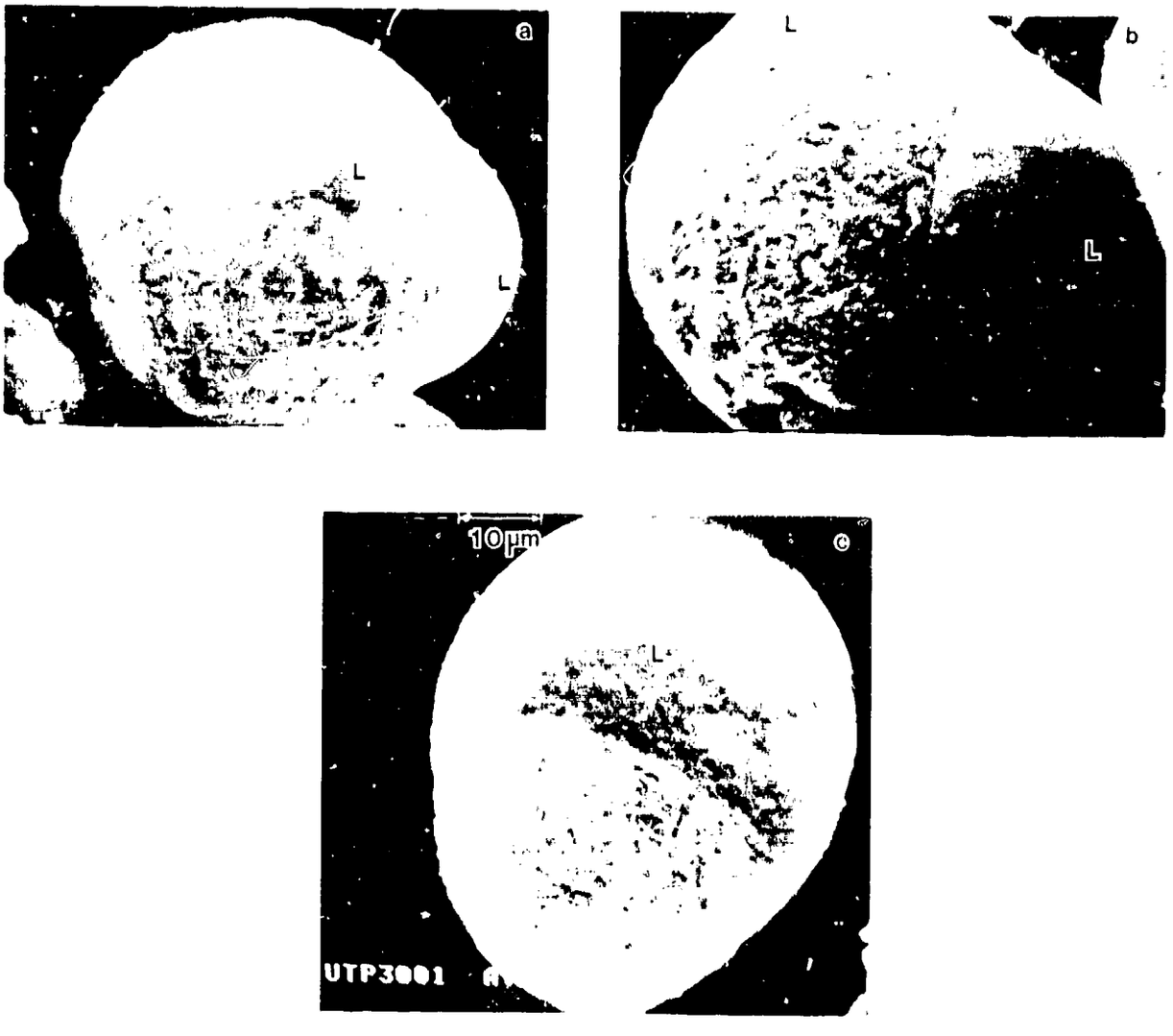

Fig. 12 Comparison of agglomerates at different quench distances, illustrating growth of relative size of the oxide lobe (test pressure 1 atm). The smooth lobe (denoted by L) is oxide. a) 1.5 cm; b) 10 cm; c) 30 cm.

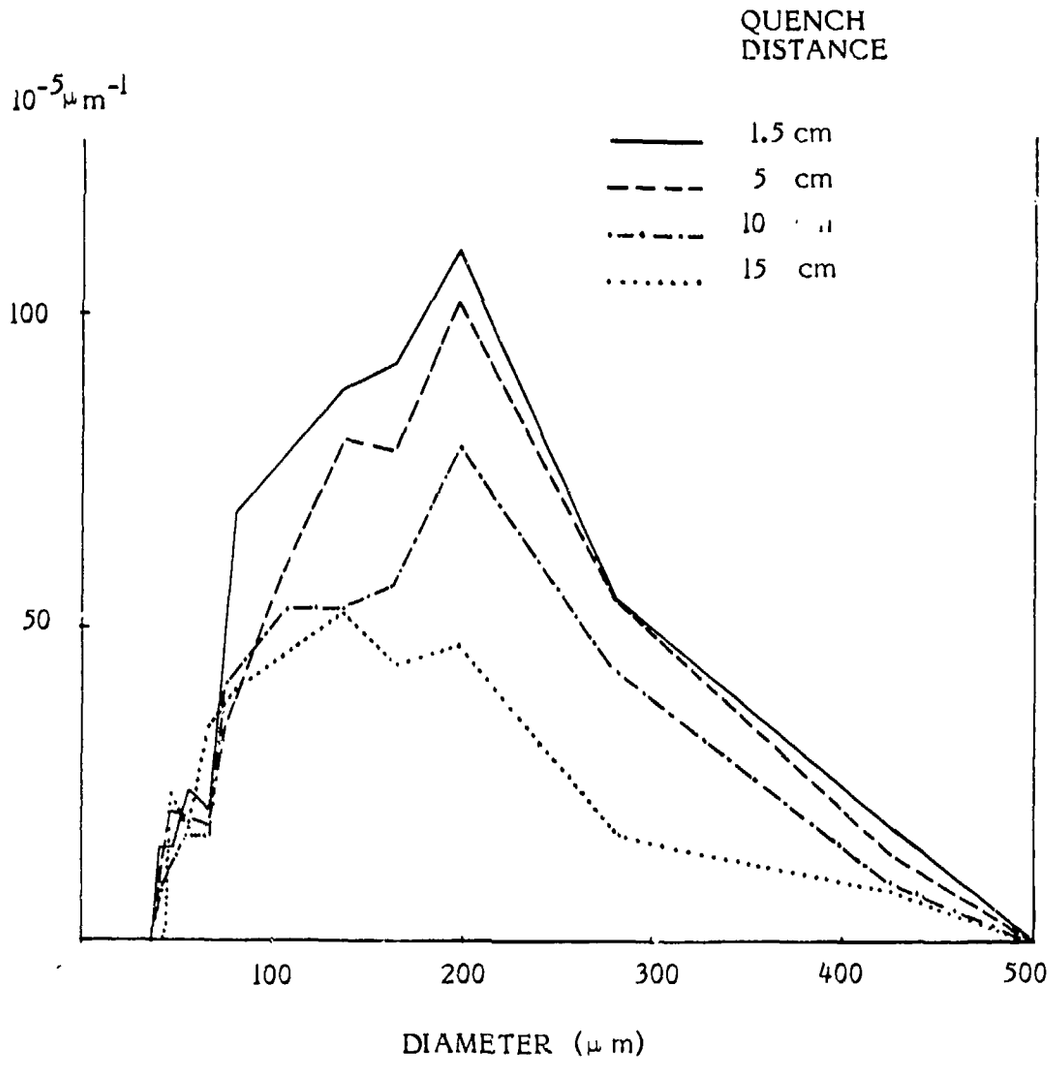

Fig. 13 Mass size distribution of agglomerates at four different quench distances (Thiokol 1780-1, 0.7 MPa test). The ordinate scale is mass per micron per initial aluminum mass.

(including oxide on the agglomerates, but excluding oxide particles). It is interesting to note that the size distribution curves don't change much with burning distance, although each particle is getting smaller and the total mass is decreasing. This relatively constant size distribution of the agglomerate population was noted earlier in an analytical study of burning agglomerate populations (Ref. 12), and is due in part to the nature of the original size distribution, and in part to the fact that some of the burned aluminum is retained on the agglomerate in oxide form, with weight gain due to the oxygen uptake. Some idea of agglomerate burning rate can be obtained from the curves in Fig. 13, in which the total agglomerate sample weight at a quench distance of 1.5 cm is about 32% of the original aluminum weight. Allowing for the weight of the oxide on the agglomerates in the sample, this corresponds to a combustion efficiency of about 78% at a distance of 1.5 cm from the propellant surface (0.7 MPa test). From estimates of flow velocity, this corresponds to 0.005 sec of burning, assuming the agglomerates started burning when they left the burning surface.

The actual aluminum combustion rate was determined by chemical analysis of the quenched samples obtained at different quench distances. The samples were analyzed for free aluminum content by dissolution in dilute HCl followed by a titration process to determine the aluminum content in the resulting solution. This measurement was made for several quench distances and for two propellants, and the results are shown in Fig. 14. These results are similar to those in previous reports on this study (Ref. 7, 13), but are considered to be more accurate because of a more accurate method for analysis of aluminum content, and elimination of igniter residue present in earlier tests. For completeness, the results of the previous tests are presented in Fig. 15 and 16. While results in these latter figures indicate an artificially high free aluminum content, the error is only about 20% of the indicated values, and the error is relatively insensitive to other test variables. The results thus provide valid trends with pressure and formulation variables. Systematic testing of the effect of relevant variables is continuing, using the improved method of Fig. 14. The collected results to date (Fig. 13 - 16) indicate:

1. An initially rapid decrease in unburned aluminum (high aluminum consumption rate), which presumably reflects burn-up of the smaller agglomerates and unagglomerated particles.

2. A drop-off in combustion rate, to a rather low rate by 10 cm from the burning surface, reflected in quenched samples consisting of agglomerates

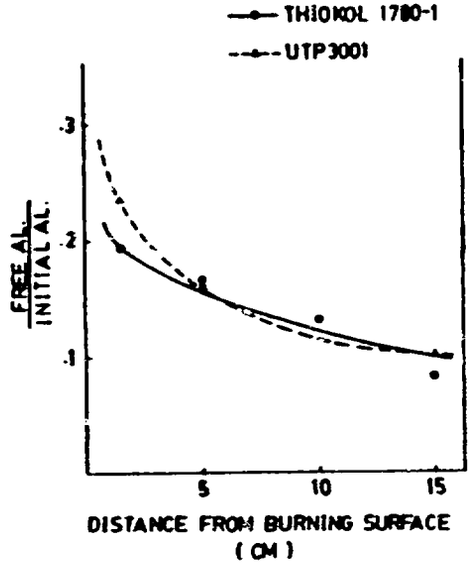

Fig. 14 Unreacted aluminum remaining at various quench distances. Tests using titration method of aluminum analysis and "clean" ignition. The ordinate is fraction of original aluminum remaining.

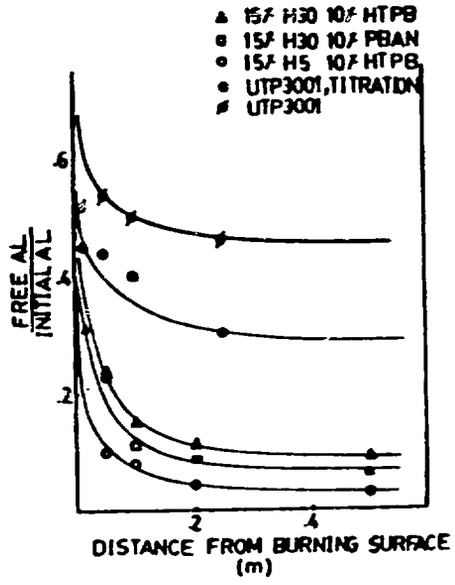

Fig. 15 Unreacted aluminum remaining at various quench distances with various propellants. Atmospheric pressure tests. Lower three curves are for propellants with 10% binder; 15% Al; 75%, 100 μm AP. All tests in this figure used ignition and chemical analysis procedure that gave a positive error in aluminum content of about 20%.

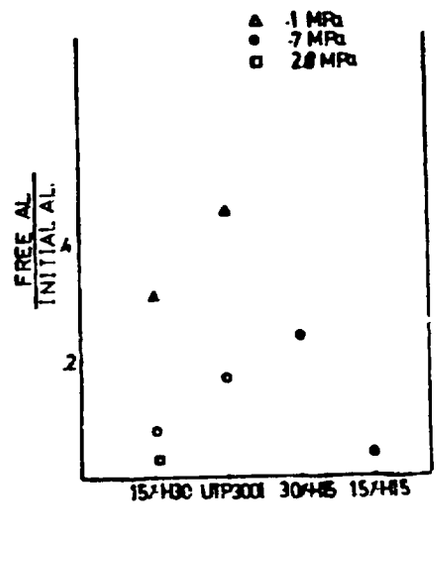

Fig. 16 Unreacted aluminum remaining at 1.5 cm for different propellants and pressures. Propellants are 10% HTPB binder; 15% Al; 75%, 100 μm AP; except as noted. Results include bias described in Fig. 15.

that now have relatively large oxide lobes.

3. A significant dependence of the observed aluminum level on propellant and test variables (Fig. 15,16).

Discussion of Chemical Analyses Results, and Outstanding Issues Regarding Agglomerate Population

The foregoing results are qualitatively consistent with the agglomerate size distribution effects in Fig. 13 and with earlier calculations of burning of droplet populations (Ref. 12). However, the results raise a number of questions that are the objects of continued study. Some of the questions relate to combustion mechanisms, and some relate to available experimental methods, which are only marginally adequate for quantitative work. These questions merit some discussion.

On the fundamental side, relatively little is known about the roles of the various oxidizing species present in the propellant combustion environment, and how they affect aluminum combustion. This means that the relevance of much past research on aluminum combustion is uncertain. Likewise, relatively little is known about the combustion of aluminum droplets with the large oxide accumulation typically present in the latter part of burning of agglomerates (e.g., beyond 5 cm quench distance in Fig. 14). Little is known about combustion of any aluminum droplets in the fuel-rich, high temperature conditions present in the propellant combustion environment at locations where the larger oxide-loaded agglomerates complete their burning. These conditions of oxide-burden and low oxidizer concentration are not very favorable for burnup of large agglomerates, and this is no doubt a factor in the "tail-off" of the curves in Fig. 14. It is also the key to the question of aluminum combustion efficiency in motors, since it is this prolonged phase of combustion that might not go to completion in a rocket motor. In this connection, one would anticipate that the outcome in the rocket motor would be quite sensitive to such variables as aluminum agglomeration, propellant stoichiometry, pressure, convective flow situations and motor stay time. These trends are implied by results of the present experiments, and generally recognized by developers of high performance motors.

Regarding the adequacy of the quenching experiment, the more serious limitations are most manifest in the same "tail-off" region that controls combustion efficiency. At low pressures, experiments are appreciably non-adiabatic and the temperature tends to drop off in the flow away from the

propellant surface even while the aluminum is still burning (Ref. 14). This is presumably due in part to the very effects one is anxious to study; retardation of reaction rate by depletion of oxidizing species and encroachment of oxide on the agglomerate surfaces. Under some conditions, the agglomerate temperature apparently falls below the oxide freezing point, a situation that virtually arrests agglomerate burning. At this point in the laboratory experiment the simulation of the nearly adiabatic rocket motor environment is totally broken down. This situation appears to have happened in the case of atmospheric pressure tests on UTP 3001 propellant shown in Ref. 7 and Fig. 15, in which combustion of aluminum seems to have ceased at about 55% burned (top curve). Visual examination of samples in this particular test sequence shows little change in appearance of agglomerates beyond 5 cm. In an earlier study (Ref. 14) of this same propellant in a similar, but larger, experimental apparatus (lower proportional heat loss), the agglomerate combustion rate at atmospheric pressure was also low, but did not appear to be arrested. Likewise, there is no evidence of arrested burning of agglomerates at higher pressure (Fig. 14), or in the service rocket motor. Thus the apparent cessation of agglomerate burning in the atmospheric pressure tests on UTP 3001 propellant seems to reflect poor simulation of rocket motor behavior late in agglomerate burning, aggravated in this case by the low pressure of these tests and relatively poor stoichiometry of this particular propellant (16% binder). As can be seen in Fig. 14, the combustion efficiency is much better at 0.7 MPa (100 psi), and a similar pressure dependence is evident with the other propellants noted in Fig. 16.

In the determinations of unreacted aluminum in the quench samples, the procedure was revised part way through the studies summarized in Fig. 14-16. Also a change was made in sample ignition method that affected results somewhat. While tests are now being re-run with the improved procedures, some of the results (most of Fig. 15 and all of Fig. 16) are based on tests by the "old" method. The trends in those tests are valid, but indicate artificially high aluminum content (and incorrect characterization of oxide products, as noted later). The original procedure for aluminum analysis was to dissolve the aluminum in HCl, wash it away, and compare dry sample weights before and after aluminum removal. It was later decided that this procedure was removing some of the oxide as well (see later), giving an indicated aluminum content higher than the true value. A further source of error resulted from use of an igniter paste on the propellant samples that

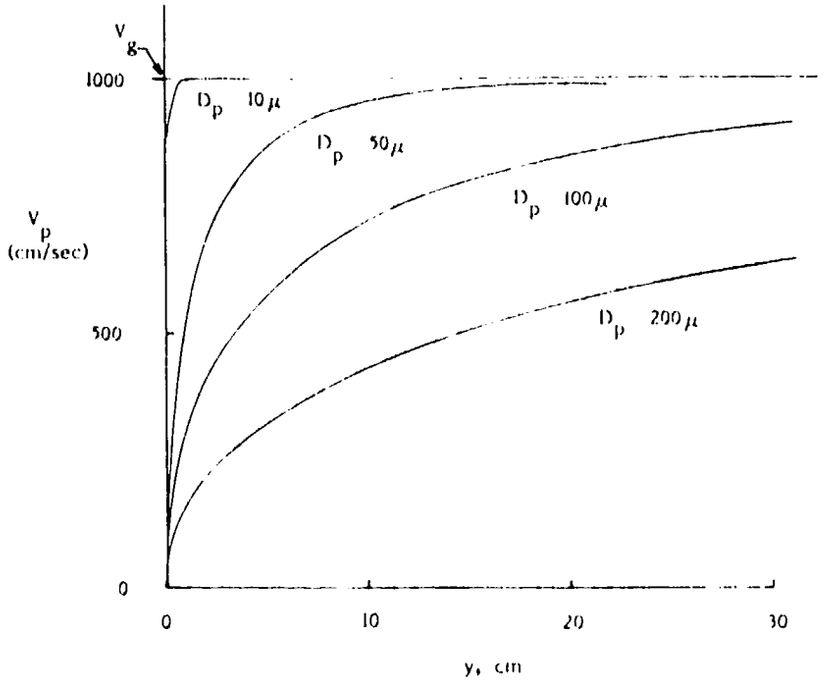

Fig. 17 Agglomerate velocity vs distance from the burning surface (calculated, see Ref. 12).

contained titanium and boron. The data in Fig. 15 and 16 are affected by these error sources, but were included because the error is only about 10-20%, and the repeat tests were not completed at report time. The tests summarized in Fig. 14 used a nonmetallized igniter paste, and an improved method of determining free aluminum content that measured the amount of aluminum directly rather than by weight differencing.

One further experimental problem, applicable particularly to short quench distances and fast-burning samples, is related to determination of the actual time-to-quench. As noted in Ref. 12, large agglomerates do not come up to speed as fast as small ones when they leave the propellant surface. (Fig. 17 shows the result from Ref. 12, which is for an upward flowing plume.) Further, the actual distance to quench depends on undetermined details of the alcohol behavior during the test. Finally, at higher pressures, the burning rate increases producing a higher mass flux in the tube. Correspondingly, the density and velocity of the gas flow change. Thus even small particles which convect at the gas velocity would experience different burning times if quenched at the same distance at different pressures. The problem of nonuniform, nonconstant velocity near the propellant surface is common to all quench experiments; but could be circumvented by use of

complementary combustion photography tests if deemed sufficiently important. The problem of uncertainty about the site and details of the quench event is being attacked by a modified design of the experiment that controls the location of the alcohol surface. In the present work, testing at high pressure would have been more extensive if these problems could have been resolved. Regardless of quantitative problems, such tests did provide comparative results at different pressures, and provided information on pressure effects on the detailed nature of agglomerates and oxide products, described in the following.

Nature of Agglomerates

In discussing combustion of aluminum agglomerates, it is often assumed for convenience that they are aluminum droplets, or aluminum droplets with oxide lobes. Experimental investigators are generally aware that the agglomerates are much more complex (Ref. 14, 15). These added complexities may not be important during much of the burning period of the agglomerate, but they merit study for at least two reasons. First, they provide information about how agglomerates are formed. Second, the complexities become important in the later, slow burning part of the agglomerate burning history, and the transition to residual oxide droplets.

The external appearance of quenched agglomerates was shown in Fig. 12. The trend with burning time is qualitatively independent of the initial agglomerate size, pressure, and propellant formulation, except under marginal conditions noted before, when the agglomerate droplet temperature drops low enough to allow flame collapse and oxide freezing. Examination of the interior of normal agglomerates reveals a relatively complex structure (Ref. 7). Cleaved agglomerates show voids, of non-characteristic shape, size and location (Fig. 18). Voids are larger in low pressure tests and early in burning, and usually include one under the oxide lobe (making it somewhat like a bubble early in burning). Agglomerates from atmospheric pressure tests are fairly soft, while agglomerates from tests at higher pressure are brittle and don't cut easily. These trends have not been studied thoroughly (e.g., as a function of propellant composition). Void volume was generally less than 15% of agglomerate volume, except in atmospheric pressure tests.

Another feature of the interior of the aluminum lobe of the agglomerate is revealed by careful acid etching to remove the aluminum. It is found that the interior contains an intricate structure of oxide flakes (See Fig. 11.). These

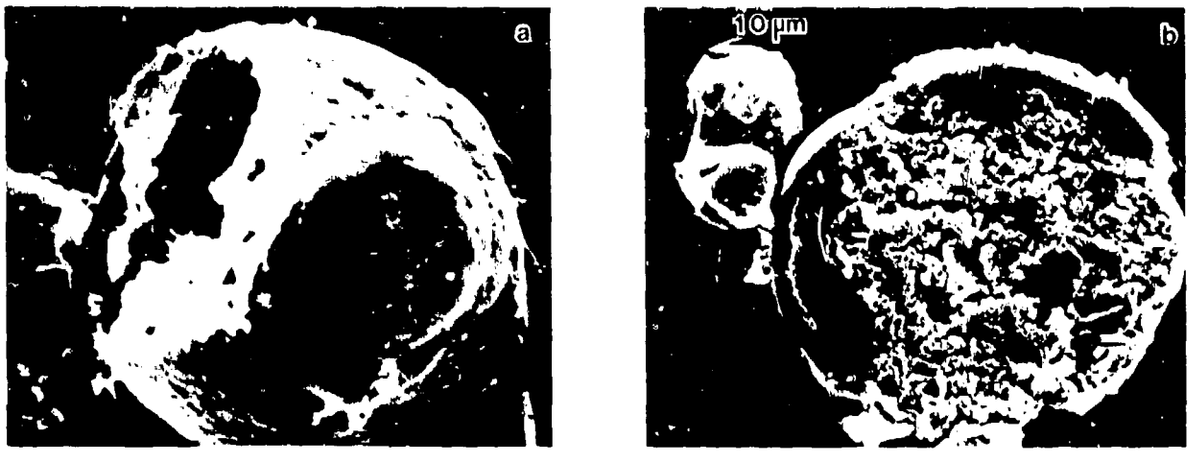

Fig. 18 Agglomerates cleaved to show interior.
a) Soft agglomerate from atmospheric pressure test.
b) Brittle agglomerate from test at 2.8 MPa.

structures are not recognizable in cleaved samples, but are evidently responsible for the brittle quality of agglomerates from quench tests at elevated pressure. The flake structure is much more extensive in agglomerates from tests at elevated pressure.

The inhomogeneous nature of the aluminum section of the agglomerate poses two practical questions suggested above. First, does the inhomogeneity have any significant effect on combustion? Is it telling us something about formation of agglomerates? The answers are speculation at present. As indicated in Fig. 9-11, the agglomeration event involves the melt-down and coalescence of a very complex structure, under the influence of surface tension forces of the molten aluminum. It seems likely that this event would trap some solid oxide shell structures in the interior of the agglomerate, and that this insoluble oxide would change during inflamation, into thin molten films in the interior of the agglomerate. If the melt-down and coalescence of the accumulate is gradual enough (e.g., at low pressure), the aluminum probably withdraws into a sphere with the oxide changing from a solid aggregation on the surface to a molten oxide lobe. At higher pressure, coalescence is more abrupt, and more oxide aggregate is trapped inside the

agglomerate. The test results suggest that trapped aggregate is first converted to very thin oxide sheets, insoluble in the molten aluminum, which become concentrated as the aluminum evaporates away. If the agglomerate is quenched, the films apparently freeze into the flake arrays noted above and in Fig. 11. It seems likely that it is these flakes that make agglomerates brittle.

Regarding the voids in the agglomerates, there is no direct evidence as to their source. They may be blown by aluminum vapor, or possibly formed by gas entrapment during coalescence as suggested by agglomerates frozen during coalescence (Fig. 10). Given the complexity of the accumulate, the coalescence event and the gaseous environment, there is no shortage of hypotheses. There is no clear evidence that the voids affect burning, except as they affect agglomerate surface area to mass ratio. They will cause agglomerates to weigh less than would be judged on the basis of visual (motion picture) observations of diameter.

The aluminum agglomerate is typically characterized as an aluminum droplet with an oxide lobe as in Fig. 12. Actual characterization of the oxide lobe has proven to be difficult because its character changes during burning, is different at different pressures, and depends on the propellant. In general, the oxide lobe appears to be more well defined in low pressure tests. This is very likely due to greater pre-ignition oxidation of accumulates at low pressure, and more complete coalescence of the oxide into a lobe (as opposed to formation of flakes in the aluminum lobe) at low pressure. The oxide lobes increase in size during agglomerate burning at low pressure, and tend to change from transparent to white as burnout is approached (inferred from agglomerate size distribution trends and detailed agglomerate features). The data at higher pressure are too sparse to identify trends, but oxide lobes on agglomerates are less conspicuous, suggesting that more of the oxide is inside the agglomerate and/or that less oxide is formed or retained on the agglomerate.

It is relevant to raise the question of final fate of an agglomerate that is near burnout, and dominated by the oxide lobe (Fig. 19). During burning, the flake oxide is concentrated in the contracting aluminum lobe, and may concurrently be reduced to lower oxides and/or flow into the oxide lobe (or neither). During this burnout stage, the state of the droplet's flame envelope is a matter of speculation. The fragmentation events observed in many studies in non-propellant environments apparently do not consistently occur, because oxide droplets continue to be added to the population in sizes comparable to the residual oxide in the agglomerate that are burning out. This will be examined in greater detail in the next section.

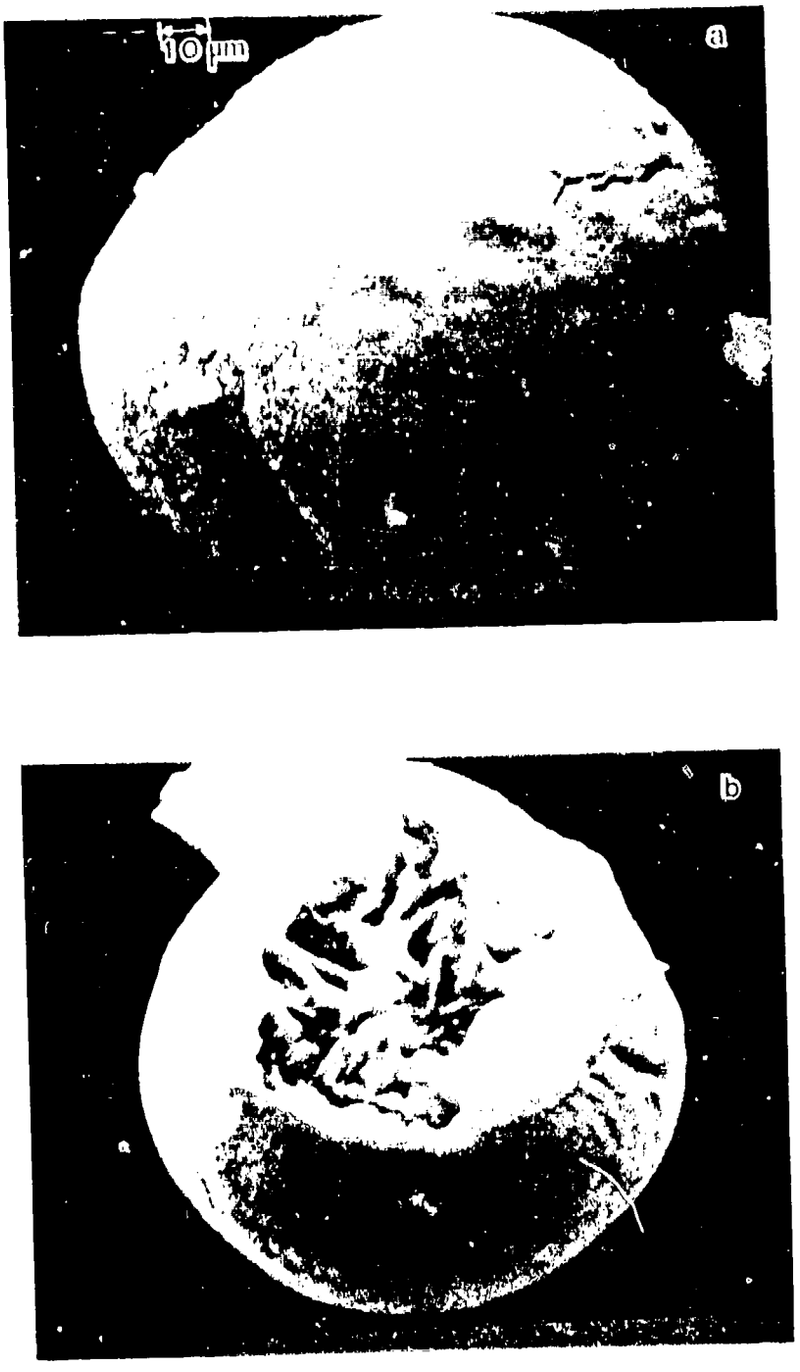

Fig. 19 Agglomerates quenched near burnout. Atmospheric pressure tests.
a) As quenched.
b) Acid-etched.

PRODUCT ALUMINUM OXIDE PARTICLES

It has often been noted (Ref. 16-18) that burning of aluminum droplets leads to two kinds of oxide product droplets, i.e., "smoke" formed in the flame envelope of the aluminum droplet, and "residual oxide" droplets left over when the agglomerates burn out. These are two entirely different populations of droplets, the former being generally less than two microns in diameter and the latter being substantially larger. Being governed by different formation processes, their size distributions are subject to entirely different constraints. In particular, the residual oxide droplet size distribution is linked to the agglomerate size distribution, and hence to all the processes discussed above that govern agglomerate size.

The importance of the combustion-generated size distributions was noted earlier. The effects on combustor stability, component erosion, thrust loss, etc., depend on the details of the size distribution. The effects cannot be fully characterized in practice without consideration of subsequent population changes in the combustor and nozzle flow, a subject beyond the scope of the present study. However, calculations of populations in the flow field cannot be made properly without use of correct starting populations, which are the combustion-generated ones discussed here. Particular attention was paid here to the residual oxide droplet population because, although it represents only 5-20% of the total oxide, its role in motor performance problems is relatively large, relatively unpredictable, and closely related to other aspects of the present study.

Kinds of Oxide Particles and Size Trends

Quenched samples yield a variety of particles other than agglomerates. After all the smoke particles are washed away (separated from the larger particles by repeated sedimentation-decanting operations), the remaining particles consist of white oxide spheres, transparent oxide spheres, and various debris originating from igniter materials and carbonaceous binder residue. In previous reports (Ref. 7, 13), reference was made to black shiny spheres thought to represent a burnout transition state between agglomerates and white oxide spheres. These have been found to be a product of the igniter paste, used in those tests, that contained titanium and boron. While black shiny product spheres have been reported in the past from tests that did not use such igniter materials, none have been obtained in recent

tests on this project using a nonmetallic igniter paste.

In this report, the combination of white and transparent oxide particles and of oxide contained on and inside agglomerates is referred to collectively as "residual oxide", because it consists of that oxide that is believed to be converted to relatively large "non-smoke" oxide when agglomerates burn out. White and transparent oxide particles are the product of those agglomerates that are already burned out. Their external appearance is illustrated in Fig. 20. The transparent oxide particles represent a relatively small portion of the residual oxide. They are generally less than 35 μm, and of smaller average size than the white oxide particles. The size distributions of the oxide particles is illustrated by Fig. 21. These results correspond to the agglomerate size distributions in Fig. 13. The ordinate in Fig. 21 is normalized by a mass corresponding to complete oxidation of all of the aluminum in the propellant sample, referred to below as "ultimate" oxide. Thus, the curves corresponding to longer quench distance have larger ordinates; the area under each curve is indicative of mass fraction (of ultimate oxide) in the particular sample. The jagged nature of the curves is due to the rather crude method of determining the mass in different size intervals. The method consists of sieve-sizing the test samples, weighing the size fractions, and visually determining the relative number of agglomerates vs oxide particles in each size interval. No correction was made for difference in density of particles.

From the particle size distributions, it appears that particles on the small end of the distribution (transparent oxides, typically 20-25 μm continue to be formed as the flow moves away from the burning surface. This suggests that the small transparent oxide particles are not simply the residue of burnout of the smaller aluminum droplets (in fact very few oxide particles are present in samples quenched 1.5 cm from the burning surface). Since the transparent oxide particles continue to be formed further downstream, they can presumably be produced from the initially large agglomerates remaining further downstream, possibly by expulsion during burnout, or by fragmentation. At the same time, increasingly larger oxide particles (white oxide) are added further downstream, indicating that the initially large agglomerates that burn out further downstream make larger residual oxide droplets as well. At this point it is not determined whether the continued growth of both ends of the size distribution is a consequence of alternative modes of agglomerate burnout, or a mode of burnout that typically produces both kinds of oxide particles.

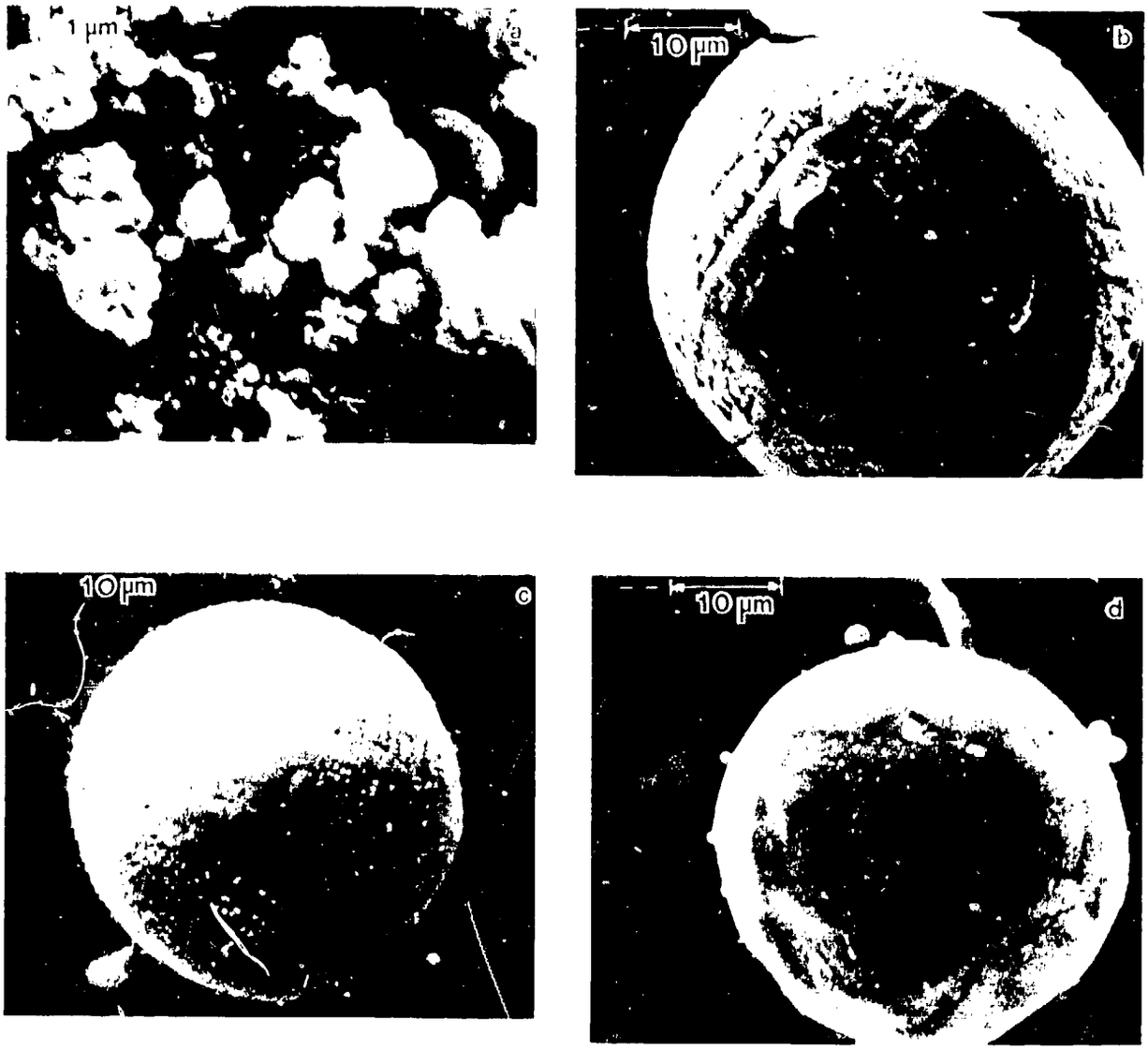

Fig. 20 Exterior appearance of oxide particles.
a) Smoke oxide (2.8 MPa test).
b) White oxide (atmospheric test).
c) White oxide (2.8 MPa test).
d) Transparent oxide (2.8 MPa test).

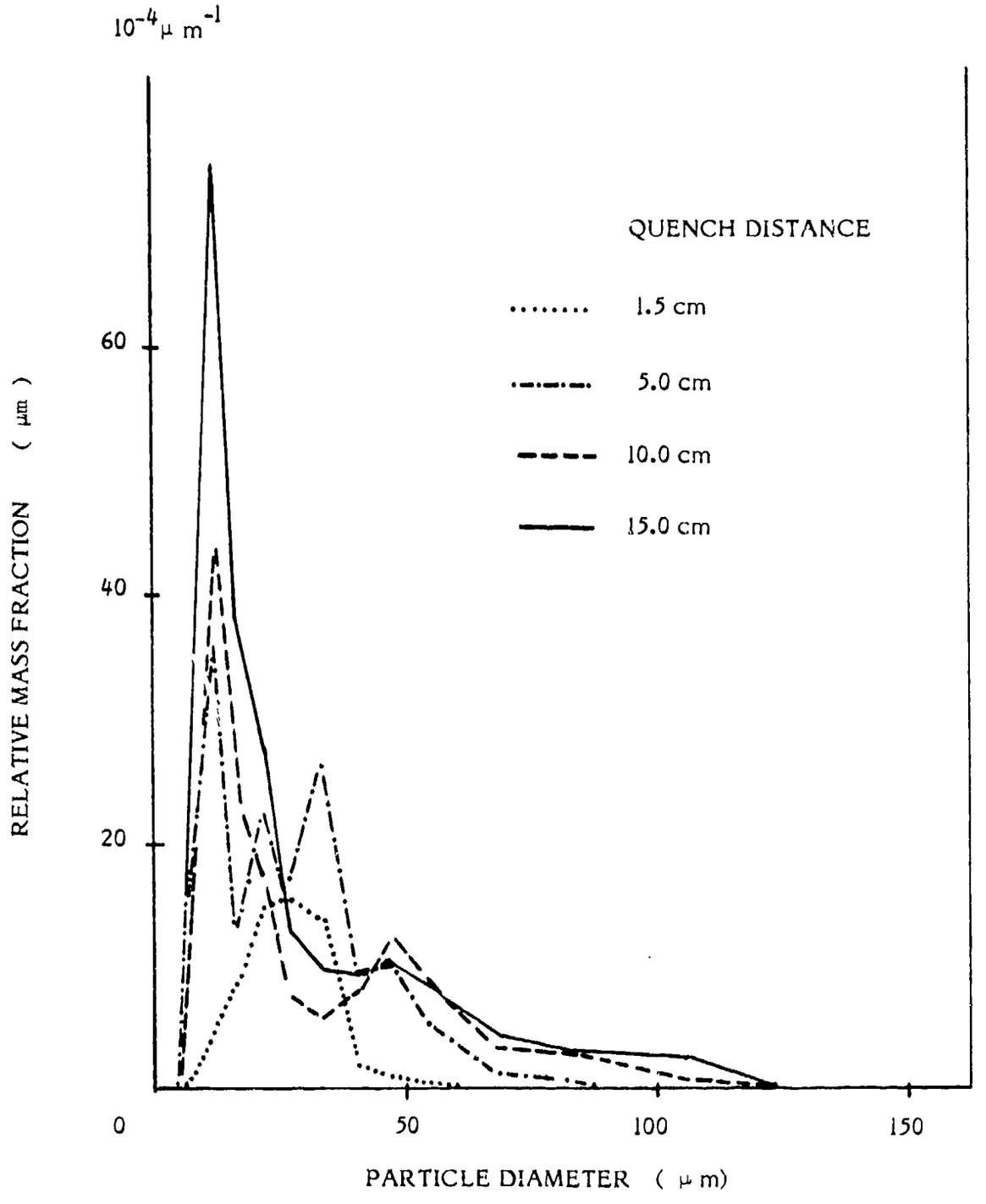

Fig. 21 Oxide particle size distribution; Thiokol batch 1780-1, test pressure 0.7 MPa. (Smoke "oxide" was removed from samples. Mass fraction is based on mass compared to oxide that would result from conversion of all original aluminum.)

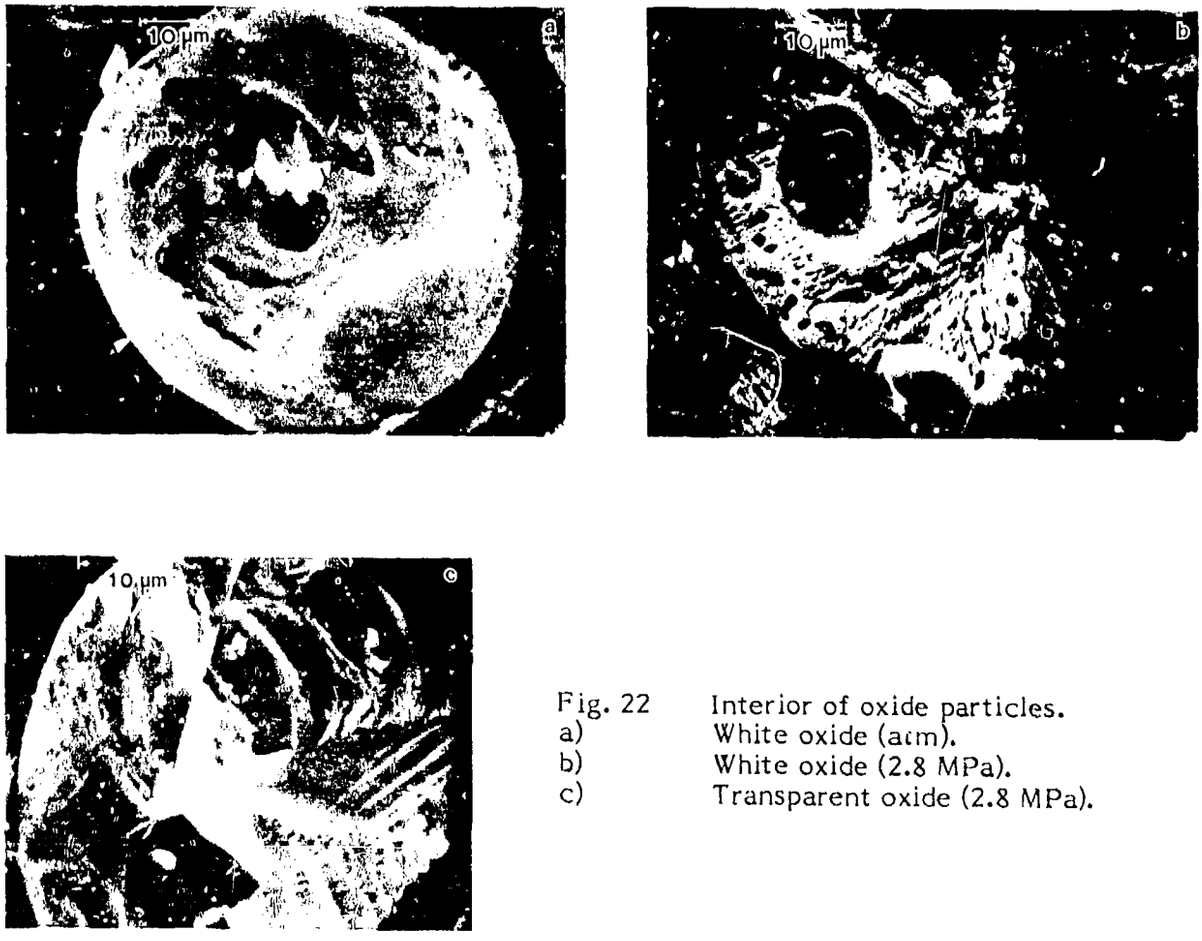

Fig. 22 Interior of oxide particles.
a) White oxide (atm).
b) White oxide (2.8 MPa).
c) Transparent oxide (2.8 MPa).

Detailed Nature of Oxide Particles

The nature of oxide particles was examined by microscopic study of the exterior surface, and of the interior as revealed by broken particles. Particles were subjected to acid etching and to observation during heating to 1200°C. The exterior appearance of the particles is shown in Fig. 6 and 20. White oxides are nearly spherical, but show surface striations suggestive of crystallization patterns (especially at atmospheric pressures). In an optical microscope, transparent oxides look like glassy spheres, but SEM's show them to be slightly irregular in shape.

The interior nature of transparent oxide particles is glassy and void free (Fig. 22). The interiors of white oxide particles are extraordinarily complex (Fig. 22), with a typically sponge-like structure. White oxide particles recovered from atmospheric pressure tests are often hollow with nearly 40% void. The appearance

is believed to be a consequence of conversion of the oxide-capped, flake-containing agglomerates during the slow burning and burnout phase of the agglomerates. The oxide lobe and flake oxide apparently do not coalesce completely into a homogeneous droplet, even though surface tension seems to close the exterior surface. This interpretation of the origin of white oxides is consistent with the appearance of agglomerates captured in the late stage of burning.

The oxide particles show no reactivity when placed in 3% HCl in water for prolonged periods of time. The particles show no change when heated to 1200°C in argon or oxygen.

Relative Mass of Different Forms of Oxide

In the present studies, the oxide reaction products have been classified as either "smoke" or "residual". The former constitutes the majority of the oxide, is in particle sizes under 2 μm, and is produced in the detached flame envelope around the burning agglomerates. In the experiments reported here, these particles were not subjected to detailed study. They are only partially captured in the quench experiment and were removed from the sample to facilitate study of the agglomerates and residual oxide. The total weight of smoke oxide could be determined by mass balance, since all other weights were measured. Smoke masses so determined are reported in the following.

The term "residual oxide" refers to all the oxide remaining in the sample after the repeated washing (sedimentation and decanting) operations. This includes transparent oxides, white oxides, and oxide on and in the agglomerates. The oxide on and in the agglomerates consists of the oxide lobes, flake oxide, and surface oxide (surface oxide probably is minimal except under adverse burning conditions). In a previous section, it was noted that the mass of unreacted aluminum was determined by a solution-titration method. The mass of residual oxide was taken to be the difference between the initial weight of the washed sample and the unreacted aluminum weight so determined. The smoke oxide mass was then determined as the difference between the total oxide (based on the mass of aluminum consumed) and the residual oxide weight. Fig. 23 shows the trend of residual and smoke oxide with quench distance for several test conditions (masses have been normalized by dividing by the mass of the total oxide that would result from oxidation of all of the aluminum in the test sample). Also shown is the ratio of residual oxide to smoke oxide for the tests reported. The trend of oxide masses

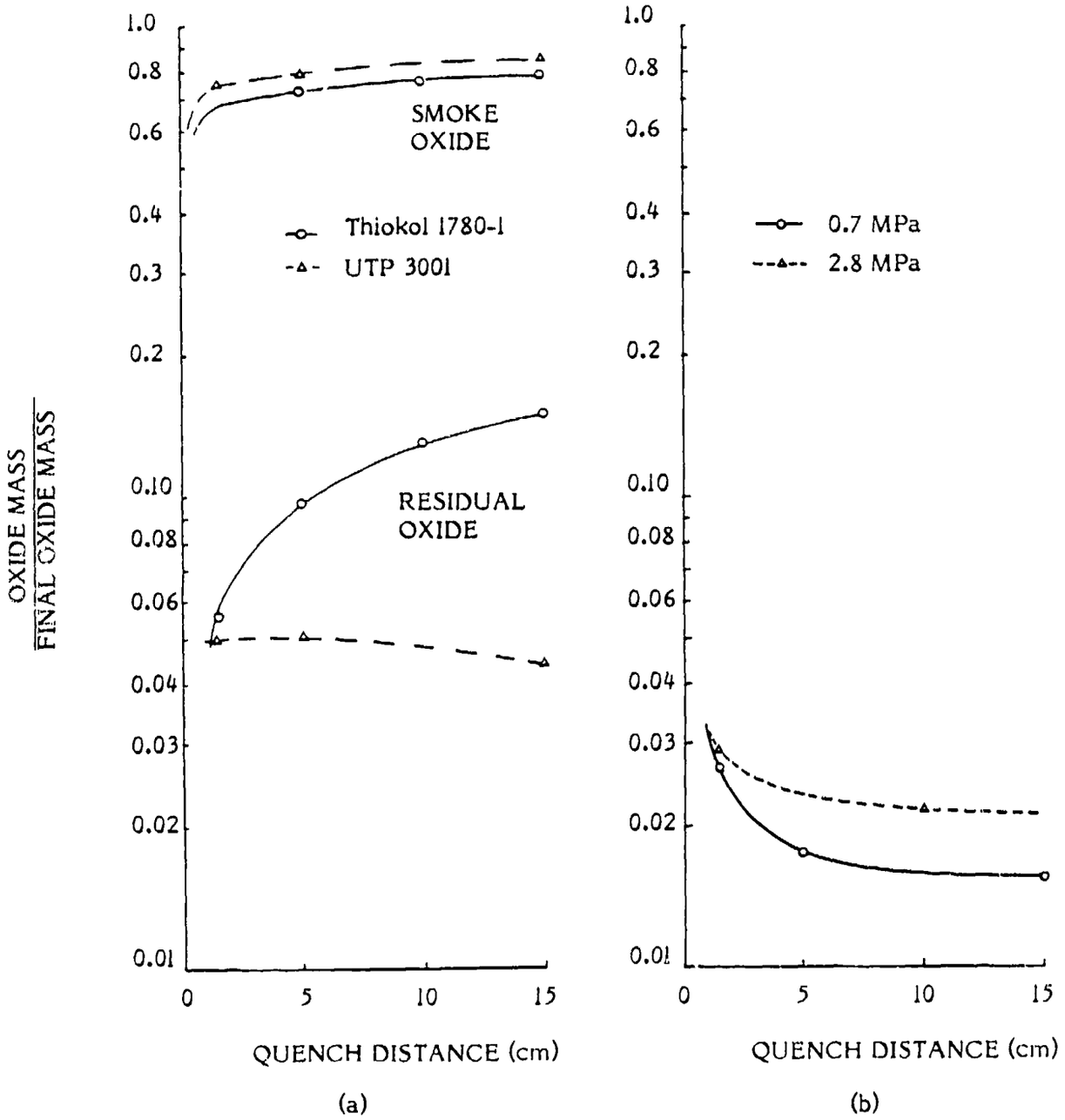

Fig. 23 Oxide mass fractions vs quench distance.
a) Smoke and residual oxide for UTP 3001 propellant and Thiokol batch 1780-1, test pressure 0.7 MPa.
b) Mass fraction of residual oxide in flake form for UTP 3001 propellant at two pressures.

with quench distance simply reflects the consumption of aluminum shown in Fig. 14 and 15. The trend at large distances is pressure and propellant dependent, but indicates that final residual oxide totals 5-15% of oxide formed and smoke 95-85%. The ratios of residual oxide to smoke oxide are slightly dependent on pressure and quench distances, although it appears that the nature of agglomerate combustion is not critically sensitive to time during agglomerate burning or other conditions. On the other hand, it is clear from collected results that instances of rapid consumption of aluminum correspond to conditions that produce small initial agglomerate size, and that the size of the white oxide particles is then correspondingly small.

One further aspect of the quenched samples was examined by determinations of mass fraction, i.e., the relative amount of residual oxide in flake form, and in consolidated (i.e., oxide particles and lobe) forms. It was found that the structure of the oxide flake was so delicate that it would break up during acid etching of agglomerates and as a result could be carried away in the washing operation. Oxide samples remaining were weighed, and the mass was compared with the higher total residual oxide masses indicated by the acid dissolution-titration method. The difference in the two masses was assumed to correspond to the mass of flakes removed in the acid etch-washing operation. While this method gives somewhat erratic results for flake mass, some useful results are evident. In interpreting results, it should be remembered that the flake oxide is distinguishable only when it is still dispersed in the aluminum lobes of agglomerate particles, becoming an indistinguishable part of the residual oxide particles upon burnout. In the plume, flake oxide is thus progressively converted to residual oxide as the smaller agglomerates burn out. At a quench distance of 1.5 cm, the indicated amount of flake oxide is roughly 1-4% of the "ultimate" oxide, suggesting that the mass of accumulated oxide engulfed during agglomerate formation is of this same order. This is an estimate of pre-agglomeration oxidation of aluminum on the propellant burning surface (the estimate is somewhat low, because even at 1.5 cm quench distance, some of the smaller agglomerates have burned out and converted their flake oxide to residual oxide). The argument that flake oxide is progressively converted to residual oxide by agglomerate burnouts is affirmed by the decreasing trend in flake oxide with increasing quench distance (Fig. 23). Flake mass also appears to depend on propellant composition and pressure, but present data are not sufficient to establish quantitative trends. A possible exception is the trends for

UTP 3001 propellant, which has shown unusually slow combustion of aluminum in the plume (Fig. 15). This propellant also shows low sensitivity of flake oxide mass to quench distance, and lower flake mass at higher pressure, probably both attributable to slow agglomerate combustion rate, improving with increasing pressure.

COMBUSTION OF DRY-PRESSED MIXTURES OF ALUMINUM AND AMMONIUM PERCHLORATE POWDERS

Combustion of the aluminum ingredient in composite hydrocarbon binder propellants is a consequence of the availability of oxidizing species provided by decomposition of the solid oxidizer. However, the detailed accumulation-agglomeration-metal ignition process is substantially determined by events other than molecular level oxidation. In order to unravel the roles of different steps in the propellant combustion process, it is helpful to determine just how much of the aluminum "metabolism" is due purely to interaction with the ammonium perchlorate oxidizer. It had been established before that aluminum could survive the environment on the surface of burning ammonium perchlorate for an appreciable time (Ref. 19, 20) without ignition, while there are some recent conflicting claims that intermediate reaction products of AP (present primarily in the AP decomposition-flame zone) might be particularly important to ignition of aluminum (Ref. 21). Previous work on the present project had confirmed a substantial body of literature (e.g., Ref. 22-24) concerning the protective character of the oxide "skin" on aluminum particles. Those collected results had indicated that temperatures in the range 1200 to 2030°C might be required to ignite particles. The AP flame would thus be marginal as an ignition source. However, the ignition requirements referred to in Ref. 22 to 24 were not determined in chemical environments typical of an AP deflagration wave, nor on assemblages of aluminum particles typical of propellant burning surfaces. Thus it was important to determine whether accumulating aluminum on an AP burning surface would adhere there (as implied by results in Ref. 11, 19, 25 and elsewhere), and if it would, whether it would sinter, ignite, and agglomerate.

In order to resolve these questions, combustion tests were run on hard-pressed (175 MPa) samples of Al/AP powder mixes. Tests consisted of interrupted burning by rapid depressurization, and combustion cinemicrophotography. Tests were run with different mixture ratios of Al and AP, different particle size combinations, different kinds of aluminum powder, and different pressures. A summary of test conditions is shown in Table I, and a description and interpretation of results was reported in Ref. 20. These results indicated the following critical points about aluminum behavior and Al-AP interactions:

Table I
Summary of Tests on Dry-Pressed AP/Al Mixtures*

Sample		85% 10 μm AP 15% 5 μm Al (H-5)	85% 60 μm AP 15% 30 μm Al (H-30)	85% 100 μm AP 15% 30 μm Al (H-30)			85% 100 μm AP 15% 95 μm Al (H-95)		
Pressure					Movie			Movie	
MPa	PSI	Movie	Movie	dp/dt Quench	Hi Mag	Lo Mag	dp/dt Quench	Hi Mag	Lo Mag
4.2	600			✓✓✓ ✓			✓✓✓ ✓		
5.5	800			✓	35	38		5, 9, 13	c
6.9	1000	55	57	✓✓✓	33	4	✓✓✓	1,10,14	

* Check marks denote tests. Number identify the pertinent film.

1. Aluminum particles do not ingite in the AP deflagration zone (propellant-ingredient-size particles).

2. Aluminum adheres to the deflagrating AP surface, and under most conditions accumulates there. Accumulation is very limited where the aluminum particles are comparable in size to the oxidizer particles; those (large) aluminum particles do linger on the surface, but the spacing of the particles is now large enough to reduce chances of a surface particle being joined by underlying particles as occurs with small Al particles.

3. Accumulation of aluminum on the AP surface leads to rigid assemblages on the burning surface that eventually break up and detach. Break-away is usually followed by local inflamation of the accumulate. This appears to occur at break points in the detaching crust, followed by spread into the rest of the crust.

4. The spreading inflamation leads to formation of several large agglomerates, that appear to burn thereafter much in the manner observed with propellants.

The foregoing observations were based on the motion picture tests. Quench tests yielded relatively little evidence of surface accumulation of aluminum, which apparently detached during the depressurization quench.

The test results are interpreted as follows, in the light of earlier tests on behavior of aluminum powders during heating (Ref. 5, 8, 26). Upon being reached by the receding surface of the sample, an aluminum particle adheres to the surface, which is generally believed to consist of a froth layer at a temperature of about 600°C. The particle probably proceeds to higher temperature under the influence of the nearby AP flame, while continuing to reside on the surface. Underlying aluminum particles emerge and join the original ones, concentrating into contacting arrays. The oxide skin on each particle apparently limits aluminum oxidation to a continuing build up of surface oxide. This includes sintering of the particles to each other when they are contacting. As the sintered layer becomes more dense and more heavily oxidized, it becomes resistant to flow of gas from the underlying AP, and also resistant to heat flow from the AP flame to the AP surface. Under these conditions, the layer would be expected to be above the aluminum melting point, and the structural strength would be due to the sintered solid oxide structure that encases the aluminum. This structure in turn is stressed by the gas through

flow, and the stage is set for break-up of the sintered accumulation.

Break-up of the accumulation implies local break up of the oxide that has been "protecting" the aluminum, which promptly increases its oxidation rate and locally heats the sintered structure. Under favorable heat-flow conditions, this can lead to progressive breakdown of adjoining sintered structure, i.e., inflamation. Alternately, aluminum exposed in a break may simply be covered over by new solid oxide, which the AP flame is unable to melt. Both alternatives apparently occur, sometimes in the same test. The inflamation alternative is believed to proceed as follows. A breaking section of the accumulate with exposed molten aluminum self heats due to oxidation of exposed aluminum. This is aided and sustained by limited flow of aluminum under surface tension forces, with associated continual mechanical degradation of any newly forming oxide skin. Heat release goes primarily to heat-up of those particles that are actually reacting, which are insulated from their colder, unignited neighbors by the very oxide that sinters them together. Local self heating melts the protective oxide locally, permitting local coalescence of aluminum "particles" (Fig. 10a), retraction of insoluble oxide from the metal surface, and establishment of a high temperature aluminum vapor flame (photographically manifested by rapidly increased brightness and establishment of the characteristic luminous smoke trail). This state is sometimes reached at more than one site in large accumulates, and leads to a rapid propagative heat-up, oxide melt-down, and inflamation of the accumulate and transformation to one or more burning agglomerates.

While the foregoing scenario is very complex, the observed combustion behavior is hardly amenable to a simple explanation. The interpretation rests on a great deal of information about the real behavior, including not only the combustion of AP/Al samples, but also on behavior of single aluminum particles and powders. The scenario explains why larger unsintered particles don't ignite (no means to break down the oxide skin); why heavier sintering and non-ignition can occur at lower pressure (low oxidizer concentration and poor heating from the oxidizer flame permit protective oxidation of break-up surfaces); and why vigorous combustion can occur when typically reluctant ignition is finally achieved (transition to vapor phase burning). The scenario also has major implications for aluminum behavior in propellant combustion:

1. Ignition of accumulating aluminum will generally depend on exposure to high temperature flames resulting from AP-Binder interaction (i.e., the AP flame alone is not enough). Conditions that delay this AP-Binder flame exposure will yield prolonged accumulation and large agglomerates.

2. Vigorous inflamation of accumulates on or near the burning surface is favored by large specific surface of aluminum (small particles), because the eventual breakup and coalescence of the accumulates at the surface is then a highly exothermic event. Large single aluminum particles ignite further from the surface because the protective oxide won't break down at temperatures near the burning surface, even when the particles linger long enough to heat up to surrounding temperature.

3. The size of agglomerates in propellant combustion is generally recognized to be strongly affected by the degree of segregation of aluminum particles in the propellant microstructure, with local concentrations ("pockets") of aluminum tending to form single agglomerates. It is also recognized that this criterion for agglomerate size is modified by the susceptibility of the accumulating aluminum to ignition, which event usually causes the accumulated aluminum to detach from the propellant surface. In this context it is important to keep in mind that the AP flame will not cause ignition, a fact that accounts for the massive accumulations on the surface of AP/Al samples. Under adverse ignition conditions, accumulated aluminum on the burning surface of propellants may also end up on the surface of oxidizer particles of the propellant and remain during all or part of the burning of the oxidizer particle. Under some conditions (notably low pressure), delayed ignition can even give rise to interconnection ("bridging") of local accumulations to give the more massive accumulations observed with AP/Al samples. In that case, correspondingly large agglomerates may be formed.

STUDY OF THE ACCUMULATION-AGGLOMERATION PROCESS USING AP-BINDER SANDWICHES WITH ALUMINUM FILLED BINDER

One of the primary problems in the study of accumulation and agglomeration of aluminum in a propellant is the chaotic nature of the propellant on the dimensional scale of the relevant processes. In effect, it is impossible to describe what was tested or what happened. On the other hand, some success had been achieved in a companion project to the present one, through testing sandwiches of AP and binder. A sandwich consists of two layers of pre-pressed sheets of ammonium perchlorate (oxidizer) with a layer of binder (fuel) of controlled thickness cured between the sheets. Such systems do not provide the intermittency of microstructure present with granular mixes but they simplify the geometry of the combustion zone and separate the ingredients of the propellant into precisely definable regions providing a better understanding of the flame structure and greater resolution by experimental methods. Using aluminum in the binder lamina provides a means to conduct controlled accumulation-sintering-agglomeration experiments in a combustion environment simulating critical aspects of real propellants.

The investigation of aluminum combustion in sandwiches consisted of preparing sandwiches with various combinations of binder, aluminum and oxidizer in the fuel lamina; edge burning the sandwiches at various pressures; and observing combustion behavior by photography and by microscopic study of quenched samples (quenched by rapid depressurization). Fig. 24 gives the matrix of test conditions used. Only a limited number of tests with photography were run, but quench tests were run at all the indicated conditions, and two tests were run at some test conditions to determine reproducibility.

Results of Sandwich Quench Tests

All test results described below were for binder lamina thickness between 60 and 90 μm. With pure binder laminated sandwiches, it is observed on quenched samples that the binder is slightly recessed at low pressure (1.4 MPa) and is protruding at high pressures (6.9 MPa) (Fig. 25) (Ref. 19, 27, 28). The AP burning rate adjacent to the binder is retarded, with the maximum regression of the surface occuring at about 100 μm from the interface. There are bands of relatively smooth AP surface running along the edges of the interfaces in all samples. These features

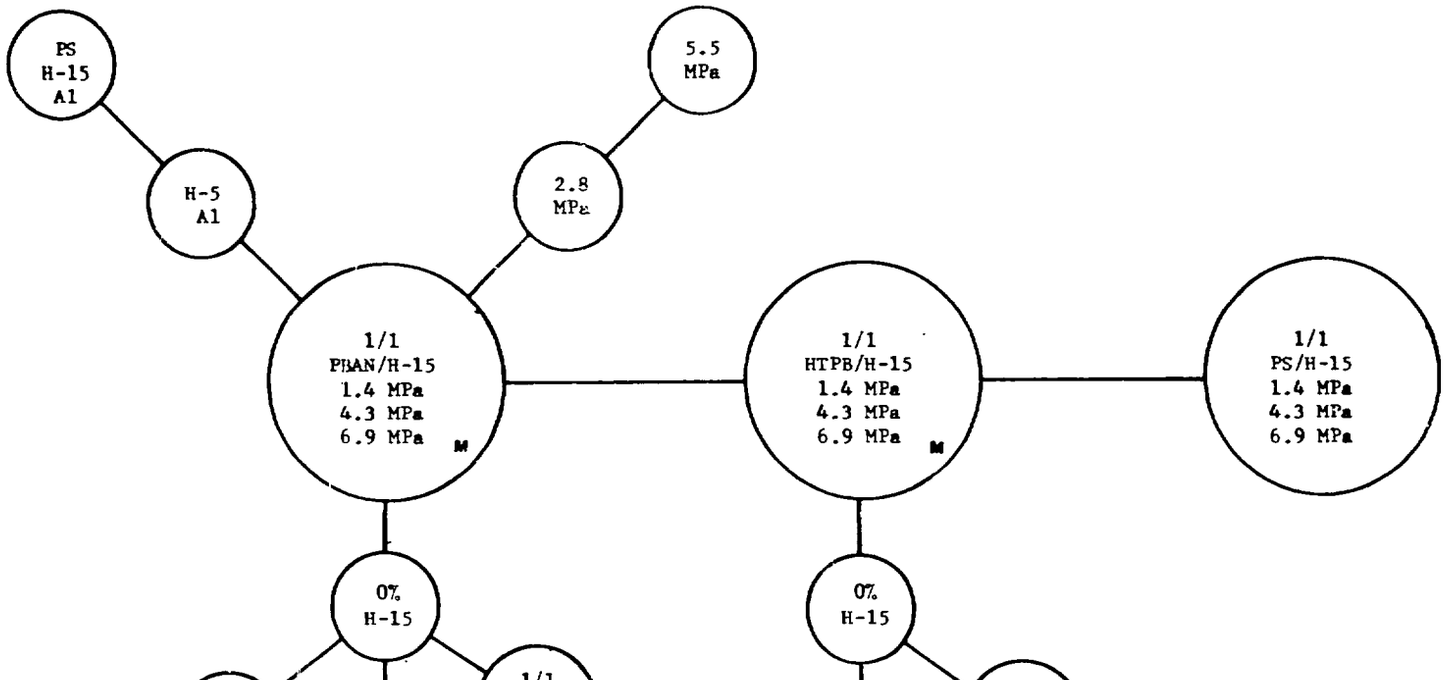

Fig. 24 Summary of conditions for sandwich burning tests (large circles denote primary burning tests (large circles denote primary conditions, small circles denote variants on primary conditions). (M denotes combustion photography.)

Fig. 25 Examples of quenched AP/PBAN sandwiches.
a) 1.4 MPa, b) 4.1 MPa, c) 6.9 MPa.

did not change with type of binder except that polysulfide has a drier appearance.

The general effect of addition of aluminum to the binder lamina is illustrated in Fig. 26 by samples with a 1/1, PBAN/H-15 Al lamina. The accumulated aluminum is visible on the binder lamina, and has the appearance of being wetted by molten binder. The volumetric loading of aluminum in the lamina is less than 50%, but the surface generally appears to have a higher concentration of aluminum. As noted later, some test conditions lead to occasional presence of dry accumulates and occasional agglomerates on the quenched surface, and some conditions lead to small accumulates or single aluminum particles on the oxidizer surface. In the example shown, the binder lamina is slightly recessed. The smooth bands on the AP surface adjoining the AP-binder interfaces are equally evident with aluminized laminae, and were present under all test conditions in this study. A tendency for the leading edge of the AP surface to be at a location some distance from the interface (i.e., interface AP protruding) was noted above for unaluminized sandwiches, and occurs also with aluminized binder (all tests with binder-Al, all pressures). Use of aluminized binder increased the burning rate in some tests (increased in the case in Fig. 26). In the following, the effect of various test variables are described in terms of the features noted above for aluminized PBAN sandwiches.

a) Effect of Pressure

In the sample case used in Fig. 26 (1/1, PBAN/H-15, at 4.1 MPa), increasing the pressure reduced the amount of distinguishable aluminum on the binder surface, as well as the amount scattered on the AP surface (almost none at 6.9 MPa). The wetted appearance of the aluminum concentrated on the binder lamina is evident at all pressures. with occasional areas of dry-sintered particles at low pressure. The surface profiles of the aluminized PBAN sandwiches (i.e., details near the fuel laminae) were alike over the pressure range 1.4 - 6.9 MPa, and similar to the unaluminized PBAN sandwiches at lower pressures. The trend of the nonaluminized laminae to protrude at higher pressure (Fig. 25) did not occur for the aluminized PBAN sandwiches (Fig. 27). In general, the overall sandwich burning rate appeared to be higher with aluminized PBAN sandwiches, a feature reflected in the overall sandwich profiles, which have more "Vee" shaped profiles.

The above observations of pressure dependence do not all apply for other binders, or other additions to the binder, as noted later.

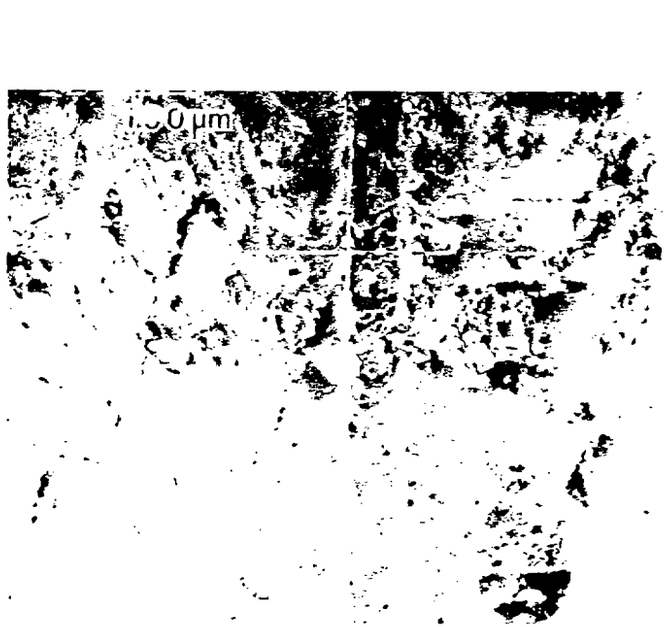

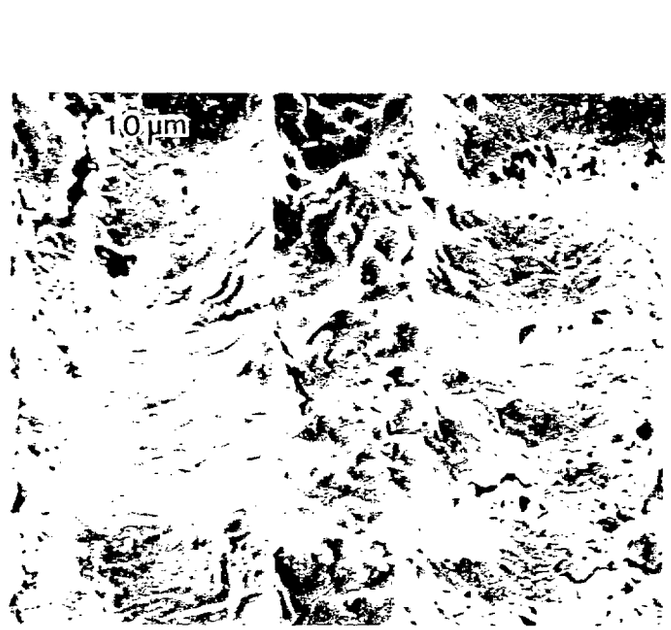

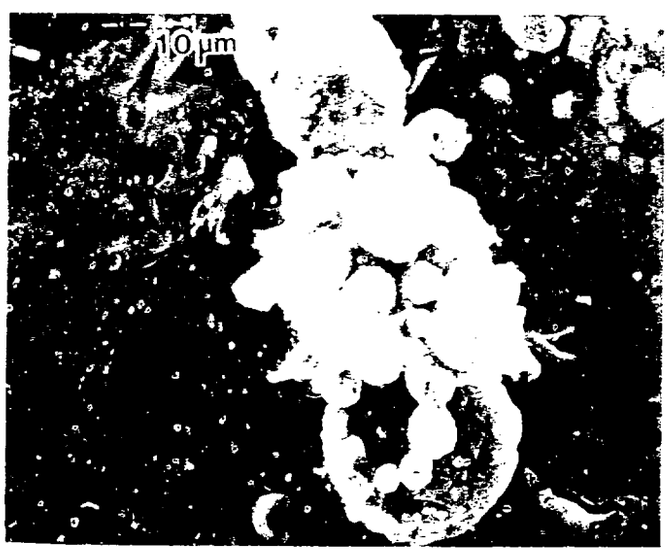

Fig. 26 Examples of quenched sandwich similar to Fig. 25b, but with fuel lamina 1/1, PBAN/H-15 Al, 4.1 MPa.

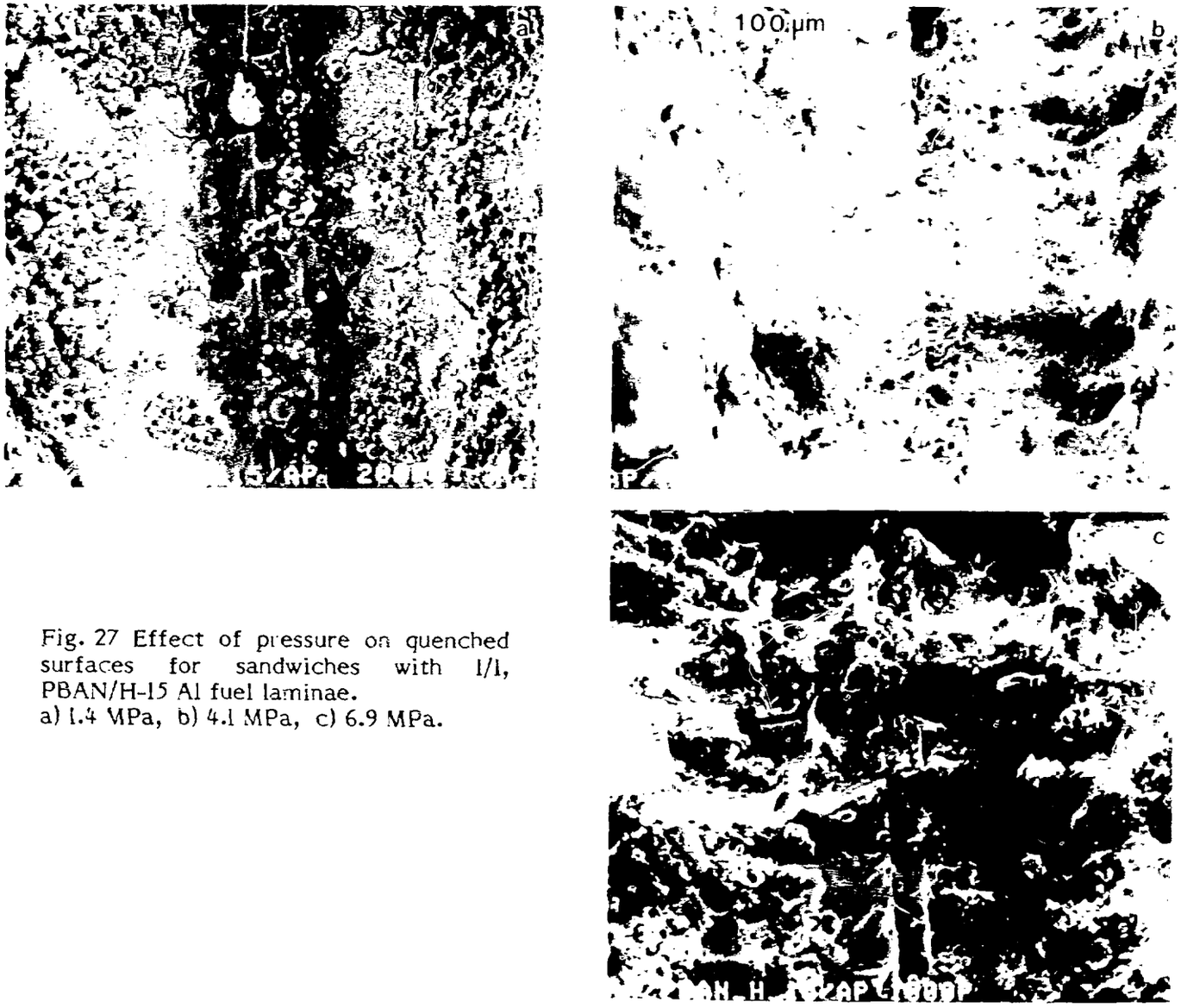

Fig. 27 Effect of pressure on quenched surfaces for sandwiches with 1/1, PBAN/H-15 Al fuel laminae.
a) 1.4 MPa, b) 4.1 MPa, c) 6.9 MPa.

b) Effects of Aluminum Variations

Changes in aluminum (with PBAN binder) had only moderate effect on quenched samples. Use of pre-stretched H-15 in place of as received H-15 (1/1, Binder/Al) produced no effect (although a substantial change was evident in the combustion photography tests described later).

Reducing the aluminum loading to 3/7, Al/Binder resulted in a somewhat lower aluminum concentration on the binder surface, and gave a somewhat smaller enhancement over the non-aluminized burning rate at pressures > 3.5 MPa (as compared to 1/1 Binder/Al).

Use of finer aluminum particles (H-5) in place of H-15 increased the level of accumulation at all pressures.

c) Effect of Binder

Changes in binder resulted in unexpectedly large effects on aluminized sandwiches. At low pressure these differences from PBAN sandwiches were not conspicuous, except for a drier, denser looking aluminum accumulation with polysulfide binder. Above 3.5 MPa, the effect of binder was more conspicuous, as shown in Fig. 28. In particular, the sandwiches with HTPB binder had aluminum accumulation that appeared to be flooded with binder melt. The HTPB/Al lamina and immediately adjoining AP protruded conspicuously at 6.9 MPa. The protrusion was significantly larger than observed in the tests with PBAN/Al fuel laminae or binder laminae alone.

d) Effect of AP in Binder

Introduction of 10 μm AP into a pure PBAN lamina in a 1 to 1 ratio (replacement of Al by AP) resulted in a binder surface that still looked wet, but irregular on a scale comparable to the oxidizer particle dimensions. No distinguishable AP particle surfaces were evident. The binder laminae were recessed slightly at all pressures (Fig. 29), as in the case of aluminized PBAN laminae, and pure PBAN binder at lower pressures. The very localized protrusion of AP immediately adjoining the fuel laminae (Fig. 25-28) is absent with the PBAN/AP lamina (Fig. 29). Instead, at a high pressure there is a wider plateau-like region of protruding AP unique to these samples (Fig. 29 b, c) and the AP/Al/Binder samples noted in the next section. The extent of protrusion of this region was more than with pure binder laminae for PBAN binder, less for HTPB

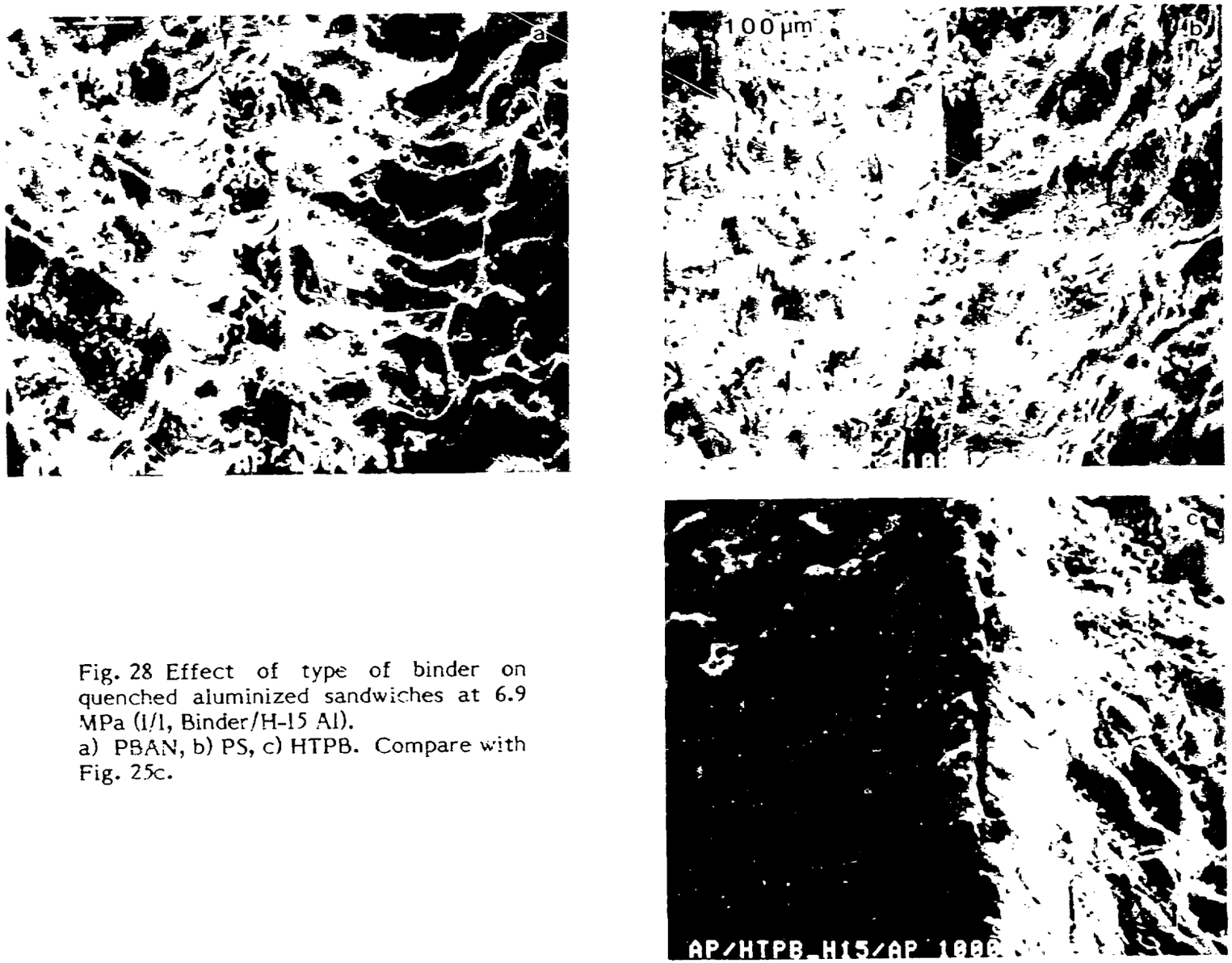

Fig. 28 Effect of type of binder on quenched aluminized sandwiches at 6.9 MPa (1/1, Binder/H-15 Al).
a) PBAN, b) PS, c) HTPB. Compare with Fig. 25c.

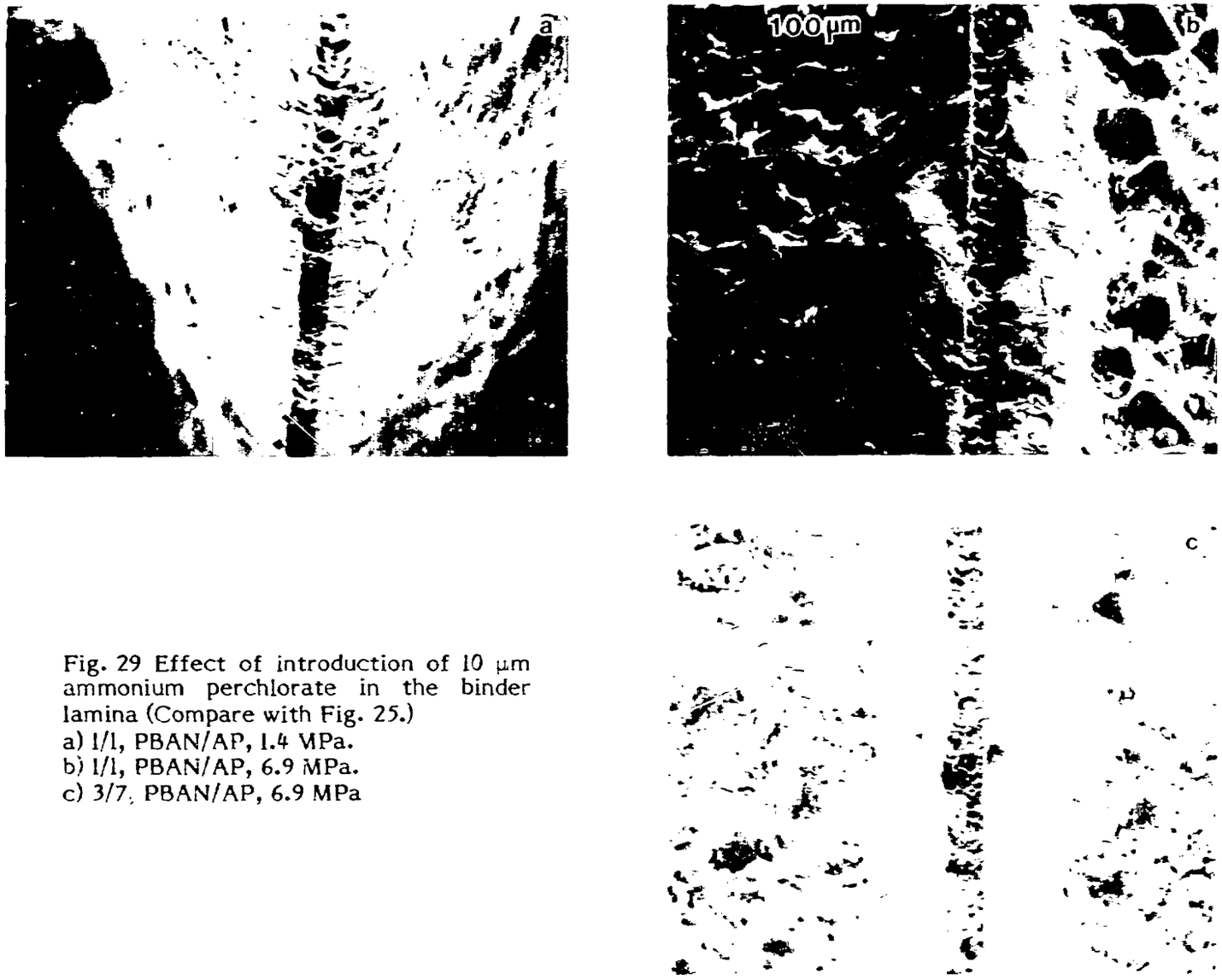

Fig. 29 Effect of introduction of 10 µm ammonium perchlorate in the binder lamina (Compare with Fig. 25.)
a) 1/1, PBAN/AP, 1.4 MPa.
b) 1/1, PBAN/AP, 6.9 MPa.
c) 3/7, PBAN/AP, 6.9 MPa

binder (Fig. 30). The test with a 7/3, AP/PBAN sandwich at high pressure exhibited less overall protrusion of the interfacial regions, and the interface was no longer the most protruding point in the interface region of the profile (Fig. 29c, not shown in Fig. 30).

e) Effect of Al and AP on the Binder

When a 1/1/1; Binder/AP/Al filled lamina was used, the lamina surface had less accumulated aluminum compared to the one with no fine AP at all pressures. The aluminum still had a wet appearance with both binders. But at 6.9 MPa with HTPB binder, the singular protruding feature of the lamina region with only aluminum (Fig. 28c) was absent when fine AP was added too. In general, the Binder/AP/Al sandwiches gave surface profiles closely resembling those obtained with sandwiches having 1/1 Binder/fine AP filled lamina.

Combustion Photography

The test conditions for which combustion photography was used are denoted by the symbol "M" in Fig. 24. From these few tests it was evident that aluminum left the surface primarily as ignited particles and agglomerates (6.9 MPa). Agglomerates were larger, and fewer original particles were present with HTPB binder than with PBAN binder. Addition of fine AP resulted in a reduction of agglomerate size, but did not seem to change the amount of unagglomerated aluminum leaving the surface. There was an appearance of distinguishable diffusion flame sheets or flamelet arrays extending from each AP/Binder interface. It is judged that these are smoke (carbon) trails from the true flames. Aluminum ignition tends to occur in these (presumably hot) regions, in the manner noted by previous investigators (Ref. 19). However, this was not completely systematic in these thin binder sandwiches. Some agglomerates appeared to form up and ignite while straddling the fuel lamina. Such agglomerates are probably of a size comparable to the lamina width. In the case of the HTPB/Al sandwiches at 6.9 MPa, the protruding lamina was easily visible and the top edge appeared to sway locally from one side to the other. In this situation, most of the aluminum emerged burning from one side or the other, not from the tip of the lamina.

In general, the photographic tests were too limited to make generalizations except for the following points:

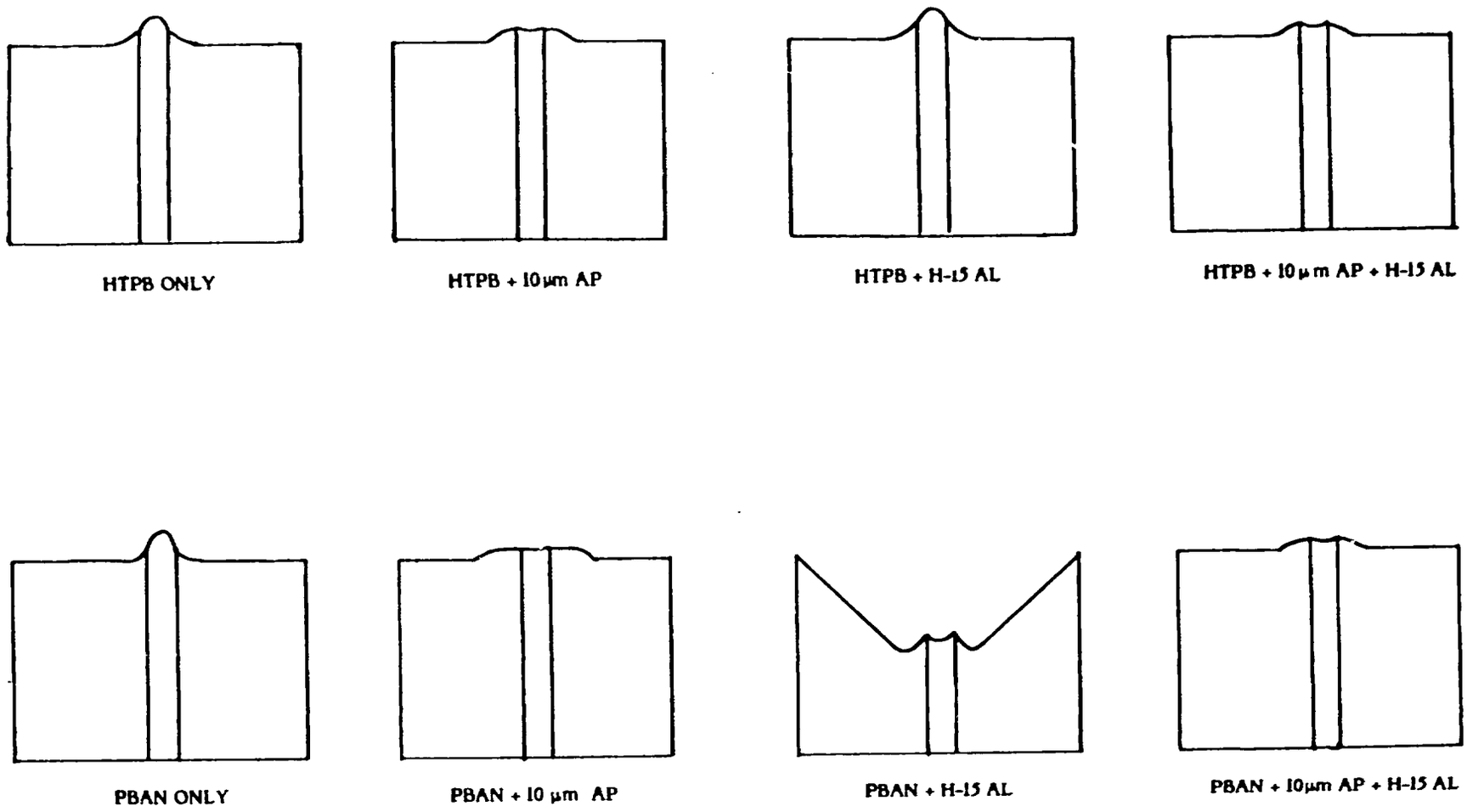

Fig. 30 Sandwich surface profiles for two binders and different combinations of AP and/or Al in the binder lamina.

a) There was extensive agglomerate formation at the sandwich surface. No unignited material was evident leaving the surface.

b) Agglomerates were smaller with PBAN binder than with HTPB binder.

c) Replacement of a 1/1, PBAN/Al lamina by a 1/1/1 PBAN/Al/AP lamina resulted in smaller agglomerates.

d) Separate AP/Binder flame sheets were evident for the two AP-fuel interface planes of the sandwiches, manifested by fluctuating smoke sheets.

e) Ignition of aluminum was favored in proximity of the AP/Binder flame, but with thin sandwiches the agglomerates were of comparable size to the fuel laminae and sometimes ignited and detached from a symmetrical position relative to the fuel lamina.

f) The test in which "pre-stretched" aluminum was used in place of as-received aluminum (H-15) exhibited substantial reduction in size of agglomerates.

Discussion of Sandwich Tests

The original objective of the aluminized binder sandwich tests was to provide a more controlled experiment for observation of aluminum accumulation, sintering, agglomeration and ignition. In particular, it was desired to examine the condition of the aluminum on the burning surface of thin binder lamina, a critical aspect of the behavior that had received only limited attention in a previous study (Ref. 18). Relative to this behavior, the principal result was the notable difference in appearance of the accumulated aluminum with different binders. HTPB binder resulted in a binder-flooded appearance; PBAN binder resulted in obvious aluminum accumulation, with appearance of wetting of particle surfaces and bridging between particles by binder melt; PS binder resulted in a dry-looking accumulation of aluminum. These results, observed on quenched samples, did not provide clues to subsequent development of agglomerates, except in the context of photographic observations of burning. The motion pictures showed that the size of agglomerates was greater with the "flooded look" of the HTPB sandwiches. Since HTPB appears to be the more thermally stable of the binders tested (Ref. 8,29), this suggests that the binder melt plays an important role in protecting the aluminum from ignition while it is concentrated and heated on the burning surface. The fact that use of sintering-resistant pre-stretched aluminum reduces agglomeration suggests that concentration and heat-up of the aluminum do not assure agglomeration, i.e., that a

final particle-to-particle sintering step is necessary for agglomeration. Likewise, the reduction of agglomeration by addition of fine AP to the aluminized binder lamina suggests that improvement of ignition conditions can block agglomeration. These speculations are consistent with propellant experience; additional combustion photography tests are needed to fully interpret the quenched surface observations.

The original plan for the sandwich tests covered only the study of aluminized binder lamina samples. However, the conspicuous effect of binder type on both surface profiles and aluminum wetting led to a series of tests on nonaluminized sandwiches, to determine to what extent the presence of aluminum was involved. The tests with fine AP additions were then conducted because of observations of the effect of fine AP in propellant testing (Ref. 11, 21, 30). Interpretation of the results of these further tests cannot be made yet, but the key results regarding surface profiles of the whole series of sandwich tests merit recapitulation.

1. Surface profiles with and without aluminum were similar with PBAN binder, except that the mildly protruding binder at higher pressure was changed to a mildly recessed profile when aluminum was added. A corresponding increase in sample burning rate resulted, accompanied by a corresponding "V" shaped overall sample profile.

2. With HTPB binder the effect of addition of aluminum had the opposite effect at high pressure. The extent of protrusion of the fuel lamina and adjoining AP was conspicuously increased (compared to nonaluminized HTPB sandwiches). The enhancement of sample burning rate observed with PBAN binder was absent with HTPB binder.

3. Addition of fine AP to PBAN binder laminae resulted in mildly recessed binder laminae at all pressures, as with the addition of aluminum. The corresponding increase in burning rate at higher pressure did not occur. Instead, the usually narrow region of protruding AP adjoining the lamina interfaces was widened. Similar effects were observed with HTPB binder.

4. Addition of both fine AP and aluminum to the binder laminae produced profiles similar to those with only AP added. The primary difference from sandwiches with aluminized binder was the widened region of AP protrusion at 6.9 MPa, and reduction of the unique height of protrusion of the lamina region with HTPB binder.

MODIFICATION OF ALUMINUM TO CONTROL AGGLOMERATION

Background

In view of the obvious importance of the role of the oxide skin on aluminum particles in controlling the onset of sintering, agglomeration and ignition of aluminum, it is reasonable to seek beneficial modification of the oxide. A method explored by Kraeutle (Ref. 31) was to enhance the oxide by further oxidation, by holding powders at elevated temperature in oxidizing atmospheres. This modification method was called "pre-oxidation", and was conducted at temperatures below the aluminum melting point.

A method explored earlier in the present project (Ref. 20,32) was called "pre-stretching" the oxide, by heating particles through the aluminum melting point. The oxide skin deforms to accomodate the relatively greater thermal expansion and phase change expansion of the aluminum. The oxide deformation is presumably by both inelastic stretching and cracking. In the presence of a low concentration of oxygen, the cracked areas will close rapidly by further oxidation. Upon cooling, the particles shrink, the oxide skin wrinkles or exhibits depressions (Ref. 32), but the oxide surface area is believed to remain sufficient to enclose the aluminum when the particle later melts in the combustion zone. This argument was developed from growing understanding of ignition behavior of aluminum powder, and was evaluated earlier in the project using the hot stage microscope to produce and test the pre-stretched oxide particles (Ref. 32). In those tests the tendency of aluminum powders to sinter and agglomerate when heated was sharply reduced by pre-stretching the oxide.

In subsequent combustion studies on this program, modified aluminum has been carried as one of the test variables, thus giving a systematic demonstration of the potential of modificiation of the oxide skin as a means of controlling agglomeration. For those combustion studies aluminum with pre-stretched oxide was produced in greater quantity by heating the powder in a half open quartz tube to 700°C, using a tube furnace flushed with a nitrogen flow (with some entrained air). The "pre-stretched" aluminum was subsequently sieved to eliminate any large agglomerates or sintered accumulates formed during the "pre-stretching" process. Since the smallest sieve mesh is 37 μ, it is probable that some small accumulates were included, but the mean particle diameter was not significantly altered.

The "pre-stretched" aluminum was compared with as received, and pre-

oxidized aluminum in a series of "propellant" formulations. The formulations included dry pressed AP/Al, and AP/Al/Wax samples. Sandwiches were also prepared consisting of an aluminum filled PBAN lamina between AP slabs. The results of some of these tests have been reported in interim reports (Ref 28, 32), but will be repeated here for completeness.

Combustion of AP/Al Samples

Samples were prepared from mixturs of AP and Al powders by dry pressing mixtures of 85%, 100 μm AP and 15% Alcoa 123 Al to pressure of 170 MPa for 20 minutes. Similar samples were made with pre-stretched Alcoa 123 Al, and samples with pre-oxidized Alcoa 123 Al (provided by Karl Kraeutle of Naval Weapons Center). Tests were run at 6.9 MPa (1000 psi), and observations were made by combustion photography.

Tests on the samples with untreated aluminum exhibited massive accumulation and sintering of aluminum on the burning surface, with ignition occurring only during break-up of detaching accumulate layers. Very large agglomerates formed. Results with the pre-oxidized and with the pre-stretched aluminum were alike. In the tests with pre-stretched aluminum, only small accumulates were evident, with more or less continual detachment of small fragments. Aluminum ignition was only occasional. This result supports the mechanistic argument that led to "pre-stretching" experiments (Ref. 20,32), and suggests a means of controlling accumulate size, using a modification of aluminum powder that is economically viable in production, possibly by simply changing process control variables in the original powder manufacture. The observation of only limited ignition of the pre-stretched aluminum supports the earlier argument that conditions in the AP flame are not conducive to ignition of aluminum unless some mechanical breakage of the hot sintered accumulate exposes aluminum, and thus provides the opportunity for localized exothermic reaction.

Combustion of AP/Al-Binder/AP Sandwiches

Sandwiches were prepared using the usual method (Ref. 27, 28) of laminating a thin layer of binder between two AP slabs. In this case the binder was a 1/1 mixture of PBAN and Valley Met H-15 aluminum. Samples were prepared using as received and pre-stretched H-15, and combustion tests were run at a pressure of 6.9 MPa (1000 psi) and observed by high speed cinephotography. The sandwiches

prepared with as-received H-15 burned with large slow moving agglomerates, and the ignition and detachment of agglomerates was noticably intermittent, almost periodic. The sample with pre-stretched aluminum burned with small agglomerates and single ignited particles that left the surface in a more or less continuous manner. In this test the pre-stretched aluminum was shown to substantially reduce agglomeration thus improving the combustion behavior of the aluminum. In contrast to the tests on dry-pressed AP/Al samples, use of pre-stretched aluminum in sandwich tests led to improved aluminum ignition, presumably because ignition is induced by the hot AP-Binder flame instead of by aluminum exposure during accumulate break-up.

Combustion of AP/Al/Wax Samples

A set of propellant samples were prepared by dry pressing 30% Valley Met H-30 aluminum, 7% carnauba wax, and 63% 100 μ AP. One sample was prepared using as received H-30, a second sample used pre-stretched H-30, and a third sample used "pre-oxidized" H-30. A fourth sample was prepared in a manner that illustrated the differences in aluminum behavior more graphically in a single motion picture, by using as-received and pre-stretched aluminum in different parts of the same sample. As in the AP/Al tests, dry pressed samples are prepared by mixing the ingredients, pouring the ingredients into a die and pressing the mixture in a hydraulic press to obtain a compact disc of propellant. The fourth sample was prepared by using a piece of card stock to divide the die into two halves. One half of the die was loaded with the mixture containing as received aluminum while the other half contained the mixture with pre-stretched H-30. The mixture was carefully tamped down and the card separator was carefully removed. The sample was then hydraulically pressed to obtain a disc of propellant. After careful cutting, a 10 mm x 6 mm x 1.6 mm sample was obtained, one half containing as-received H-30 and one half with pre-stretched H-30. Motion pictures of these "half and half" propellants are comparable to split frame motion pictures, i.e., a direct comparison of the combustion behavior of the aluminum is possible.

Motion pictures were filmed for each of the samples burning at 6.9 MPa (1000 psi). The sample with as received H-30 exhibited relatively unfavorable Al combustion characteristics. The surface was covered with large filigrees, aluminum ignition was sporadic, and moderately large to large agglomerates were formed. Significant improvement was seen with the samples with pre-stretched

and pre-oxidized H-30. The surface was rough but fewer filigrees were evident. The aluminum left the surface (ignited) in small agglomerates or single particles. Viewing the "half and half" sample was quite convincing. In any single frame, the region above the half of the sample with as-received aluminum was dark with two or three large burning agglomerates. The region over the other half of the sample surface (pre-stretched aluminum) was nearly a continuous white field of burning particles (Fig. 31).

Combustion of the samples prepared with "pre-oxidized" H-30 was indistinguishable from the "pre-stretched". Both modifications of the aluminum resulted also in higher sample burning rates.

Summary of Aluminum Modification Tests

Combustion photography was used to compare aluminum behavior in tests on three kinds of samples:

Dry-pressed mixtures of AP and Al powders.

Dry-pressed mixtures of AP, Al, and Carnauba wax powders.

Sandwiches with aluminum in the binder lamina.

Both pre-oxidation and pre-stretching treatments of aluminum particles resulted in reduction of accumulation of aluminum on the burning surface, and major reduction of the size of aggregates leaving the surface. In those tests where an AP-hydrocarbon flame was present, the changes resulting from use of modified aluminum led to more prompt ignition of accumulating aluminum and to correspondingly smaller agglomerates. In the tests on AP/Al samples (no hydrocarbon fuel), aluminum ignition was not improved, apparently because conditions in the combustion zone of the AP are not conducive to ignition of the aluminum. In general, the results are consistent with those obtained earlier by Boggs, et al (Ref. 33), with pre-oxidized aluminum, although detailed comparison cannot be made of the two aluminum modifications because of differences in other test sample variables.

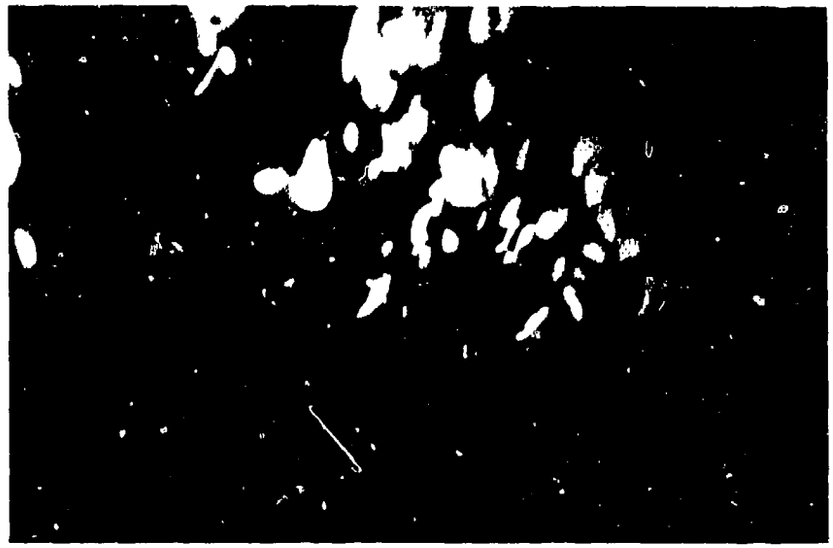

Fig. 31 Comparison of aluminum combustion with dry pressed AP/Al/Wax samples: pre-stretched on the right and as-received aluminum on the left.

STUDIES OF A FAMILY OF PROPELLANTS PREPARED AT THIOKOL-ELKTON

Background

Variation of composition and ingredient particle sizes is probably the most critical factor available in conduct of propellant combustion research. The high cost of preparation of propellant mixes, unfortunately, tends to limit the systematic use of this critical variable as an investigative tool in research and often forces the use of samples prepared by improvised means of unevaluated relevance (e.g., use of samples prepared by dry pressing powder mixes). During the present study, a family of samples became available, which has a systematic variation of composition, prepared by state-of-the-art method (Ref. 34). These same formulations were studied by the suppliers (Ref. 11, 34) using a variety of combustion experiments. In the present program this series of propellants was studied by combustion photography, and by scanning electron microscope analysis of sample surfaces quenched by rapid depressurization. The objectives were three-fold: first, it was desired to establish a basis of comparison of test results on conventional propellants with work on the present program using samples prepared by various improvised methods; second, it was desired to take advantage of the available range of systematic variations of formulations; and third, it was desired to provide a independent set of test results that could be compared with those of the propellant supplier (for reproducibility or possible mutual improvement of experimental methods). In the following, information regarding the propellants, tests, results, and interpretation is summarized.

Propellant Formulations

The range of test variables covered in this investigation is given in Table 2. The actual composition of the propellants can be obtained from Ref. 11 and 34; they are high solids HTPB propellants with variations on a baseline propellant having 18% aluminum and a trimodal AP blend. One or two variables were changed at a time to study the effect of these variations on the combustion behavior of the propellant. All the propellants studied are low burning rate composite propellants. The sample designated 1780-1 was used here as a baseline formulation. Not all the formulations in the supplier's original program were available, and not all those supplied were tested in the present investigation. Choices were based in part on anticipated results, and in part on supplier's test results.

Table 2

Range of Major Propellant Variables Investigated

HTPB BINDER	
LEVEL:	9 to 14%
ALUMINUM	
LEVEL:	18 to 22.4 %
SIZE:	7.5 to 84 μm
AMMONIUM PERCHLORATE	
LEVEL:	55 to 71%
SIZE:	6 to 400 μm
MODALITY:	
Bimodal:	400/fine
Trimodal:	400/200/fine
HMX	
LEVEL:	0 to 15%
SIZE:	6 and 9 μm
ALTERNATIVE:	RDX

Experimental Procedures

Combustion Photography: The experimental set up and the procedure are similar to those described in Ref. 35. The sample dimensions were 10 mm x 6 mm x 1.6 mm. Ektachrome 7241 high speed color film was used for motion pictures. The film framing rates and the aperture f-stop setting varied with test pressure, and are given in Table 3. The samples were externally illuminated by a Xenon lamp under all test conditions. Test conditions are tabulated in Table 4.

Quench Procedure: Quenching was accomplished by rapid depressurization of the combustion vessel by diaphragm rupture. The experimental set up and technique are described in Ref. 36. The sample dimensions were maintained the same as in combustion photography for ease of comparison of results. The quenched samples were then prepared for study under a scanning electron microscope. Quench test conditions are tabulated in Table 5.

Results

Combustion Photography: Combustion photography provides details regarding the combustion efficiency, nature of accumulates on the burning surface, size of agglomerates leaving the surface, burning rate, etc.. The combustion photographs were initially compiled into edited motion pictures for three different pressures and then spliced together into one picture for easy comparison of combustion of different samples. The results of combustion photography allow a comparison of combustion behavior as a function of size of aluminum, % binder, size of AP particles, addition of HMX, usage of DDI curative in propellant and pressure. The pictures were examined for:

(a) Degree of accumulation of aluminum on the surface.

(b) Duration of retention of accumulated aluminum on the surface.

(c) Qualitative estimate of the size range of agglomerates leaving the burning surface.

(d) Ignition characteristics of agglomerates.

(e) Burning rate of sample.

(f) Brightness of field of view which in turn is a measure of the vigorousness of combustion.

(g) Qualitative estimate of unignited aluminum leaving the burning surface.

Behavior in each test was ranked in Table 6, and can be interpreted by comparison with behavior of the baseline propellant No. 1780-1 as described below, in terms of

Table 3

High Speed Camera Settings for Combustion Photography

Pressure MPa (psi)	Film Speed f/sec	F-Stop
1.4 (200)	3000	5.6
3.45 (500)	3400	8.0
6.9 (1000)	4000	11.0

Table 4

Test Conditions for Combustion Photography

PRESSURE / FORMULATION	1.4 MPa (200 psi)	2.62 MPa (350 psi)	3.45 MPa (500 psi)	6.9 MPa (1000 psi)
BASELINE	X	X	X	X
AL EFFECT (SIZE)				
Fine Al	X		X	X
Coarse Al	X		X	X
BINDER EFFECT				
High Binder	X		X	
DDI	X		X	
Catalyst Fe_2O_3			X	
AP SIDE EFFECTS				
400/200/71	X		X	
400/71			X	
400/41			X	
HMX	X		X	X

Table 5

Conditions for Quench Tests of Propellants

1.	6.9 MPa Quenches of all formulations.
2.	Quenches of baseline formulation at progressively lower pressures of 6.9, 5.2, 3.45, 2.42, 1.41, 0.7 MPa.
3.	Quenches of 400/200/71 (no fine AP) at the same series of pressures as in 2.
4.	Quenches of DDI curative propellant at the same series of pressures as in 2.

accumulating insight into the aluminum behavior and the observed results ranked in the table.

At a pressure of 1.4 MPa (200 psi) the combustion of the baseline formulation is as follows. As the burning surface recedes, the ingredient aluminum particles accumulate on the surface due to the concentration of the surface aluminum particles with the underlying particles, and retention on the surface by the surface tension forces of the molten binder, in the absence of favorable ignition conditions. The accumulation is moderate in the case of the baseline propellant. Past studies (Ref. 6, 33, 37, 38) indicate that as this accumulation progresses, a sintered filigree of particles forms and as accumulation progresses further, a part of the filigree is eventually exposed to the hot diffusion flame. This results in local breakdown of the sintered oxide skin of the filigree, followed by a spreading inflamation and coalescence into an agglomerate. In the case of the baseline propellant of the present study, most of the accumulated aluminum ignites on the propellant surface and ignition-coalescence is rapid. Some of the burning agglomerates reside on the burning surface for a short time before being swept away by the gas flow. The agglomerates leaving the burning surface range in size from single particles to about 350 μm. The field of view is moderately bright both close to the burning surface and in the far field, with a moderate amount of smoke in the combustion zone. No unignited aluminum is evident leaving the burning surface. To the extent possible in still photographs, the foregoing details are illustrated in Fig.32.

The propellant combustion behavior is not significantly different at 3.45 MPa except that the degree of accumulation is less and hence smaller agglomerates leave the burning surface.

The results of all tests are tabulated in comparative terms in Table 6 a (1.4 MPa tests) and Table 6 b (3.45 MPa). The numbers 1 - 5 used in these tables rank the indicated combustion behavior on a scale of 1-5.

It is observed from the analysis of this combustion photography that the general trend is for a bright combustion field, short residence time, smaller agglomerates, and high burning rate to go together. Conditions which favor this complex of behavior are:

a) Small (i.e., < 15 μm) aluminum particle size: Relatively fine aluminum provides more surface area and finer sintered structure of accumulates, which results in more vigorous inflamation at the moment of accumulate breakdown. However, under adverse ignition conditions, the large surface area can lead to more

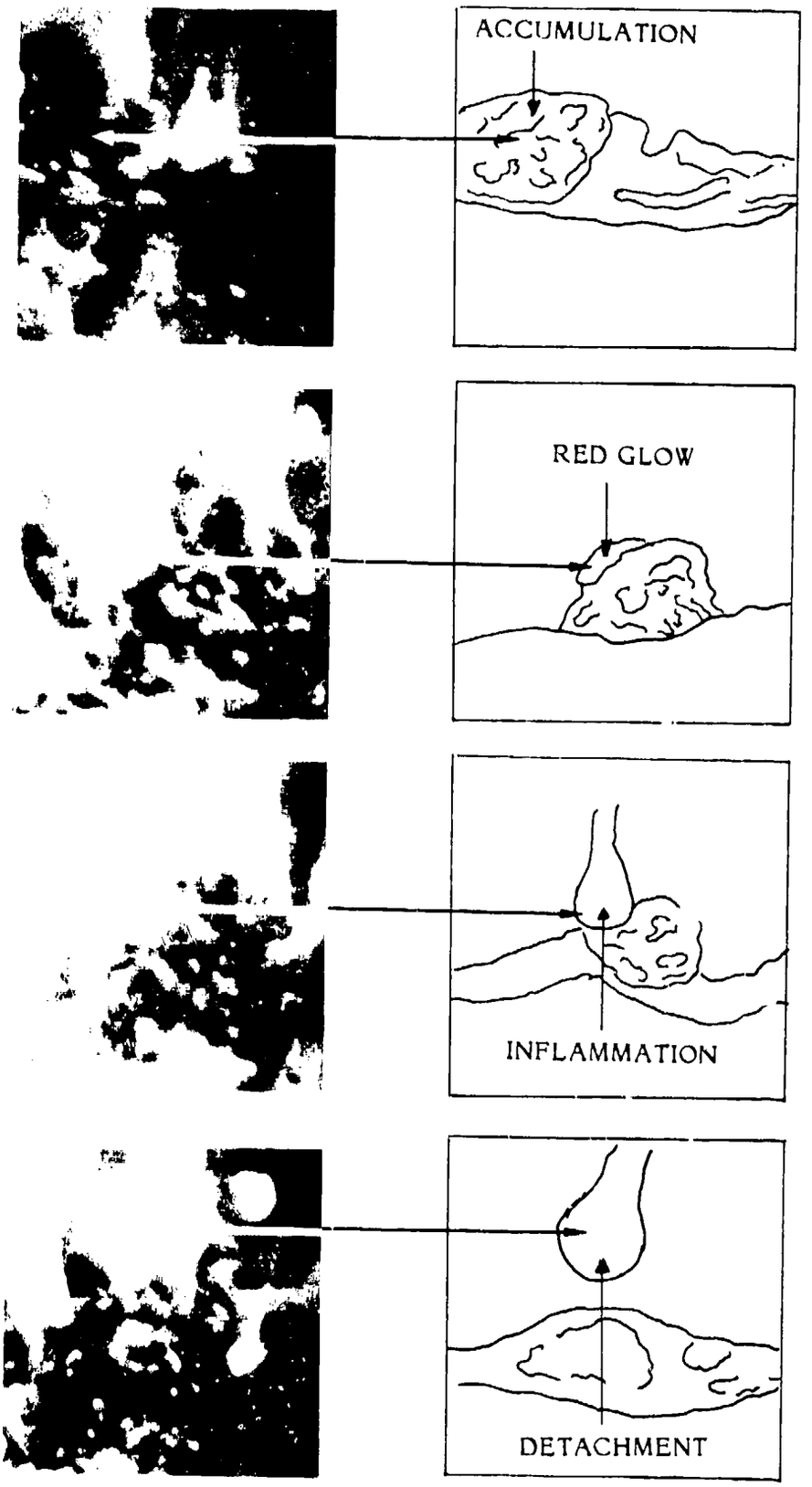

Fig. 32 Combustion field for sample 1780-1 at 1.4 MPa.

Table 6a

Comparative Results of Tests Run at 1.4 MPa

CHARACTERISTICS / FORMULATION	Degree of Accumulation	Retention on Burning Surface	Ignition		Aggl. Size		Brightness		Smoke	Burning Rate	Unburned Aluminum Leaving Surface
			Surface or Gas	Quick or Slow	Range	Avg. Size	Near Field	Far Field			
BASELINE	3	2	S	Q	3	3	2	2	2	--	1
AL EFFECT											
Fine Al	3*	2	S	S & Q Crusts	3	2	3	3	2	Higher	1
Coarse Al	5	3	S & G	S	2	2	1	1	3	Smaller	2
BINDER EFFECT											
High % Binder	4	3	S	S	4	4	1	1	3	Lower	1
DDI Curative	3	2	S	Q	3	2	2	2	2	Lower	1
AP SIDE EFFECT											
400/200/90 μm AP	2	1	S	Q	2	1	1	--	2		1
HMX	3	2	S	Q	3	2	1	1	2	Higher	1

* (Crusting occasionally)

Table 6b

Comparative Results of Tests Run at 3.45 MPa

CHARACTERISTICS / FORMULATION	Degree of Accumulation	Retention on Burning Surface	Ignition		Aggl. Size		Brightness		Smoke	Burning Rate	Unburned Aluminum Leaving Surface
			Surface or Gas	Quick or Slow	Range	Avg. Size	Near Field	Far Field			
BASELINE	3	2	S	Q	3	3	2	2	2	--	1
AL EFFECT											
Fine Al	3*	2	S	Q	3	2	3	3	2	Higher	1
Coarse Al	4	3	S & G	S	2	2	1	1	3	Lower	2
BINDER EFFECT											
High % Binder	4	3	S	S	4	4	1	1	3	Lower	1
DDI Curative	2	2	S	Q	3	2	2	2	2	Lower	1
Fe_2O_3 Catalyst	3	2	S	Q	3	2	3	2	2	Higher	1
AP SIDE EFFECT											
600/200/90 μ m	2	1	S	Q	2	2	3	2	2	Higher	1
400/90 μ m	2	1	S	Q	1	1	3	--	2	Lower	1
400/50	3	2	S	Q	2	2	2	2	2	Higher	1
HMX	3	2	S	Q	3	3	1	1	2	Higher	1

* (Crusting occasionally)

extensive sintering and larger agglomerates, as observed here with the finest aluminum particle size.

b) Low binder to oxidizer ratio: The "bright burning" complex is apparently favored by the more oxidizer-rich environment and perhaps even more by the less prolonged surface retention and protection from oxidizing species, due to reduced binder presence in the surface accumulates.

c) Close proximity of the oxidizer-binder flame to the accumulating aluminum: Whether due to higher pressure or to propellant microstructure, proximity to these high temperature flamelets appears to precipitate early ignition of aluminum, and hence less accumulation and agglomeration and more vigorous combustion.

SEM Studies of Quenched Burning Surfaces

The general appearance of quenched surfaces is illustrated by the series in Fig. 33 for 1780-1 formulation at 5 pressures. The coarser oxidizer particles are conspicuous at lower pressures, with the intervening areas showing a binder surface that looks like it was a melt prior to quench. The aluminum concentrated in the binder is evident at lower pressure, while the fine oxidizer particles are either not evident, or not distinguishable from aluminum particles. The larger oxidizer particles generally have concave surfaces, especially at high pressure. The profiles of the oxidizer surfaces have a close resemblance to the profiles obtained in aluminized sandwich burning tests. The region adjoining the binder is protruding and has a smooth surface. Further from the interface, the sloping surface flattens out and transitions to a central area that has a frothy surface appearance, sometimes raised (low pressure). Under some conditions (low pressure), collections of aluminum particles were contained in the central froth region (Fig. 34). At pressures higher than 3.45 MPa the surfaces of the oxidizer particles were deeply concave and exhibited no froth or aluminum. In general, the array of accumulated aluminum on the burning surface reflected its original distribution in the propellant microstructure. The fine oxidizer did not manifest its presence. "Pocket" concentrations of aluminum occurred in spite of the presence of the fine AP. These trends were generally true over the whole pressure range, but the aluminum concentration became flooded with binder melt at higher pressure.

The principal effects of propellant variations on samples quenched at 6.9 MPa were the following:

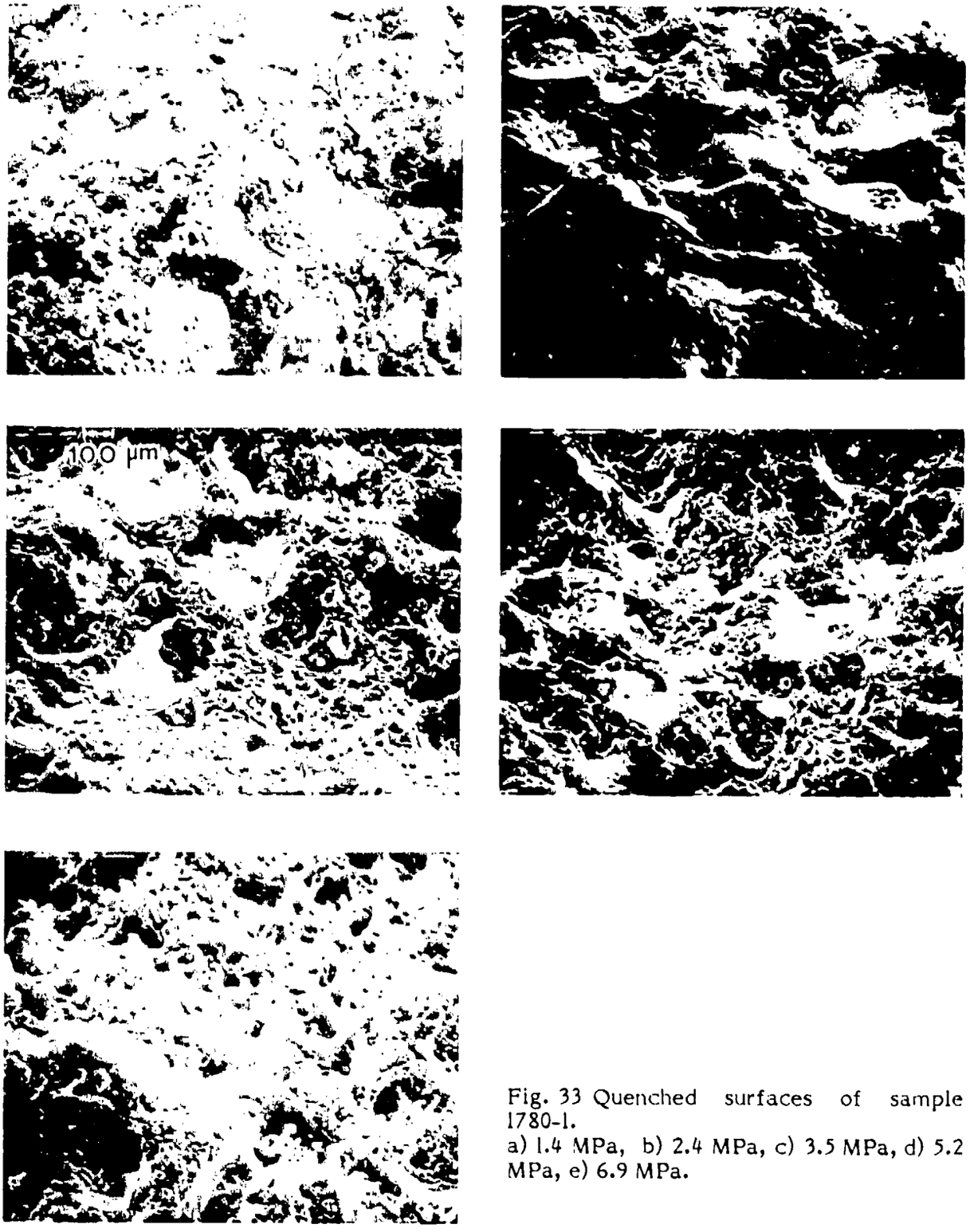

Fig. 33 Quenched surfaces of sample 1780-1.
a) 1.4 MPa, b) 2.4 MPa, c) 3.5 MPa, d) 5.2 MPa, e) 6.9 MPa.

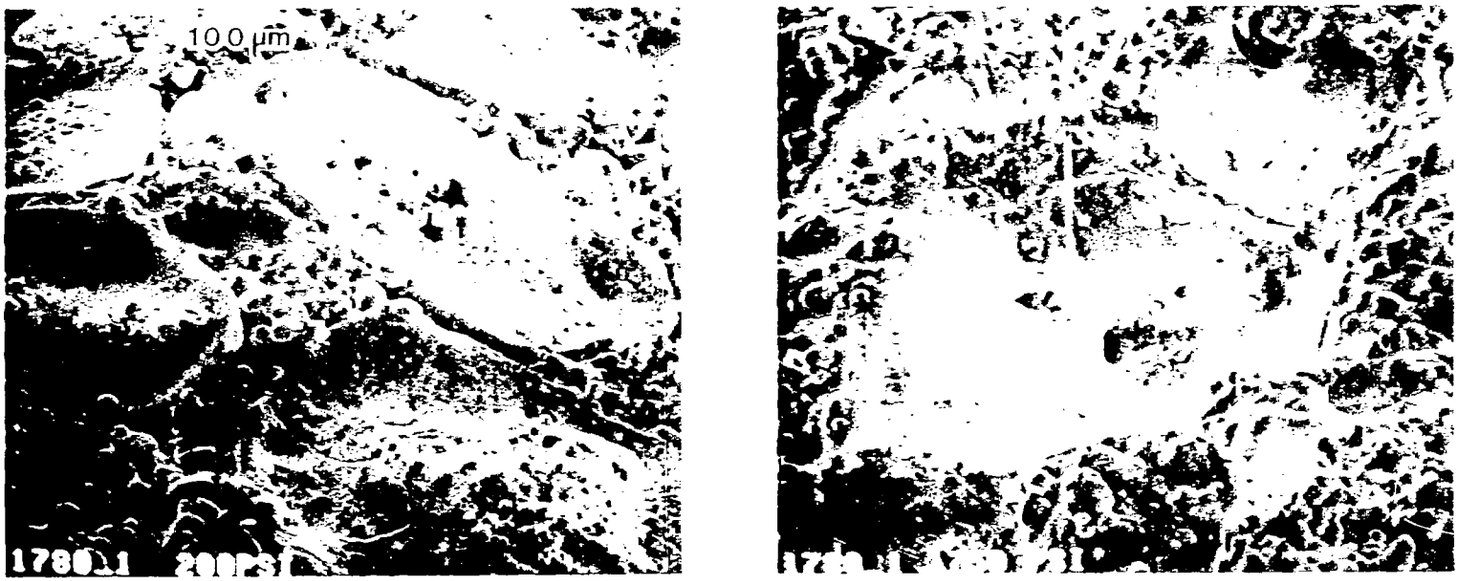

Fig. 34 Aluminum accumulation on the surface of an oxidizer particle, sample 1780-1.
a) Heavy at 1.4 MPa, b) not at 5.2 MPa.

a) Replacement of fine AP by an intermediate size resulted in a surface accumulation of aluminum that was of a filigree nature. This result is a consequence of the fact that pockets in the propellant microstructure were eliminated by being filled with the intermediate size AP particles, leaving the relatively finer aluminum particles in less concentrated clumps. The aluminum looked appreciably less flooded.

b) The sample with fine aluminum showed local areas of formation of aluminum crust, larger than typical pocket accumulations.

c) The samples with a moderate amount of HMX tended to give a more wetting binder surface, with very small holes in the binder surface.

d) The sample with coarse aluminum showed very little accumulated aluminum on the surface, localized only to individual pockets, containing 4 - 10 particles.

The reader is reminded that the description of the sample surface may reflect changes that took place during quench. It seems likely that the drier aluminum accumulates may detach during quench, and the binder may experience some local flow of the molten surface. The holes in the binder with HMX may be blown during quench, and the froth on the oxidizer surface may be disrupted. These are all believed to be of only moderate importance to surface appearance, except for the possible detachment of accumulates in transition (which limits their observation to the relatively poor resolution obtainable from the combustion photography).

Discussion

The results indicate the relevance of the early comments on propellant microstructure to the formation of surface accumulates and agglomerates. Pocket-forming oxidizer particle blends form agglomerates of pocket size. In this respect, the presence of a moderate amount of fine AP does not prevent pocket size accumulates, but apparently aids ignition of aluminum enough to give somewhat more vigorous inflamation and burning. Using fine aluminum seems to have aided sintering, which in turn led to some very large agglomerates, a behavior that was not prevented by presence of fine oxidizer. The presence of aluminum accumulations in the middle of oxidizer burning surfaces has been observed in previous studies (Ref. 11, 25, 37), and is believed to result from a failure of the pocket accumulation to ignite at the time of transition as the underlying surface passes from binder to an underlying oxidizer particle. This is consistent with

observations reported in earlier sections regarding survival of accumulates on oxidizer surfaces. In general, this type of behavior is more common under the unfavorable ignition conditions at low pressure. Of particular importance is the effect ing the "pockets" with oxidizer particles large enough to displace the aluminum into thinner "sponge" elements of binder, oxidizer particles large enough to deflagrate on the surface like the larger particles. This leads to a more tenuous filigree of aluminum a ulation, that forms in close proximity with hot oxidizer-binder flamelets. The result is relatively small and vigorously burning agglomerates.

COMBUSTION OF HIGH ALUMINUM CONTENT SOLID PROPELLANTS

Most rocket propellants with aluminum as a fuel ingredient contain 12 - 18% aluminum. Motor performance calculations generally indicate that optimum performance would be obtained at a higher aluminum content, and particularly so in volume-limited applications where high propellant density is also advantageous. In addition, there is some indication that high aluminum content reduces susceptibility to detonation. However, there are problems with high aluminum content that reduce its actual performance, problems that would have to be minimized before increased aluminum would be advantageous. However, the seriousness of these problems (low combustion efficiency and high two-phase flow losses in the nozzle flow) has remained substantially unevaluated, as have the possibilities of reducing the problems by better "design" of combustion. Results and methods of the present research offered the means to achieve improved combustion and control of product oxide droplet size distribution, and an exploratory study was made. This work was reported in Ref. 39 and is summarized here.

Three types of experiments were conducted on propellants containing 5 - 35% aluminum. These consisted of high speed cinemicrophotography; microscopic studies of quenched burning surfaces; and microscopic and chemical analysis of the efflux from the burning surface (quench-collected in ethanol at various distances from the burning surface). In order to permit a large range of propellant formulations, the propellant was simulated by one of two different processes.

1. Dry-pressing powder mixtures in which polymeric binder is replaced by carnauba wax powder.
2. Hand mixing small samples of conventional ingredients, followed by pressing and then curing.

The modifications in formulation that were tested are shown in the test summaries in Fig. 35 to 37. The charts show a central reference formulation and test pressure, and sequences of values of different variables, changed one at a time from the central reference condition. At least one test was run for each condition in the charts.

A motion picture sequence is available summarizing the combustion photography. The effects of test variables on combustion characteristics are

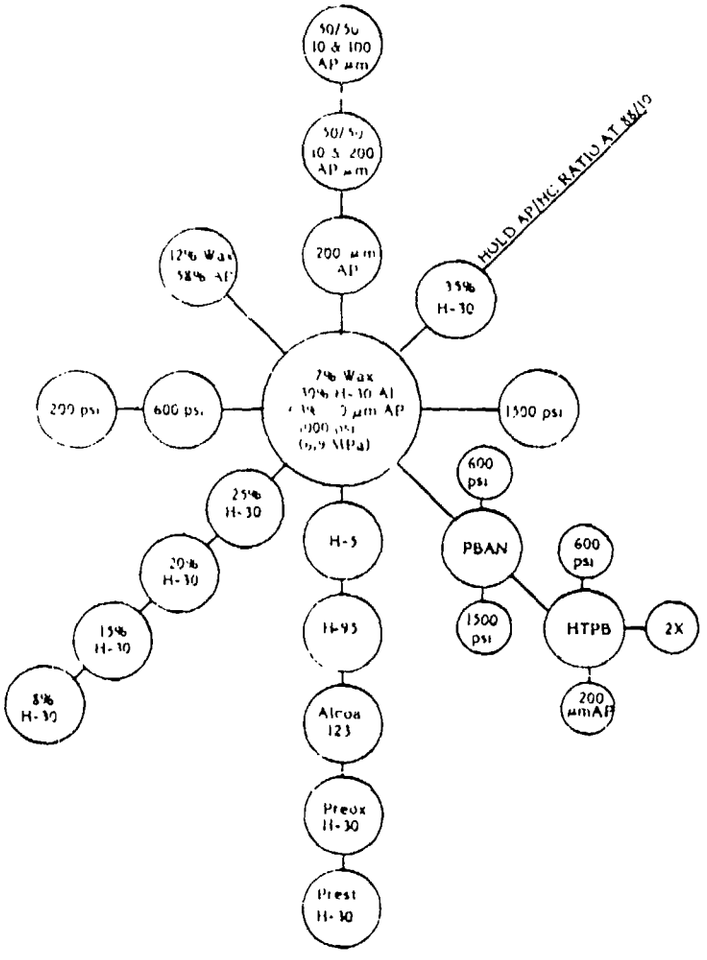

Fig. 35 Test conditions for combustion photography: AP-Wax-Al, "dry pressed" samples. Each small circle indicates one or more tests with indicated modification of test conditions relative to the "reference state" inside the large circle.

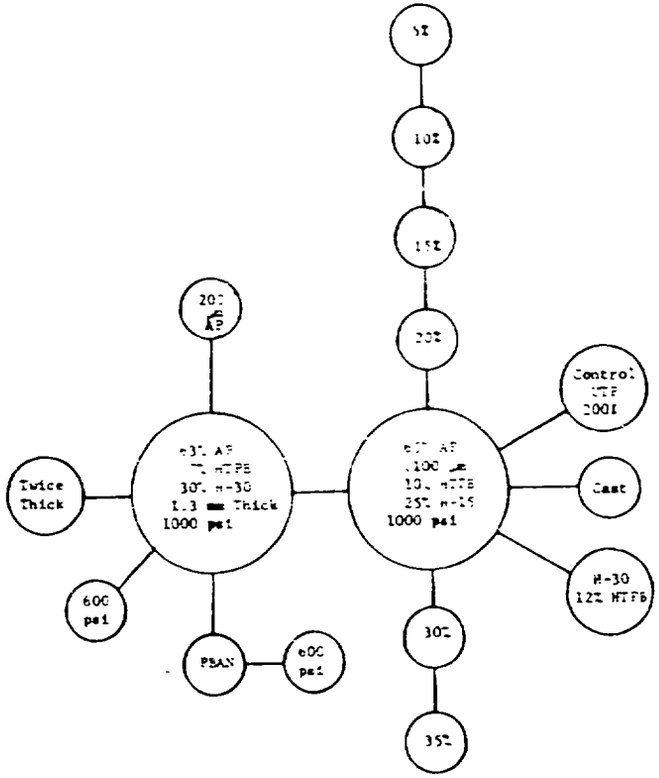

Fig. 36 Test conditions for combustion photography: AP-HTPB-Al, "wet pressed" samples.

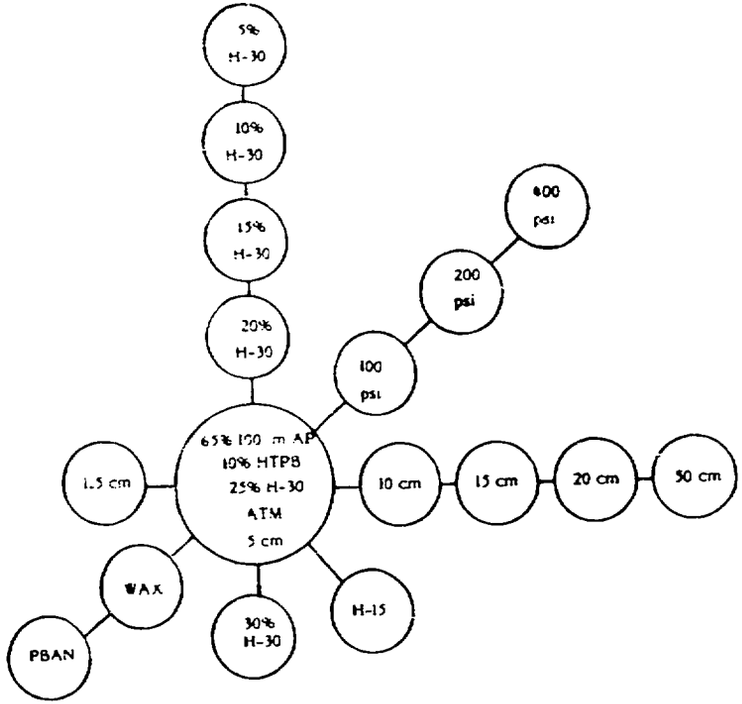

Fig. 37 Test conditions for plume quench samples.

tabulated in Table 7. Fig. 38 shows the effect of aluminum content on the burning surface as revealed by microscopic examination of quenched samples. Fig. 39 shows typical size distribution of aluminum agglomerates from plume quench tests and Fig. 40 shows amounts of unreacted aluminum remaining in plume quench samples for various test conditions (indicative of combustion efficiency). These and other results are presented in more detail in Ref. 39. From the combined results, the following conclusions were drawn regarding high aluminum content propellants.

1. Combustion efficiency of aluminum remains high to 25% aluminum. It is pressure-dependent in the range tested, and would apparently be better at typical rocket motor pressures than in the tests reported here.
2. Burning rate tends to a maximum around 18% aluminum, and the brightness of the combustion field peaks at about the same aluminum content.
3. The size of aluminum agglomerates (and degree of agglomeration) increase with aluminum content, especially above 25% aluminum. Other indicators of slow combustion also follow this trend (burning rate, brightness of field, combustion efficiency at 5 cm).
4. Several measures for improving combustion were found to be effective, including: treatment of aluminum powder to minimize agglomeration; choice of relative size of AP and Al particles so as to isolate groupings of accumulating aluminum particles on the burning surface from each other; choice of propellant and motor conditions conducive to aluminum ignition (particle size control, low binder content, high pressure).
5. An accompanying study (summarized elsewhere in this report and in Ref. 7) shows that the oxide products of burned agglomerates consist of about 85% smoke particles (< 2 μ m) and 15% burnout residuals of agglomerates. The size of the latter depends on the size of the parent agglomerate, and increases with % aluminum. The size range is 5 - 80 μ m. With a 25% aluminum propellant, the size could probably be kept around 10 -25 μ m by appropriate choices of aluminum powder and of ingredient particle size distribution (this is a "projection"). Flow effects may modify the combustion-generated sizes.
6. Combustion behavior appears to be significantly dependent on propellant binder type, content, and/or distribution in the matrix. However,

Table 7
Summary of Effect of Test Variables on Combustion Behavior
As Indicated by Combustion Photography

Behavior / Variables	Accumulation on Surface	Accumulate Attachment to Surface	Ignition of Agglomerate	Size of Agglomerate
Effect of Increase in % Aluminum	Increases	Effect not clearly visible from movie; seems to be no effect. Oscillating sintered Al increases.	More agglomerates ignite on surface and remain longer on surface.	Increases
Effect of Increase in Pressure	Decreases but the effect is not significant between 1000 & 1500 psi.	At low pressure stays attached and glows red. Effect vanishes with pressure.	No significant variation. Mostly surface ignition.	Decreases, but not significantly between 1000 & 1500 psi.
Effect of Increase in Aluminum Particle Size	Increases	Stays attached to the surface longer; and with 95 μm particle intensively.	Ignition in the gas phase to surface ignition mostly.	Increases, but with 95 μm particle very little agglomeration.
Effect of Pre-treatment of Al (pre-oxidizing & pre-stretching)	Decreases considerably	Residence time on surface is reduced.	Ignition mostly in gas phase.	Decreases significantly.
Effect of Increase in Oxidizer Particle Size	Increases	Could not be detected very well.	No significant difference except with 200 μm AP Al agglomerates were spewed in all directions.	Increases
Effect of Addition of Fine AP	Decreases	No significant difference, but spewing of Al in 200 μm AP sample was absent.	No noticable difference.	Decreases
Wet Pressed Effect of Binder				
(a) PBAN	Decreases compared to wax.	Not observable.	Mostly surface ignition.	Decreases compared to wax.
(b) HTPB	Sample did not burn to completion (thickness effect) and sample burned almost like PBAN sample when made twice as thick.			
Second Series Effect of % Al Increase in HTPB Series.	Not observable because of bright field of view in all tests.		Ignition mostly after leaving surface in all samples.	Increases gradually.

Table 7 (Continued)
Summary of Effect of Test Variables on Combustion Behavior
As Indicated by Combustion Photography

Behavior / Variables	Burning Rate	Brightness Near Burning Surface	Additional Remarks
Effect of Increase in % Aluminum	Peaks between 15 & 20% Al loading.	Peaks at 15 and 20% Al loading.	Amount of unburned Al leaving surface increases.
Effect of Increase in Pressure	Increases gradually.	Increases	Amount of unburned Al decreases, but not very significantly.
Effect of Increase in Aluminum Particle Size	Decreases	Decreases	Amount of unburned particle increases and is considerable with H-95.
Effect of Pre-treatment of Al (pre-oxidizing & pre-stretching)	Increases	Increases. Pre-oxidized gives higher burning rate.	Very little unburned Al leaving surface.
Effect of Increase on Oxidizer Particle Size	Decreases	Decreases	More unburned Al leaving surface.
Effect of Addition of Fine AP	Increases	Increases	Less unburned Al leaving the burning surface.
Wet-Pressed			
Effect of Binder			
(a) PBAN	Increases	Increases considerably.	Less unburned Al leaving surface.
(b) HTPB	Sample did not burn to completion (thickness effect), and sample burned almost like PBAN sample when made twice as thick.		
Second Series			
Effect of % Al Increase in HTPB Series	Peaks between 15 & 20% Al loading.	Peaks about 20% Al loading.	Very little unburned Al leaving the surface.

a

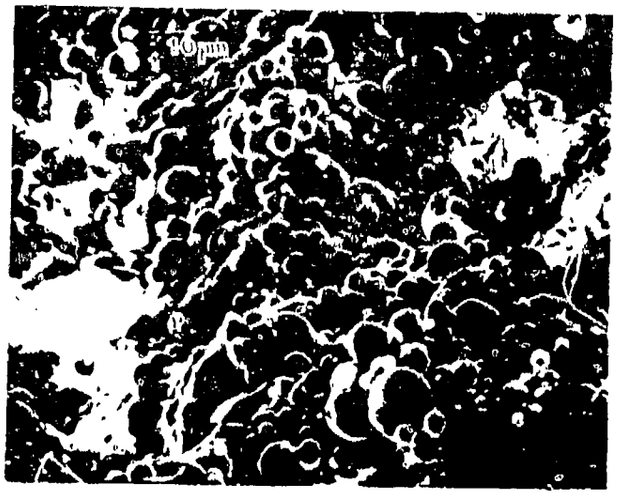

b

Fig. 38 Aluminum accumulation on the burning surface of AP-HTPB-Al sample quenched by rapid depressurization at 6.9 MPa. (a) Low % aluminum (5%). (b) High % aluminum (35%).

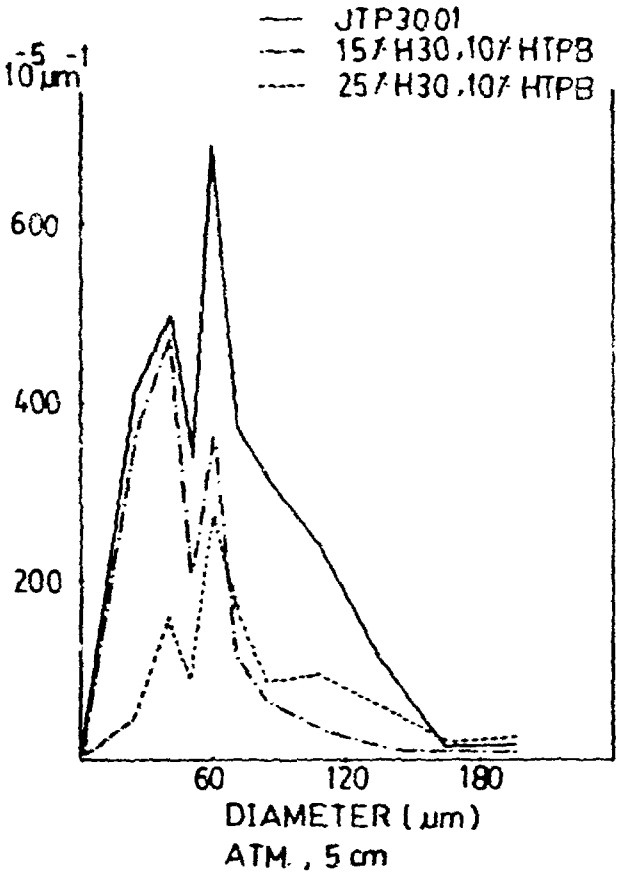

Fig. 39 Size distribution of particles in plume quench samples. Atmospheric pressure tests, quench distance = 5 cm.

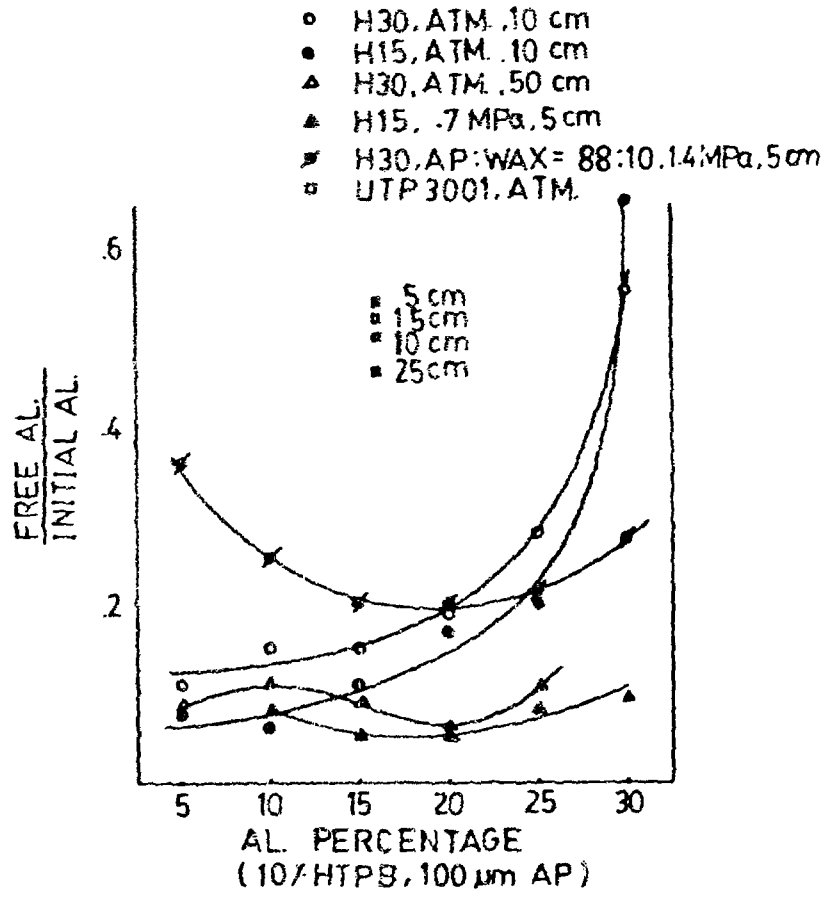

Fig. 40 Mass fraction of unreacted aluminum in plume quench samples (weight difference method of Al determination).

this variable was not adequately evaluated because of the improvised methods for propellant processing available in the study.

In general, the results suggest that combustion efficiency can be held to conventional levels with aluminum contents up to about 25%, provided propellant ingredients are tailored for that purpose. In the process, combustion-generated aluminum oxide size distributions can be kept comparable to present ones. This conclusion needs further support by tests on propellants with conventional binders and processing.

REFERENCES

1. Price, E. W., et al, "Combustion of Solid Propellants and Low Frequency Combustion Instability," NOTS TP 4244, June 1967.
2. Povinelli, L. A., and R. A. Rosenstein, "Alumina Size Distributions from High-Pressure Composite Solid Propellant Combustion," AIAA J., Vol. 2, No. 10 (1964), pp. 1754-1760.
3. Miller, R. R., "Some Factors Affecting the Combustion of Aluminum in Solid Propellants," ICRPG 2nd Combustion Conference, CPIA Publication 105, Vol. I, May 1966, p. 331-335.
4. Cohen, N. S., "A Pocket Model for Aluminum Agglomeration in Composite Propellants," AIAA/SAE/ASME 17th Joint Propulsion Conference, AIAA Paper 81-1585.
5. Price, E. W., "Combustion of Aluminum in Solid Propellant Flames," 53rd Meeting of AGARD Propulsion and Energetics Panel, 1979, AGARD-CP-259, pp. 14-1-14-15.
6. Hubbartt, J. E., E. W. Price, W. C. Strahle and B. T. Zinn, "Rocket Research at Georgia Tech," AFOSR Interim Scientific Report, November 1978.
7. Price, E. W., C. J. Park, R. K. Sigman and J. K. Sambamurthi, "The Nature and Combustion of Agglomerates," 18th JANNAF Combustion Meeting, CPIA Publication 347, October 1981.
8. Price, E. W., and R. K. Sigman, "Behavior of Aluminum in Solid Propellant Combustion," AFOSR-TR-77-0050, November 1976.
9. Caveny, L. H., and A. Gany, "Aluminum Combustion Under Rocket Motor Conditions," 53rd Meeting of the AGARD Propulsion and Energetics Panel, 1979, AGARD-CP-259, pp.13-1-13-13.
10. Price, E. W., "Relevance of Analytical Models for Perturbation of Combustion of Solid Propellants," AIAA J., Vol. 7, No. 1, (1969), pp. 153-154.
11. Brundige, W. N., and L. H. Caveny, "Combustion of Low-Burn-Rate HTPB Propellants in an Acceleration Field - Part III," 18th JANNAF Combustion Meeting, CPIA Publication 347, October 1981.
12. Price, E. W., et al, "The Fire Environment of a Solid Rocket Propellant Burning in Air," AFWL-TR-78-34, March 1979.
13. Price, E. W., W. C. Strahle, B. T. Zinn, J. E. Hubbartt, R. K. Sigman and B. R. Daniel, "Rocket Research at Georgia Tech," AFOSR Final Technical Report,

Georgia Institute of Technology, November 1981.

14. Price, E. W., E. A. Powell and R. K. Sigman, "Further Studies of the Fire Environment of a Solid Rocket Propellant Burning in Air," AFWL-TR-79-55, April 1980.
15. Micheli, P. L., and W. G. Schmidt, "Behavior of Aluminum in Solid Rocket Motors, Vol. I" AFRPL-TR-77-29, December 1977.
16. Kraeutle, K. J., and H. H. Bradley, Jr., "Combustion of Aluminized Propellants: The Influence of Pressure and Propellant Combustion on Formation of Aluminum Combustion Residue," 14th JANNAF Combustion Meeting, CPIA Publication 292, Vol. I, December 1977, pp. 209-219.
17. Price, E. W., J. E. Crump, H. C. Christensen and R. Sehgal, "Comments on 'Alumina Size Distributions from High-Pressure Composite Solid-Propellant Combustion'," AIAA J., Vol. 3, No. 9 (1965), pp. 1790-1791.
18. Brzustowski, T. A., and I. Glassman, "Vapor-Phase Diffusion Flames in the Combustion of Magnesium and Aluminum: I. Analytical developments, and II. Experimental observations in oxygen atmospheres," AIAA Progress in Astronautics and Aeronautics: Heterogeneous Combustion, edited by H. G. Wolfhard, I. Glassman, and L. Green, Jr., Academic Press Inc., New York, 1964, Vol. 15, pp. 75-158.
19. Boggs, T. L., D. E. Zurn, W. C. Strahle, J. C. Handley and T. T. Milkie, "Mechanisms of Combustion," NWC-TP-5514, July 1973.
20. Price, E. W., W. C. Strahle, B. T. Zinn, J. E. Hubbartt, D. H. Neale, R. K. Sigman and B. R. Daniel, "Rocket Research at Georgia Tech," AFOSR Interim Scientific Report, November 1979.
21. Schmidt, W., and R. Poynter, "Zirconium/Aluminum Combustion," AFRPL-TR-80-8, March 1980.
22. Mellor, A. M., and I. Glassman, "Augmented Ignition Efficiency for Aluminum," Combust. Sci. Technol., Vol. 1, No. 6 (1970), pp. 437-447. (See also: same title, Princeton University, Dept. of Aerospace Sciences Technical Report No. 791, 1967.)
23. Frolov, Yu. V., P. F. Pokhil, and V. S. Logachev, "Ignition and Combustion of Powdered Aluminum in High-Temperature Gaseous Media and in a Composition of Heterogeneous Condensed Systems," Fizika Goreniya i Vzryva, Vol. 8, No. 2 (1973), pp. 213-236.

24. Glassman, I., "Combustion of Metals: Physical Considerations," ARS Progress in Astronautics and Rocketry, Vol. 1, Solid Propellant Rocket Research, Academic Press, New York, 1960, pp. 253-258.

25. Boggs, T. L., et al, "Combustion of Solid Propellants and Low Frequency Combustion Instability," Progress Report, 1 October 1967-1 November1968, NWC-TP-4749, June 1969.

26. Prentice, J. L., and K. J. Kraeutle, "Metal Particle Combustion," Progress Report, 1 May 1967-30 September 1968, NWC-TP-4658, January 1969.

27. Price, E. W., J. C. Handley, R. R. Panyam, R. K. Sigman, and A. Ghosh, "Combustion of Ammonium Perchlorate-Polymer Sandwiches," AIAA J., Vol. 19, No. 3, (1981), pp. 380-386.

28. Price, E. W., R. K. Sigman and R. R. Panyam, "Combustion Mechanisms of Solid Propellants," Annual Technical Report 1 August 1979-31 July 1980 for Office of Naval Research, Georgia Institute of Technology, September 1981.

29. Cohen, N. S., R. W. Fleming, and R. L. Derr, "Propellants and Combustion -- I, Role of Binder in Solid Propellant Combustion," AIAA/SAE 8th Joint Propulsion Specialist Conference, AIAA Paper 72-1121. (See also: AIAA J., Vol. 12, No. 2 (1974), pp. 212-218.

30. Miller, R. R., M. T. Donohue, R. A. Young, and J. R. Martin, "Control of Solids Distribution in HTPB Propellants," AFRPL-TR-78-14, April 1978.

31. Kraeutle, K. J., "The Behavior of Aluminum During Subignition Heating and Its Dependence on Environmental Conditions and Particle Properties," 9th JANNAF Combustion Meeting, CPIA Publication 231, December 1972, pp. 325-340.

32. Price, E. W., W. C. Strahle, B. T. Zinn, J. E. Hubbartt, R. K. Sigman, and B. R. Daniel, "Rocket Research at Georgia Tech," AFOSR Interim Scientific Report, Georgia Institute of Technology, November 1980.

33. Boggs, T. L., K. J. Kraeutle, and D. E. Zurn, "The Combustion of As-Received and Preoxidized Aluminum in Sandwich and Propellant Configurations," 9th JANNAF Combustion Meeting, CPIA Publication 231, December 1972, pp. 341-345.

34. Brundige, W. N., "Space Motor Combustion Technology, Phase I. Data Base Development," AFRPL-TR-80-52, December 1980.

35. Boggs, T. L., J. E. Crump, K. J. Kraeutle, and D. E. Zurn, "Cinephotomicrography and Scanning Electron Microscope as Used To Study

Solid Propellant Combustion at the Naval Weapons Center," NWC-TP-5944, May 1977.

36. Varney, A. M., "An Experimental Investigation of the Burning Mechanisms of Ammonium Perchlorate Composite Solid Propellants," Ph.D. Thesis, Georgia Institute of Technology, 1970.
37. Price, E. W., K. J. Kraeutle, R. K. Sigman, J. E. Crump,T. L. Boggs, D. E. Zurn, "Behavior of Aluminum in Solid Propellant Combustion, NWC-TP-6120, in press.
38. Crump, J. E., J. L. Prentice, and K. J. Kraeutle, "Role of Scanning Electron Microscope in the Study of Solid Propellant Combustion: II. Behavior of Metal Additives," Combust. Sci. Technol., Vol. 1 (1969), pp. 205-223.
39. Price, E. W., J. K. Sambamurthi, R. K. Sigman and C. J. Park, "Combustion of High Aluminum Content Solid Propellants," 18th JANNAF Combustion Meeting, CPIA Publication 347, October 1981.

DISTRIBUTION LIST

	Copies
Aerojet Solid Propulsion Company P. O. Box 13400, Bldg. 2019/Dept. 4350 Sacramento, CA 95813 Attn: Mr. Michael J. Ditore	1
Aerojet Strategic Propulsion Co. P. O. Box 15699C Sacramento, CA 95813 Attn: Dr. R. L. Lou Dr. Wilfred Schmidt	2
Aerospace Corporation P. O. Box 92957 Los Angeles, CA 90045 Attn: Ellis M. Landsbaum	1
U. S. Air Force Academy FJSRL/NC USAF Academy, CO 80840 Attn: Dr. John S. Wilkes, Jr.	1
AFATL Code DLDL Eglin AFB, FL 32542 Attn: Mr. Otto K. Heiney	1
Air Force Office of Scientific Research Directorate of Aerospace Sciences Bolling Air Force Base Washington, DC 20332 Attn: Dr. L. H. Caveny	10
Air Force Office of Scientific Research Directorate of Chemical Sciences Bolling Air Force Base Washington, DC 20332 Attn: Mr. Donald L. Ball	10
AFRPL Code PACC Edwards AFB, CA 93523 Attn: Mr. W. C. Andrepont Mr. Wayne Roe	2
AFRPL Code MKP/MS24 Edwards AFB, CA 93523 Attn: Mr. R. Geisler	1
AFRPL Code DYSC Edwards AFB, CA 93523 Attn: Mr. Daweel George	1
AFRPL Code LK Edwards AFB, CA 93523 Attn: LTC B. Loving	1
AFRPL Code CA Edwards AFB, CA 93523 Attn: Dr. R. R. Weiss	1
Aeropropulsion Laboratory Wright-Patterson AFB Fairborn, Ohio Attn: Dr. F. D. Stull	1
Army Ballistic Research Labs ARRADCOM Code DRDAR-BLI Aberdeen Proving Ground, MD 21005 Attn: Mr. J. M. Frankle Dr. Ingo W. May Mr. L. A. Watermeier	3
Army Ballistic Research Labs ARRADCOM Code DRDAR-BLP Aberdeen Proving Ground, MD 21005 Attn: Dr. A. W. Barrows	1
Army Ballistic Research Labs ARRADCOM Code DRDAR-BLT Aberdeen Proving Ground, MD 21005 Attn: Dr. Philip Howe	1
Army Frankford Arsenal Bridge & Tacony Streets Philadelphia, PA 19137 Attn: J. Lannon	1
HQ US Army Material Development Readiness Command Code DRCDE-DW 5011 Eisenhower Avenue Room 8N42 Alexandria, VA 22333 Attn: Mr. S. R. Matos	1
Army Missile Command Code DRSMI-R Redstone Arsenal, AL 35898 Attn: Dr. R. G. Rhoades	1
Army Missile Command Code DRSMI-RKL Redstone Arsenal, AL 35898 Attn: Dr. W. W. Wharton	1
Army Research & Development Command ARRADCOM Code LCWSL Dover, NJ 07802 Attn: Mr. C. Lenchitz	1
Army Research & Development Command ARRADCOM Code DRDAR-SCA-PF Dover, NJ 07802 Attn: Mr. L. Stiefel	1
U. S. Army Research Office P. O. Box 12211 Research Triangle Park, NC 27709 Attn: D. Squires	2
Atlantic Research Corp. 5390 Cherokee Ave. Alexandria, VA 22314 Attn: Dr. C. B. Henderson Dr. Merrill K. King Dr. W. Waesche	3
Brigham Young University Provo, UT 84601 Attn: Dr. Merrill W. Beckstead	1
British Embassy Munitions Directorate Propellants and Explosives Defence Equipment Staff 3100 Massachusetts Ave. Washington, DC 20008 Attn: Dr. T. Sinden	1
Case Western Reserve Univ. Dept. of Mechanical & Aerospace Engineering Cleveland, Ohio 44106 Attn: James S. T'ien	1
California Institute of Tech. 204 Karman Lab 1201 E. California St. Pasadena, CA 91109 Attn: Fred E. C. Culick	1
California Institute of Tech. Jet Propulsion Laboratory 4800 Oak Grove Drive Pasadena, CA 91103 Attn: Leon D. Strand	1
Mr. Norman Cohen 858-A Pine Ave. Redlands, CA 92373	1
Defense Technical Information Center Code DTIC-DDA-2 Cameron Station Alexandria, VA 22314	12
Georgia Institute of Tech. School of Aerospace Eng. Atlanta, GA 30332 Attn: Prof. Edward Price	1
Hercules Inc. Aerospace Division Alleghany Ballistic Lab P. O. Box 210 Washington, DC 21502 Attn: Dr. Rocco C. Musso Dr. R. R. Miller	2
Hercules Inc. Bacchus Works P. O. Box 98 Magna, UT 84044 Attn: Dr. E. H. Debutts Dr. James H. Thacher Dr. K. McCarty	3

DISTRIBUTION LIST

	Copies
Hercules Inc. Eglin Code AFATL/DLDL Eglin AFB, FL 32542 Attn: Dr. Ronald L. Simmons	1
Institute for Defense Analyses 400 Army-Navy Drive Arlington, VA 22202 Attn: R. C. Oliver	1
Johns Hopkins University APL Chemical Propulsion Info. Agency Johns Hopkins Road Laurel, MD 20810 Attn: Mr. Thomas W. Christian Mr. Theodore M. Gilliland	2
Lawrence Livermore Laboratory University of California Code L-324 Livermore, CA 94550 Attn: Dr. R. McGuire	1
Los Alamos Scientific Lab Code NSP/DOD, MS-245 P. O. Box 1663 Los Alamos, NM 87545 Attn: Dr. B. G. Craig	1
Los Alamos Scientific Lab Mail Stop 920 Los Alamos, NM 87545 Attn: Ms. Joan L. Janney	1
Los Alamos Scientific Lab Code WX-2 P. O. Box 1663 Los Alamos, NM 87545 Attn: Dr. R. Rogers	1
Los Alamos Scientific Lab P. O. Box 1663 Los Alamos, NM 87545 Attn: Dr. J. M. Walsh	1
NASA/George C. Marshall Space Flight Center Code EP 25 Huntsville, AL 35812 Attn: J. Q. Miller	1
NASA/George C. Marshall Space Flight Center Code EP 24 Huntsville, AL 35812 Attn: Robert J. Richmond	1
NASA/HQ Code RP 600 Independence Ave., SW, Rm. 625 Washington, DC 20546 Attn: Frank W. Stephenson, Jr.	1
Scientific Advisor Commandant of the Marine Corps Code RD-1 Washington, DC 20380 Attn: Dr. A. L. Slafkosky	1
Office of Naval Research Code 413 Arlington, VA 22217 Attn: Dr. Richard S. Miller	1
Office of Naval Research Western Office 1030 East Green Street Pasadena, CA 91106 Attn: Dr. R. J. Marcus	1
Naval Air Systems Command Code 330 Washington, DC 20361 Attn: Mr. R. Brown	1
Naval Air Systems Command Code 03P25 Washington, DC 20360 Attn: Mr. B. Sobers	1
Naval Air Systems Command Code NAIR-954-Tech Library Washington, DC 20361	1
Naval Explosives Dev. Engineering Department Assistant Director Naval Weapons Station Yorktown, VA 23691 Attn: Dr. L. R. Rothstein	1
Naval Explosive Ordnance Disposal Tech Center Code D Indian Head, MD 20640 Attn: Dr. Lionel Dickinson	1
Naval Materiel Command Strategic Systems Project Office Department of the Navy Room 901 Washington, DC 20376 Attn: Dr. J. F. Kincaid	1
Naval Material Command Strategic Systems Project Office Propulsion Unit Code SP 2731 Department of the Navy Washington, DC 20376	1
Naval Material Command Strategic Systems Project Office Department of the Navy Room 1048 Washington, DC 20376 Attn: Mrs E. L. Throckmorton	1
Naval Ordnance Station CM PM4 Indian Head, MD 20640 Attn: Mr. C. L. Adams	1
Naval Ordnance Station Code 5253 Indian Head, MD 20640 Attn: Mr. S. Mitchell	1
Naval Ordnance Station Indian Head, MD 20640 Attn: Mr. Peter L. Stang	1
Naval Postgraduate School Dean of Research Monterey, CA 93940 Attn: Dr. William Tolles	1
Naval Postgraduate School Physics & Chemistry Dept. Monterey, CA 93940 Attn: Prof. Richard A. Reinhardt	1
Naval Postgraduate School Department of Aeronautics Monterey, CA 93940 Attn: Mr. David W. Netzer	1
Office of Naval Research Mechanics Program Code 432 Arlington, VA 22217 Attn: Dr. N. L. Basdekas	1
Naval Research Lab. Code 6100 Washington, DC 20375	1
Naval Research Lab. Code 6510 Washington, DC 20375 Attn: Dr. J. Schnur	1
Naval Sea Systems Command Code SEA 64E Washington, DC 20362 Attn: Mr. R. Beauregard	1
Naval Sea Systems Command Code 62R2 Washington, DC 20362 Attn: Mr. J. Murrin Mr. R. Cassell	2
Naval Ship Engineering Center Materials Branch Philadelphia, PA 19112 Mr. John Boyle	1
Naval Ship Research & Development Center Applied Chemistry Division Annapolis, MD 21401 Attn: Dr. G. Bosmajian	1

DISTRIBUTION LIST

	Copies
Naval Surface Weapons Center Commander Silver Spring, MD 20910 Attn: Mr. G. B. Wilmot	1
Naval Surface Weapons Center Code R10 White Oak Laboratory Silver Spring, MD 20910 Attn: Dr. S. J. Jacobs	1
Naval Surface Weapons Center Code R11 White Oak Laboratory Silver Spring, MD 20910 Attn: Dr. H. G. Adolph	1
Naval Surface Weapons Center Code R13 White Oak Laboratory Silver Spring, MD 20910 Attn: Dr. R. Bernecker	1
Naval Surface Weapons Center Code R16 Indian Head, MD 20640 Attn: Dr. T. D. Austin	1
Office of Naval Technology Chief MAT Code 0716 Washington, DC 20360 Attn: Dr. A. Faulstich	1
Office of Naval Technology Chief MAT Code 0712 Washington, DC 20360 Attn: LCDR J. Walker	1
Naval Underwater Systems Center Energy Conversion Dept. Code 5B331 Newport, RI 02840 Attn: Mr. Robert S. Lazar	1
Naval Weapons Center Code 385 China Lake, CA 93555 Attn: Dr. A. Amster	1
Naval Weapons Center Code 388 China Lake, CA 93555 Attn: Mr. T. L. Boggs Dr. R. L. Derr Dr. R. Reed, Jr.	3
Naval Weapons Center Code 3205 China Lake, CA 93555 Attn: Mr. Lee N. Gilbert Dr. L. Smith Dr. C. Thelen	3
Naval Weapons Center Code 3272 China Lake, CA 93555 Attn: Mr. R. McCarten	1
Pennsylvania State University Dept. of Mechanical Engineering University Park, PA 16802 Attn: Prof. Kenneth Kuo	1
Princeton Combustion Research Laboratories, Inc. 1041 U. S. Highway One North Princeton, NJ 08540 Attn: Dr. Martin Summerfield	1
Princeton University School of Engineering and Applied Sciences Dept. of Mech. Eng. & Aero Eng. The Engineering Quadrangle Princeton, NJ 08544 Attn: Dr. Forman A. Williams	1
Purdue University School of Mechanical Engineering TSPC Chaffee Hall West Lafayette, IN 47906 Attn: Mr. John R. Osborn	1
Rockwell International Corp. Rocketdyne Division BA08 6633 Canoga Ave. Canoga Park, CA 91304 Attn: Mr. Joseph E. Flanagan	1
Rohm and Haas Company Huntsville, AL 35801 Attn: Dr. H. Shuey	1
Sandia Laboratories Division 2513 P. O. Box 5800 Albuquerque, NM 87185 Attn: Dr. S. Sheffield	1
Science Applications, Inc. Suite 423 20335 Ventura Blvd. Woodland Hills, CA 91364 Attn: Mr. R. B. Edelman	1
Space Sciences, Inc. 135 Maple Avenue Monrovia, CA 91016 Attn: Dr. M. Farber	1
Southwest Research Institute Institute Scientist P. O. Drawer 28510 San Antonio, TX 78228 Attn: Mr. William H. McLain	1
Thiokol Corporation Elkton Division P. O. Box 241 Elkton, MD 21921 Attn: Mr. W. Brundige	1
Thiokol Corporation Government Systems Group Technical Director P. O. Box 9258 Ogden, UT 84409 Attn: Dr. T. F. Davidson	1
Thiokol Corporation Huntsville Division Huntsville, AL 35807 Attn: Dr. D. A. Flanigan Mr. G. F. Mangum Mr. J. D. Byrd	3
Thiokol Corporation Wasatch Division P. O. Box 524 Brigham City, UT 84302 Attn: Dr. J. C. Hinshaw Mr. John A. Peterson Dr. G. Thompson	3
United Technologies Corp. Chemical Systems Division P. O. Box 358 Sunnyvale, CA 94088 Attn: Dr. Robert S. Brown Dr. C. M. Frey Dr. R. Hermsen	3
University of Illinois AE Dept. Transportation Building, [illegible] Urbana, [illegible] Attn: Dr. Herman Krier	1
University of Southern California Mechanical Engineering Dept. OHE 200 Los Angeles, [illegible] Attn: [illegible]	1
University of Utah Salt Lake City, UT 84112 Attn: Dr. G. [illegible] Flandro	1
University of Waterloo Dept. of Mechanical Engineering Waterloo, Ontario CANADA Attn: Dr. Clarke E. Hermance	1
Whittaker Corporation Bermite Division 22116 W. Soledad Canyon Road Saugus, CA 91024 Attn: Mr. L. Bloom	1